Carina Sampl, BSc.

Synthesis and Characterization of functionalized Organobismuth compounds and Conversion with Saccharides

MASTER'S THESIS

to achieve the university degree of

Diplom-Ingenieurin

Master's degree programme: Technical Chemistry

submitted to

Graz University of Technology

Supervisor

Assoc.Prof. Dipl.-Ing. Dr.techn. Roland Fischer

Institute for Inorganic Chemistry

Graz, March 2018

Meiner Familie

Danksagung

Zuallererst gilt mein Dank Herrn Prof. Dr. Roland Fischer, nicht nur für die Möglichkeit an diesem großartigen Thema zu arbeiten und die hervorragende Betreuung, sondern besonders für die sehr vielseitigen Gespräche über die Chemie und das allgemeine Leben. Lieber Roland, ich danke dir für dein Vertrauen in mich und meine Fähigkeiten.

Besonderer Dank gilt Dr. Martin Thonhofer für seine unendliche Geduld und sein offenes Ohr für meine Probleme. Lieber Martin, danke dass du mich zu jeder Zeit unterstützt hast und mir mit Rat und Tat zur Seite standest.

Dem gesamten CONQUER-Team, insbesondere Frau Prof. Dr. Karin Stana-Kleinschek, Dr. Rupert Kargl und Herrn Prof. Dr. Hermann Scharfetter danke ich für die großartige Unterstützung und den unermüdlichen Wissensdurst.

Bei Herrn Prof. Dr. Stefan Spirk bedanke ich mich für die Unterstützung sowie auch bei der gesamten AG Spirk für die immer lustige Zeit und die gute Zusammenarbeit.

Mein aufrichtiger Dank gilt darüber hinaus natürlich der gesamten Arbeitsgruppe, für die Hilfsbereitschaft, den gegenseitigen Wissensaustausch sowie die freundliche Arbeitsatmosphäre. Besonders zu erwähnen sind hier Beate und Judith, für ihr immer offenes Ohr, ihre herzlichen Worte und Unterstützungen in jeglicher Hinsicht. Ein großes Dankeschön gibt vorallem auch Moni, Babsi und Astrid, durch deren organisatorischen und wissenschaftlichen Anstrengungen das Insitut bzw. die Fakultät so erfolgreich ist. Bei allen anderen Institutskollegen bedanke ich mich für die schöne gemeinsame Zeit.

Außerdem bedanke ich mich bei meinen Freunden und Studienkollegen, die mich auf diesem Weg begleitet haben. Besonders bei Johanna, Silvan, Thomas, Peter, Andi, Werner, Cori, Ferula und Maria, sowie Sarah, Anita und Chrissi für die ununterbrochene Unterstützung und die schöne Zeit mit euch.

Meinen Eltern, Geschwistern und Großeltern - meiner ganzen Familie - gebührt unendlicher Dank. Danke, dass ihr mir immer zur Seite standet und immer an mich geglaubt habt. Ein besonderer Dank gilt Stefan, der mir immer Mut zugesprochen hat und immer für mich da war. Auch Traudi, Anni und Hildegard gebührt außerordentlicher Dank, für ihre herzlichen Worte und Unterstützungen in jeder Hinsicht.

Ich bedanke mich bei der Europäischen Union für die Finanzierung des Horizon 2020 research and innovation Programmes (FET Open, CONQUER, grant agreement No. 665172) und damit für die Finanzierung meiner Diplomarbeit.

AFFIDAVIT

I declare that I have authored this thesis independently, that I have not used other than the declared sources/resources, and that I have explicitly indicated all material which has been quoted either literally or by content from the sources used. The text document uploaded to TUGRAZonline is identical to the present master's thesis.

08.03.2018
Date

Carina Sampl
Signature

Abstract

Contrast agents used in magnetic resonance imaging (MRI) are commonly based on Gd^{3+} compounds. In search of novel, "smart" contrast agents (CA's) with high potential for molecular imaging, certain quadrupolar nuclei with a high spin quantum number (I) have become of interest. A particularly favourable element represents bismuth (^{209}Bi) due to the high spin quantum number $I = 9/2$, the variety of possible organometallic reactions and the reported low toxicity. Since the electric quadrupole moment of the Bi-nuclei, interacts with the electric field gradient (EFG), which is caused by charge distribution of the chemical environment of the nucleus, a quadrupole splitting - essential for NQR/MRI measurements - becomes possible. A change of the charge distribution, caused by variation of the ligand species, can shift the NQR transition frequencies (TF) close to the predefined frequency of 121 MHz (3 T) of the MRI scanner.

In this thesis, synthetic approaches of different known and novel trivalent organobismuth compounds, showing a suitable quadrupole transition frequency are described. The experimental focus of further synthesis is on coupling reactions with more polar, water soluble compounds - like *monosaccharides* – to enable the introduction of the NQR-active bismuth compound in aqueous environments, like the human body. The developed synthetic strategies allow various modifications for both components, in particular however for the carbohydrate species. Therefore different monosaccharide compounds are included in the synthetic concepts and coupled to the bismuth-compounds.

Kurzfassung

Die heute in der Magnetresonanztomographie (MRT) verwendete Phasenkontrastmittel basieren hauptsächlich auf Gd^{3+} Verbindungen. Auf der Suche nach neuen, "intelligenten" Kontrastmitteln, welche ein hohes Potenzial zur molekularen Bildgebung aufweisen, sind insbesonders Kerne mit einer hohen Spin-Quanten-Zahl (I) in den Fokus der Forschung geraten. Das Element Bismuth verbindet vielerlei Eigenschaften die einen Einsatz als Kontrastmittel begünstigen, vorallem durch die hohe Spinquantenzahl von $I = 9/2$, die Vielzahl möglicher metallorganischer Reaktionen und die sehr geringe Toxizität. Durch die Ladungsverteilung der chemischen Umgebung des Bismuthkerns, wird ein elektrischer Feldgradient (EFG) generiert, der in Folge einer Interaktion mit dem Quadrupolmoment der Bismuthkerns, eine für die NQR/MRI Messung essenzielle Quadrupolaufspaltung ermöglicht. Bei einer Änderung der Ladungsverteilung, die aus einer Variation der Substituenten resultiert, können die NQR-Übergangsfrequenzen (TF) in den Bereich der vom MRI Scanner vorgegebenen 121 MHz (3 T) verschoben werden.

Im Rahmen dieser Arbeit werden synthetische Zugänge zu verschiedenen bekannten und neuen trivalenten Organobismuthverbindungen, welche geeignete NQR-Übergangsfrequenzen zeigen, erarbeiten. Der experimentelle Fokus der weiteren Synthese liegt in "Kopplungsreaktion" mit polaren, wasserlöslichen Verbindungen. Hierfür eignen sich beispielsweise *Monosaccharide*, die das Einbringen von NQR-aktiven Bismuthspezies in wässrige Umgebungen, dargestellt durch den menschlichen Körper, ermöglichen können. Die synthetischen Ansätze erlauben unterschiedliche Modifikationen an beiden Komponenten, insbesondere aber auf Seite der Kohlenhydrate. Verschiedene Monosaccharide werden hierfür in die Synthese mit einbezogen und an die Bismuthverbindungen geknüpft.

Index

Abbreviations

n-BuLi	*n*-butyllithium
C	cyclohexane
CA	contrast agent
CT	computed tomography
CuI	copper iodide
DMF	dimethylformamide
DMSO	dimethylsulfoxide
EA	ethylacetate
EFG	electric field gradient
Et_3N	triethylamine
Et	ethyl
EtOH	ethanol
Et_2O	diethylether
I	spin quantum number
LG	leaving group
Me	methyl
MW	molecular weight
NMR	Nuclear Magnetic Resonance
MRI	Magnetic Resonance Imaging
MRT	Magnetic Resonance Tomography
NaH	sodium hydride
NP	nano-particle
PG	protecting group
PS	polystyrene
QN	quadrupolar nuclei
QRE	quadrupole relaxation enhancement
TBAF	tetrabutylammoniumfluorid
TBS	*tert*-butyldimethylsilyl
TF	transition frequency
THF	tetrahydrofuran
TLC	thin-layer chromatography
TMS	trimethylsilyl
XRD	X-Ray Diffraction

1 Introduction

1.1 CONQUER - Contrast by Quadrupole Enhanced Relaxation

This thesis is part of the FET-open Horizon 2020 EU funded project CONQUER (Contrast by Quadrupole Enhanced Relaxation). CONQUER aims at the development of a radically new type of magnetic resonance imaging (MRI) contrast agent for molecular imaging (MI).

In medicinal diagnostics, the molecular approach plays an increasingly important role for understanding diseases and development of effective treatment methods. MRI offers, beside laboratory tests and CT imaging, a particularly wide range of contrast mechanisms that not only allows to visualise the position, form and structure of body parts, organs and tissues, but also provides details of functioning. Today, these techniques have certain limits, concerning the visualization of molecular and metabolic changes - e.g. in cases of cancer, heart and Alzheimer's diseases - at a high resolution and a high level of reliability. A completely new type of "smart" contrast agents promises an improvement of these drawbacks. Visualization of molecular functions of tissues and organs could be enabled, allowing for a faster and more precise medical diagnosis and a better understanding of pathogenesis. Molecular imaging using MRT is based on the water content and MR relaxation times of the individual tissues, which produces images of different luminosities. Relaxation times of protons in biologiccal tissue can be strongly influenced by contrast agents and thus the image's contrast in areas where a CA accumulates. Contrary to commercially available CA's (often based on Gd^{3+} complexes), CONQUER's contrast agent is exploiting the cross relaxation between (water) protons and a large quadrupolar nuclei, i.e. the relaxation is frequency dependent and can be matched to the spectrometer frequcency, and therefore offers a broad spectrum of smart properties. [61]

A very promising QN represents bismuth (^{209}Bi) due to the high spin quantum number ($I = 9/2$), the manifold chemistry and it's low toxicity and so constitutes the basis of the CA. Different arylbismuth Ar_3Bi compounds were synthesized and investigated regarding their NQR properties. A variation of the aryl/ligand species, for example

from a phenyl to an anisyl ligand, changes the NQR transition frequencies of the bismuth compound and therefore a shifting towards the predefined frequency of the MRI scanner's 120 MHz becomes possible (see 3.1.1). Based on the NQR results, a selection of specific Bi compounds was carried out and follow up chemistry was performed using these. To realize the application of described compounds as a CA, connecting the bismuth species to more polar and larger ones, like mono- oligo- or polysaccharides and/or grafting them onto nano-particles, in order to ensure water solubility and appropriate correlation times, becomes necessary. To realize all these aspects, the project has to connect the expertise of quantum physics, chemical and biomedical engineering, material characterization and nanotoxicology. In this manner a cooperation between University of Umea (Sweden), University of Maribor (Slovenia), University of Olsztyn (Poland), Medical and Technical University of Graz arose.[59]

1.2 NQR-Spectroscopy - Nuclear Quadrupole Resonance Spectroscopy

Focus of the project is on the development of a new contrast agent based on relaxation enhancement of water protons by interaction with a quadrupolar nuclei having a high spin quantum number. Relaxation models based on combined perturbation and stochastic Liouville theories were developed as a theoretical basis for systems containing quadrupolar nuclei with high spin quantum numbers of $I = 9/2$, by cooperation partners in Sweden and Poland. These theories were used to predict the relaxation dispersion profiles of promising compounds as functions of the following parameters: quadrupole coupling constant Q_{cc}, anisotropy factor η and gyromagnetic ratio γ of the QN, the distance between ^{1}H atoms and the QN as well as the dynamics of the CA and the ^{1}H carrying molecules and the water exchange rate. [60] For a better understanding a brief introduction into the basic theory of NQR spectroscopy will be given.

1.2.1 NQR - Basic Theory

Nuclear quadrupole resonance spectroscopy (NQR) is a quantum physical phenomenon similar to that of magnetic resonance spectroscopy (NMR) and is used to characterize crystalline compounds containing quadrupolar nuclei. Similar as in nuclear magnetic resonance spectroscopy, NQR uses radio-frequency (RF) magnetic fields to induce and detect transitions between sublevels of a nuclear ground state.[70], [73] NMR refers to the situation where the sublevel energy splitting is predominatly due to a nuclear in-

teraction with an applied static magnetic field, while NQR refers to the case where the predominant splitting is due to an interaction of the nucleus with the electric field gradients within the material. Compared to NMR, NQR measurements can only be accomplished for crystalline solids and can be very selective for a defined temperature. A further important difference between these two spectroscopy methods is, that in NMR the resonance frequency (of a given compound) scales with the applied magnetic field, while in NQR an adjustment of the investigated compound to the field has to be accomplished. NQR measurements where no static magnetic field is used at all is called "pure NQR". Main objective for NQR spcetroscopy is to determine nuclear transition frequencies (energies) and relaxation times, to then relate those to the properties of the investigated crystalline material. Further, NQR is used to obtain detailed information, on crystal symmetries and binding situations, about phase transitions in crystalline solids and also on changes in lattice constants, at certain temperatures.[73]
In order to observe a NQR spectrum, a nucleus having a spin quantum number higher than 1/2 needs to be present, since only these have an electric quadrupole moment. A quadrupolar nuclei is decribed by a nonspherical charge distribution, hence this characteristic determines the electron orbits and the location of the nucleus in a molecule. The charge distribution is somewhat elongated as shown in Fig. 1.1 and forms a cigar shaped nucleus. The conformation of the nucleus on the right, is energetically more favoured, since it puts the tips of the positive charge closer to the negative external charges - q. Therefore the electrostatic energy varies depending on the nuclear orientation.[69]

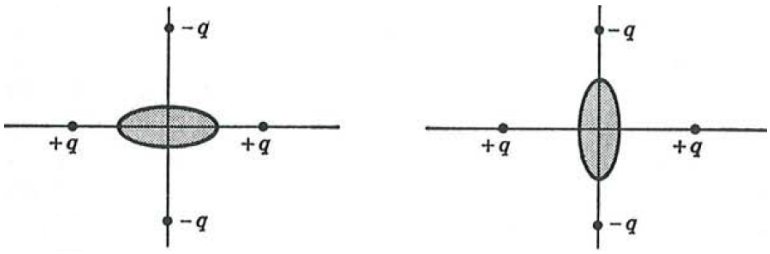

Fig. 1.1: A cigar-shaped charge distribution inside the nucleus in the field of four external charges, with + q on the x-axis and - q on the y-axis.[69]

Consequently, for a nucleus with a spin $\leq 1/2$ the charge distribution appears spherical, thus the nucleus has no electric quadrupole moment as described in Fig. 1.2. The quadrupolar momentum itself is calculated as reported in literature.[69], [73]
Depending on positive or negative prefix of the quadrupole moment, the charge distribution of the nucleus appears prolate ("stretched") or oblate ("squashed"), displayed in Fig. 1.2. ^{209}Bi having a spin quantum number of $I = 9/2$ and high transition frequencies, compared to e.g. ^{14}N/^{15}N, represents a very promising candidate for NQR

measurements. By calculating Q (nuclear quadrupole moment) for a bismuth nucleus, a value of $Q = -0.4$ barn is obtained - therefore the Bi nucleus has an oblate appearance.[73] [54]

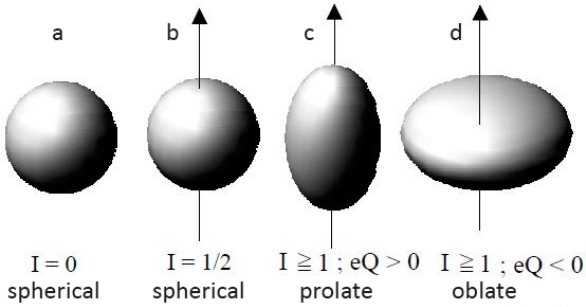

Fig. 1.2: Charge distribution whithin the nucleus for nuclei having different spin quantum numbers.

The electric quadrupole moment of the nucleus interacts with the electric field gradient (EFG), which is caused by a non-spherical charge distribution of the environment of the nucleus. Fig. 1.3 schematic represents the EFG interacting with a QN.

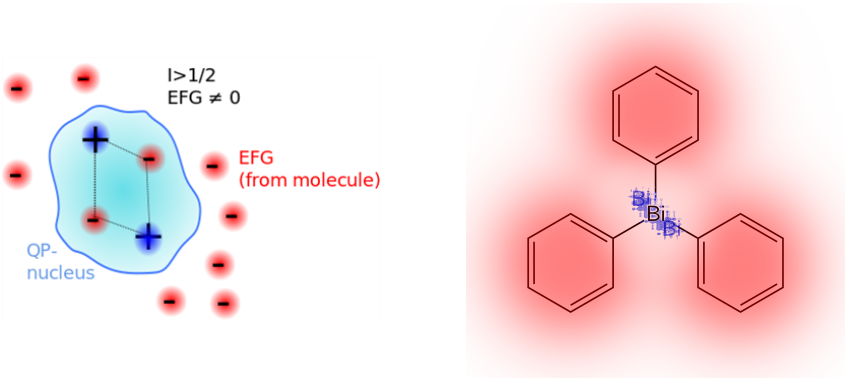

Fig. 1.3: Schematic description of a QN interacting with the EFG and $BiPh_3$ as an example for an QN (Bi) interacting with the ligands (EFG).[69]

The electric field gradient at the interacting nucleus is described by a real, symmetric, traceless 3 x 3 tensor. Such a tensor can always be made diagnonal by choosing an appropriate set of coordinate axes known as principal axes (V_{xx}, V_{yy}, V_{zz}).[62] Commonly it is described as:

$$eq = V_{zz} \quad \text{and} \quad \eta = (V_{xx} - V_{yy})/V_{zz} \tag{1.1}$$

where η is known as the asymmetry parameter, which indicates the degree of the deviation of the EFG from its axisymmetric shape. Commonly the axes are chosen as follows:

$$| V_{xx} | \leq | V_{yy} | \leq | V_{zz} | \tag{1.2}$$

giving $0 \leq \eta \leq 1$. Determination of the quadrupole coupling constant e^2qQ, also Q_{cc} and the asymmetry parameter η, which contain the information about the environment surrounding the nucleus, is one of the most important aim in NQR spectroscopy. These parameters can be used to draw conclusions in respect to changes of crystal structures of the components.[73]
For example, in case of axial symmetry, where $\eta = 2 * I + 1$, quadrupole energy levels are observable. This can be represented by:

$$A = e^2qQ/(4I(2I-1)) \tag{1.3}$$

and the quadrupole energy levels can be calculated as follows:

$$E_q(m) = A \cdot (3m^2 - I(I+1)) \tag{1.4}$$

where m is the magnetic quantum number (m = -I, -I+1,..., I-1, I).[62] Further quadrupole frequencies $f_Q(m\text{-}m')$, which are corresponding to the difference between two energy levels (E_m - $E_{m'}$).[73] For nuclei with high spin quantum numbers $I \geq 3/2$ an exact solution is not known, so in order to get accurate results, tabulated iterative calculation results, can be used.

To calculate the correct transition frequencies, the dependency between correction function f_η(m-m') and the asymmetry factor η has to be considered:[73]

$$f_Q(m - m') = A \,/\, h \cdot 3(m^2 + m'^2) \cdot f_\eta(m - m') \tag{1.5}$$

The NQR splitting, i.e. the interaction of a high spin nucleus with the electric field gradient, caused by its surrounding charge distributions (ligands), gives rise to a splitting on the spin energy levels which can be studied.[22]
The EFG is mainly caused by electrons from the p-shells, since s-shells are spherical and d- and f-shells are far-off the nucleus. Distortion and low symmetry of the chemical surrounding will in addition raise the EFG. The nuclear spin - EFG - coupling is a highly selective and very direct way to get insight in the electronic environment of the molecule. The resonance frequency can be shifted due to it's high sensitivity to

chemical or structural changes on the molecule. An understanding of these properties makes it possible to predict transitions and resonance frequencies of the quadrupole compound and thereby chemical modifications on the molecule can be proposed.[22]

1.2.2 NQR - CONQUER

CONQUER's aim is to develop a novel alternative to conventional CA, which exploits quadrupole relaxation enhancement (QRE). This effect is caused by dipol-dipol interaction of protons (from H_2O molecules in the human body) with the quadrupolar nuclei which give rise to an enhanced proton spin relxation.[32] Based on the distribution of the water protons in the human body and on their spin-spin (T_2) and spin-lattice (T_1) relaxation times, the tissue contrast of the MRT image is influenced. Involving CA's can further increase the contrast and the sensitivity by fasten up the proton spin relaxation times.[21], [22]

Most common used Gd^{+3} based paramagnetic chelating CA's shorten the longitudinal relaxation time T_1 of the free water protons. Paramagnetic iron oxid nano-particles however, predominatly shorten the transversal relaxation time T_2.[34] These CA's are insensitive towards transition frequencies and further can lower the sensitivity due to a faster net relaxation. In the last years, abundant effort has gone into the development of smart contrast agents which show a significant change in relaxation upon activation.[22] The contrast of an image can be switched in response to physiological alterations such as temperature, pH, metal ions, redox state and enzyme activity.[14],[26] Lurie et al. reported about the effectiveness of QRE for enhancing MRI contrasts for the interaction between endogenous ^1H and ^{14}N in amide groups in human muscles at very low evolution fields of 57 to 65 mT.[40] However, such CA's for clinical applications using MRT at 1.5 or 3 T have not been investigated or developed yet[22] - this is where the idea of CONQUER's CA arose.

The development of a new contrast agent based on QRE is a quite complex task, since certain conditions have to be fulfilled to make the phenomenon take place. Generally, the processes only becomes effective when the proton Larmor frequency ν_L comes close to one of the spin transition frequencies $\nu_{Q,k}$ of the quadrupolar nucleus:

$$\nu_L = \nu_{Q,k} = \nu_{Q,kpure} + \gamma_{QN} B_0 \tag{1.6}$$

where γ_{QN} is the gyromagnetic ratio of the quadrupole nucleus, $\nu_{Q,k\ pure}$ the pure quadrupolar transition frequency, which is proportional to the quadrupole coupling constant Q_{cc} and B_0 is the applied magnetic field.[22], [58], [63]
Therefore, contrast agents based on QRE are selective to the applied magnetic field B_0, the temperature, the chemical surrounding of the CA and chemical reactions. Fig. 1.4 again reflects the basic idea of QRE - by shifting the NQR resonance/transition frequency of the CA close to the MRI Larmor frequency of the ^1H atoms - an exchange of energy between CA and protons induces the cross relaxation and the ^1H spins will relax faster.

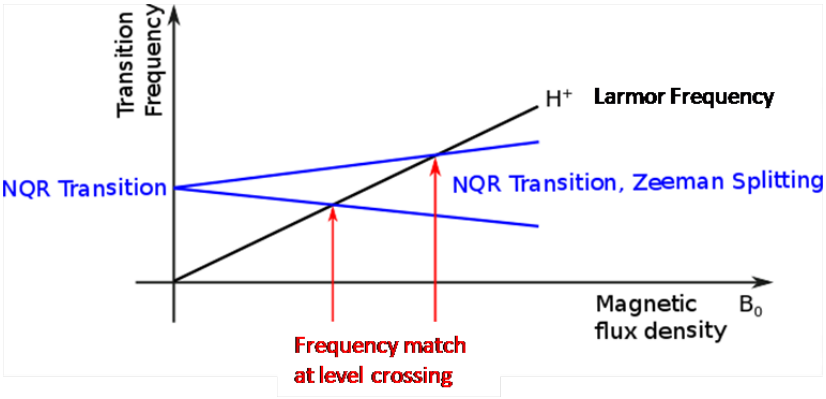

Fig. 1.4: Schematic description of a NQR transition which is split by an applied magnetic field B_0 - showing the intersection of the corresponding NQR transition of a QN with the proton Larmor frequency. At this intersection, respectively this B_0 the effect of QRE originates.

According to this, the effect can be switched on and off, by for example shifting the main field B_0 of the MRI system or changing the chemical structure of the CA (what results in a change of TF's).[22] Therefore, running measurements by sweeping B_0, a selective switch on and off of the QRE-effect is possible. This results in different relaxation times (T_1) for the water protons and thus increase the contrast of the MRT-image. Fig. 1.5 schematically displays the effect of being on and off resonance:

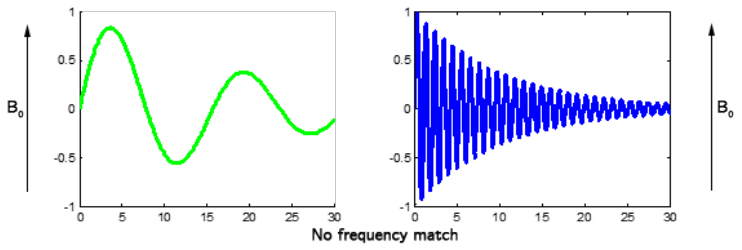

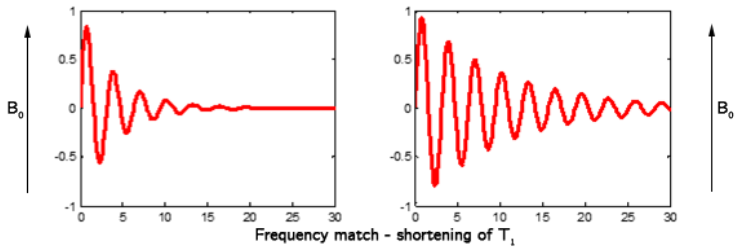

Fig. 1.5: Schematic description of the QRE-effect resulting in a shortening of T_1.

Being off resonance results in long relaxation times for protons (green), though a fast relaxation is observed for the CA/QN (blue) - here the NQR transition frequency of the QN does not intersect the Larmor frequency of the protons (see Fig. 1.4). However, if the two species are on resonance, i.e. share a common frequency, the QRE-effect works, a shortening of T_1 (spin-lattice relaxation time) of the ^{1}H atoms is achieved and therefore similar relaxation times for both, CA and protons, are observed - frequency match.
By using an additional external field input, the frequency of the MRI scanner can be altered so that either cross-relaxation is active or inactive. This will allow the observation of an additional MRI contrast (on-resonance: relaxation enhancement active; off-resonance: relaxation enhancement inactive).

Under consideration of all these factors, the development and identification of promising chemical compounds containing a suitable QN is the first step. Goesweiner et al. described a set of basic selection criteria: the nucleus needs to show a high nuclear spin I (QRE scales with I of 7/2 and 9/2) as well as a high gyromagnetic ratio γ_{QN} to provide strong D-D coupling and hence strengthens the QRE. Low toxicity, high natural abundance and a rich and well-known chemistry are of major advantage. The QN further needs to have a high quadrupole coupling constant to obtain transition frequencies $\nu_{Q,k}$ close to the scanner frequency at clinical field strengths (1.5 T or 3 T). The Q_{cc} depends on both, the quadrupolar moment of the QN and the electric field gradient EFG produced by the electronic environment of the QN and therefore the chemical environment of the compound.[22]

1.3 Bismuth

Bismuth, ^{209}Bi, is the 83th element of the periodic table, the most metallic and least abundant of the elements in group 15, the nitrogen family. For bond formation, the Bi-atom usually uses it's three $6p$ electrons and retains the two $6s$ electrons as an inert pair, thus bismuth mainly appears in oxidation state +3 compounds.[74] For three-coordinate bismuth in BiR_3 molecules, the octet rule at the bismuth nucleus is fulfilled and the resulting trigonal pyramidal geometry might be regarded as being consistant with the VSEPR theory prediction.[68] In section 3.1.1 (page 24) some crystal structures of synthesized triarylbismuth species are shown. The molecular geometry of bismuth can also be described as a result of three covalent $Bi-R_3$ bonds achieved by using the valence electrons of the p-orbital.[68] Nevertheless, Bi^{3+} is a strong Lewis acid but only a very weak Lewis base, this characteristic has dramatic consequences on Bi-chemistry - so cluster formation is favoured and many bismuth compounds, especially the halide adducts, are very poorly soluble in almost all organic solvents. Thus, follow up chemistry prove to be more complicated than expected. Beside trivalent species, organobismuth compounds also appear in the +5 oxidation state and coordination numbers 2, 3, 4, 5, 6 up to 10 become possible. Bismuth's uniqueness is also characterized by it's low toxicity in spite of the heavy metal status and being part of the "arsenic group" elements.[74] Furthermore, bismuth has a high absorption coefficient for X-ray radiation - thus making bismuth compounds suitable as CT-contrast agents, but would also represent great shielding materials for X-Ray radiation.[8], [52]
Naturally occuring bismuth consists of only one stable isotope, ^{209}Bi, with a high nuclear spin quantum number of $I = 9/2$. Due to this feature, the charge distribution of the nucleus forms an electric quadrupole moment and by interaction with the electric field gradient of the surrounding (e.g various ligands) different NRQ transition frequencies can be achieved, as described in section 1.2 on page 2.

1.3.1 Organobismuth Chemistry

Until the late 1990's bismuth chemistry has received less attention compared with that of N, P, Ar and Sb. Nevertheless, over the last one to two decades an increasing interest in the investigation of both inorganic and organometallic chemistry has started.[12] Bismuth compounds or it's chemistry is widely used, starting from medicinal chemistry,[15], [16], [31] in industry as a precursor for atomic layer deposition,[57], [78] as a reagent in cross coupling reactions[12], [25], [55] and various others.[45], [75] Triarylbismuth compounds are almost perfect reagents, since most of them are air stable, easy

to handle and do not generate toxic inorganic waste.[12] Hébert et al. described the use of functionalized triphenylbismuth compounds as proper donor molecules of phenyl species for Pd/Cu catalysed cross-coupling reactions used in organic chemistry.[25]
In this thesis, the focus is on the synthesis of trivalent organobismuth compounds and connecting them to saccharides. As mentioned above, different Ar_3Bi species are prepared, in order to investigate the NQR properties and find a compound showing appropriate NQR transition frequencies (see section 1.2). Therefore, different synthetic concepts are developed, preferable salt-free routes, to prepared them and further link the bismuth species with saccharides or comparable compounds, as described in detail in sections 3.3, 3.5 and 3.6.

1.3.1.1 Triarylbismuth and diarylbismuth chloride compounds

The synthesis of triarylbismuthines is widely reported in literature. The traditionally most common method to prepare Ar_3Bi compounds is using Grignard or organolithium reagents.

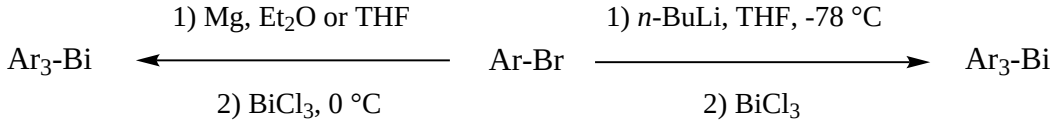

Fig. 1.6: Schematic synthesis of triarylbismuth compounds.[12]

Both synthetic strategies involve two steps. Using the Grignard approach, the first step is the synthesis of the organomagnesium reagent, this is usually made from an aryl bromide and Mg in diethylether or THF under an inert atmosphere of nitrogen. The organomagnesium bromide is further added to a solution of $BiCl_3$ in the corresponding solvent with control of temperature. Similar to this synthesis the *n*-BuLi approach works. To the aryl bromide dissolved in THF and cooled to -78 °C, *n*-BuLi is added under inert conditions. After stirring for several hours, the bismuth chloride species is added, followed by an aqueous work up, for both Grignard and organolithium method. The compounds were recrystallized and isolated.[12], [18], [35], [74]
Applying these methods, symmetric as well as asymmetric bismuth compounds were prepared. To provide asymmetric species the same approaches can be applied, just changing the chloride from $BiCl_3$ to a Ar_2BiCl species as shown in Fig. 1.7.

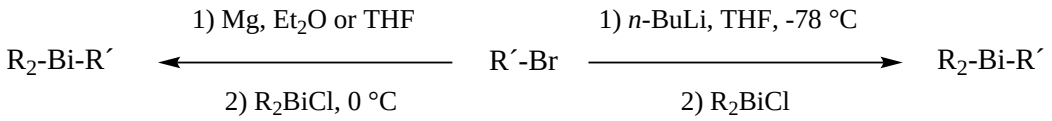

Fig. 1.7: Schematic synthesis of asymmetric triarylbismuth compounds.

Reactions of organobismuth chlorides Ar_2BiCl with Grignard reagents to yield unsymmetrical bismuthines were employed to a limited excess.[18] Norvick,[50] Gilman and Yablunky[20] and Challenger[9] reported on this subject. Their results showed that the synthesis of unsymmetrical $R_2R'Bi$ compounds is always accompanied by formation of R_3Bi, RR'_2Bi and R'_3Bi. Challenger and co-workers[9] came to the result that reactions between R_2BiCl and $R'MgBr$ compounds always yield R_3Bi species. This occurs due to redistribution reactions which already happened during R_2BiCl synthesis - and indicated that a R_2BiCl compound was in reality a double salt of R_3Bi and $BiCl_3$.[20] Subsequently Gilman and co-workers described a bismuth salt equilibrium (see Fig. 1.8) and concluded, that after formation of $R_2R'Bi$, the compound undergoes redistribution, in part or in whole, similar to Kocheshkov redistribution reactions, to R_3Bi and R'_3Bi.[20]

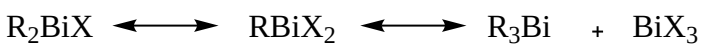

Fig. 1.8: Equilibrium of bismuth chloride species.[20]

Also Lobez and Swager,[37] Tamber[76] and Ignatious[28, 29] published their results regarding synthesis of unsymmetrical bismuth species similar to compounds **22** and **25**, discussed in section 3.1.2 on page 32.

R_2BiCl and $RBiCl_2$ species are difficult to prepare directly and especially to separate from each other by synthesizing from Ar_3Bi and $BiCl_3$, since this reaction concept is always accompanied by redistribution reactions. However, to synthesize described Ar_2BiCl compounds different ways are described in literature. Althaus and co-workers[2] reported about the synthesis of R_2BiCl and $RBiCl_2$ using RLi and $BiCl_3$ in Et_2O at -40 °C achieving yields of 93 %. Rahman et al.[53] described a route using R_3Bi and SO_2Cl_2 to obtain different pentavalent bismuth chloride compounds of R_3BiCl_2 type. Another way was published by Freedman and Doak.[18] They described the reaction of R_3Bi with halogens X_2 at low temperatures forming a dialkylhalobismuthine via cleavage of a carbon-bismuth bond.
However, mono- and dihalobismuthines are prepared in the best way by a redistribu-

tion reaction between a triorganylbismuthine R_3Bi and a bismuth halide BiX_3 as shown below:

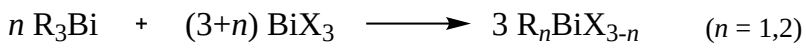

Fig. 1.9: Schematic synthesis of bismuth chloride species.[74]

Alkyl and Aryl derivatives are obtained applying this method in similar ease. To yield R_2BiCl as the main product 1 mol of BiX_3 is reacted with 2 moles of R_3Bi in Et_2O (or THF, benzene, DCM and $CHCl_3$). These reactions are essentially based on the equilibration among four different bismuth compounds R_nBiX_{3-n} (n = 0 - 3) in a given solution. Therefore, the desired chloride has to be recrystallized from a suitable solvent to be obtained as a pure compound.[74] Described monochloride synthesis is widely used and reported in literature.[3, 4], [10], [47]

1.3.1.2 Diarylbismuth amides - Ar_2BiNR_2

Chemistry concerning bismuth amides is widely used in industry. Rusek and co-workers [57] described the synthesis of $Bi(NR_2)_3$ species and use as a potential atomic layer deposition precursor for the deposition of Bi_2Te_3 films. Vehkamaki et al.[78] reported about preparation of various bismuth silylamides and application as potential atomic layer deposition and chemical vapour deposition precursors. The synthesis of different hypervalent organo-azabismocines and use as a highly reactive and recoverable reagent for cross-coupling reactions in organic chemistry was described by Shimada and co-workers.[67]
Furthermore, Gynane,[23] Nekoueishahraki,[48, 49] Mason[41] and Breunig[7] reported on synthesis of organobismuth-amides. The major part focused on the synthesis of tri-amide bismuth complexes. These are synthesized using $BiCl_3$ and the corresponding lithium amide in THF at -30 °C,[57], [74] as shown in Fig. 1.10:

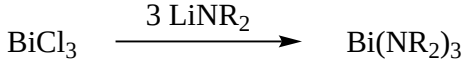

Fig. 1.10: Schematic synthesis of bismuth amides.

Gynane and co-workers described the synthesis of $MCl_n(NR_2)_{3-n}$ [M = P, Ar, Sb, Bi; n = 1, 2, 3] by addition of the lithium amide to the appropriate M(III) chloride in Et_2O:

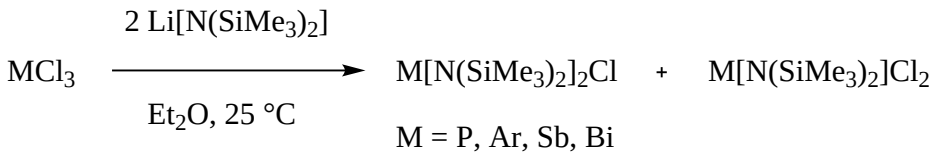

Fig. 1.11: Synthesis of $M[N(SiMe_3)_2]Cl$ and $M[N(SiMe_3)]Cl_2$ compounds.[23]

For reactions of PCl_3, $AsCl_3$ and $SbCl_3$ the desired mono- or dichloride species are obtained. However, in the case of a $BiCl_3$-$2Li[N(SiMe_3)_2]$ system, the only identified product was $Bi[N(SiMe_3)_2]_3$.[23]
$Bi(NR_2)_3$ compounds are further described as being thermolabile and light sensitive. They gradually turn black at room temperature and when exposed to sun light. This darkening indicates the formation of metallic bismuth. Therefore, storage in a freezer in the dark is recommended.[74]

However, literature concerning synthesis of diarylbismuth amides is very scarce, especially when starting from Ar_2BiCl compounds. Thus new synthetic concepts had to be developed. Bismuth amides synthesized in frame of this thesis are all prepared by addition of the corresponding lithium amide to Ar_2BiCl as shortly described in Fig. 1.12 (see Fig. 3.17).

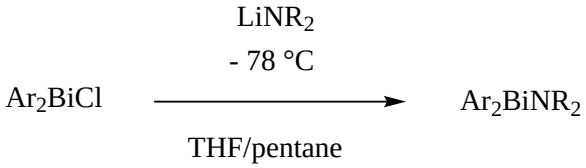

Fig. 1.12: Schematic synthesis of Ar_2BiNR_2 compounds starting from a bismuth monochloride species.

Bismuth amides, $Bi(NR_2)_3$, are known as excellent precursors for synthesis of bismuth alkoxides and bismuth thiolates.[74] Mendoza-Espinosa and Liu and co-workers have prepared various calixarene bismuth(III) and anitmony(III) complexes using bismuth triamides as precursors. Their interest in calixarene bismuth complexes stems from the development of bimetallic model molecules analogous to the Standard Oil of Ohio Company (SOHIO) Bi-Mo catalyst for study of the chemistry related to the oxidation and ammoxidation of propene.[43–46], [36]
Evans et al. reported about synthesis and characterization of $Bi(OR)_3$ compounds. They reacted $BiCl_3$ with three equivalents of $NaOCMe_3$ in THF for 24 h and yielded $Bi(OCMe_3)_3$ as a white powder in 80 % yield.[17]

Furthermore, Kou et al. described the synthesis of $Bi(OR)_3$ starting either from $BiCl_3$ or from $Bi(NR_2)_3$ as depicted in Fig. 1.13.[33]

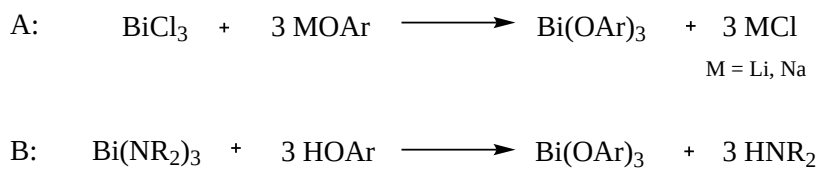

Fig. 1.13: Schematic synthesis of Ar_2BiOR compounds starting from $BiCl_3$ or $Bi(NR_2)_3$.[33]

Comparable chemical reactions using CO_2, CS_2, PhNCO and others, were reported by Suzuki et al. (Fig. 1.14). These compounds were obtained by insertion of phenyl isocyanate or phenyl isothiocyanate into the Bi-N bond of the bismuth amides in good to excellent yields. However, these compounds are not stable and decompose if not stored under inert conditions, giving the corresponding urea and thiourea derivatives.[74]

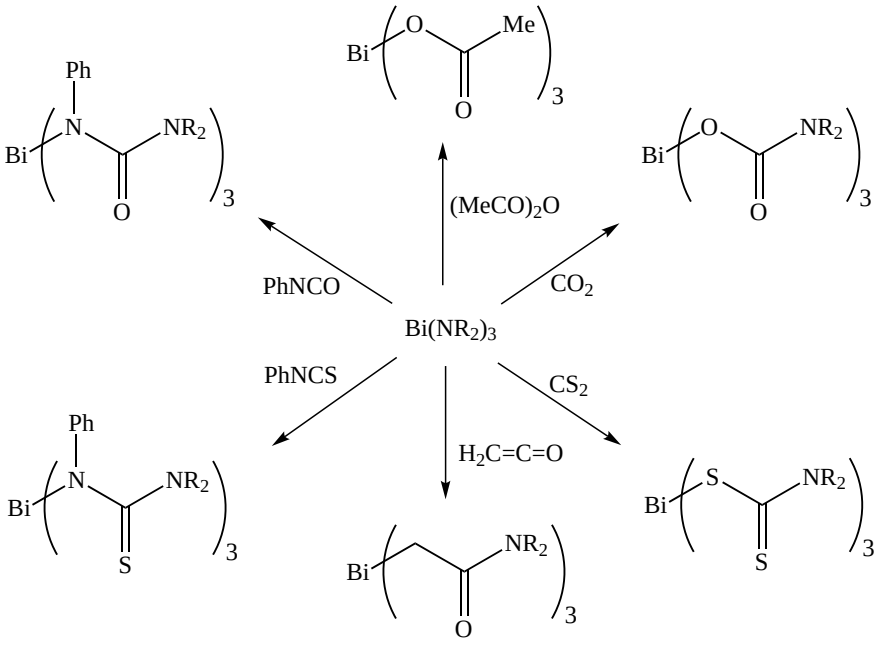

Fig. 1.14: $Bi(NR_2)_3$ and possible conversion reactions.[74]

1.3.1.3 Huisgen 1,3-dipolar cylcloaddition

Today, the copper(I)-catalyzed azide-alkyne cycloaddition - Huisgen 1,3-dipolar cycloaddition - is widely used as a reliable methode for covalently connecting diverse building blocks.[79] This cycloaddition is regarded as one of the most reliable and powerful reaction of the hetero-Diels-Alder family due to the wide variety, accessibility and relative inertness of the starting compounds.[1] In 1965, Huisgen and co-workers reported about their results on reactions of electron-rich C-C-triplebonds with electron-poor azides forming triazole rings.[27] Tornoe and co-workers[77] and Rostovtsev co-workers[56] introduced in 2002 the copper-catalysed version of the Huisgen reaction.[1] The click-chemistry's uniqueness is most likely the extraordinary stability of the azides towards H_2O, O_2 and the majority of organic synthesis conditions. The azide group, having a spring-loaded nature, last invisible unless a dipolarophile appears.[56] The cycloaddition, forming a triazole cycle usually results in a mixture of the 1,4- and 1,5-regioisomers:[56]

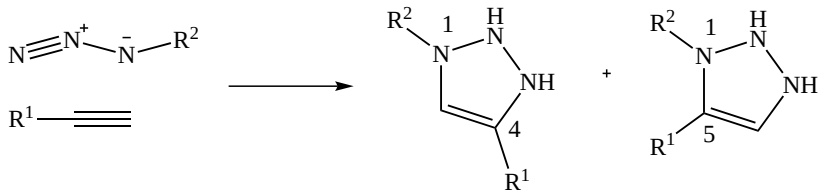

Fig. 1.15: Huisgen 1,3-dipolar cycloaddition.[56]

Copper catalysts, in form of Cu^I salts, for example CuI, $CuOTf{\cdot}C_6H_6$ and $[Cu(NCCH_2)_4][PF_6]$, usually require the presence of a nitrogen base (e.g. triethylamine, pyridine or diisopropylethylamine). The main disadvantage of this method is the formation of undesired by-products like diacetylenes, bis-triazoles and 5-hydroxytriazoles.[56] However, the use of a Cu^{II}/Cu^0 system forming Cu^I by compropartionation is a very useful alternative.[1] In Fig. 1.16 the mechanistic proposal for the catalytic cycle described by Rostovtsev et al.[56] is shown:

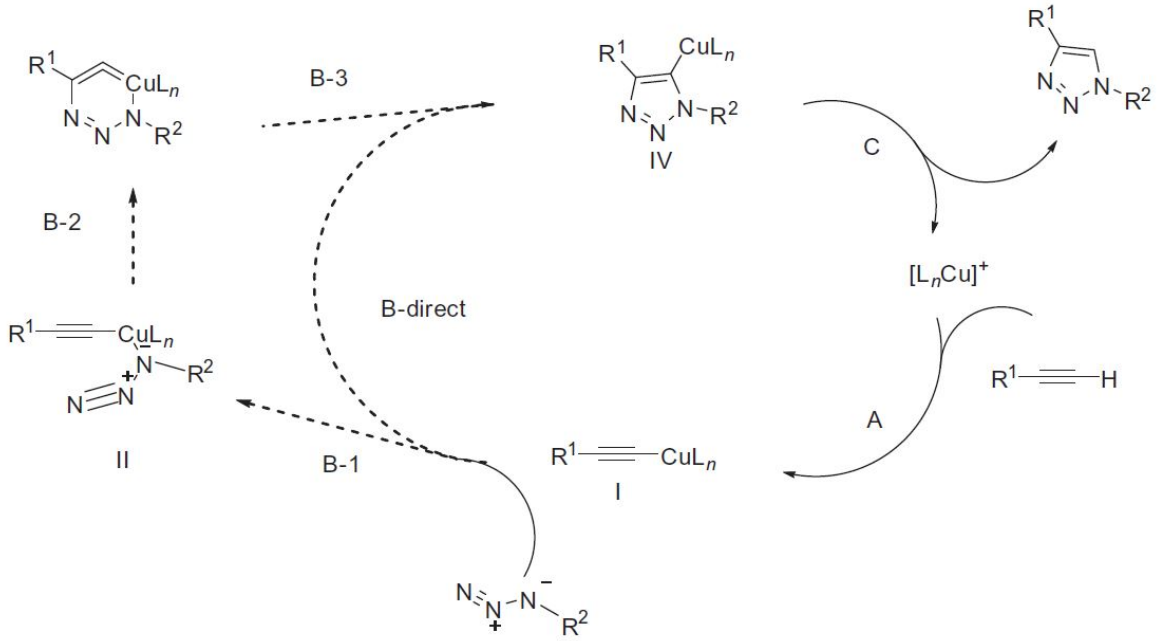

Fig. 1.16: Proposed catalytic cycle for the Cu^I-catalyzed ligation.[56]

In this manner, the Huisgen-cycloaddition is applied to connect a bismuth-alkyne with a monosaccharid-azide using CuI as catalyst. Since Cu^{II} species and Ar_3Bi compounds undergo cross coupling reactions in presence of organic molecules,[25] Cu^I catalysts are used to form the triazole-compounds. Synthesis of bismuth species showing an alkyne or azide functionality are very sparse reported in literature. Lobez et al. described a way preparing (4-ethynylphenyl)diphenylbismuthine using the corresponding bromobenzene species and *n*-BuLi and further conversion with a diarylbismuth chloride.[37, 38]
For synthesis of desired bismuth-precursors and azide-containing species, as well as for performing the click-reaction, new concepts were developed and presented in detail in section 3.5 and 5.3.5.

1.3.1.4 Polymerization of bismuth compounds

In literature, only little information regarding synthesis of polymerizable organobismuth compounds as well as bismuth-polymers is available.[42] However, Tamber and coworkers described the synthesis of styryldiphenylbismuth and the subsequent polymerization with vinylbenzylphosphonate ester and methyl methacrylate yielding bismuth-containing polymers for use as radiopaque (X-Ray contrast) resin.[76] The synthesis of the related bismuth compound was already described in section 1.3.1.1.

Polymerization of styrylbismuth compounds is performed via radical polymerization in toluene at 65 - 90 °C using AIBN as an initiator. The polymer is precipitated in cold methanol and obtained as a colourless powder.[11], [42], [76]

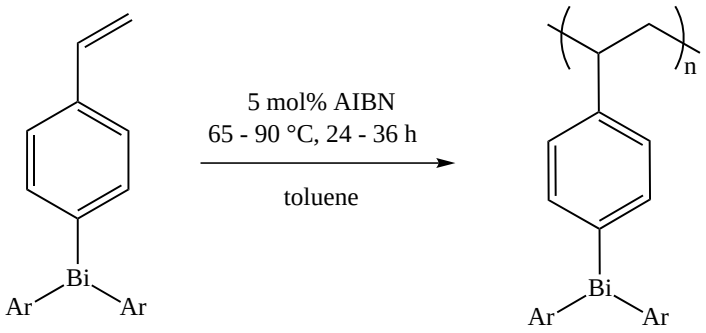

Fig. 1.17: Schematic polymerization of styryldiarylbismuth compounds using AIBN.[42]

2 General Aims and Synthetic Strategies

In search and development of novel contrast agents for molecular imaging, bismuth compounds have gained attention. The high spin quantum number of the ^{209}Bi nucleus and the very low toxicity, award the element special characteristics and makes it of special interest for medicinal applications.
The first synthetic strategy aims towards the synthesis of triarylbismuth compounds, showing transition frequencies close to the predefined frequency of 121 MHz of the MRI scanner. Therefore different known and novel arylbismuth compounds were synthesized and characterized, as depicted in Fig. 2.1

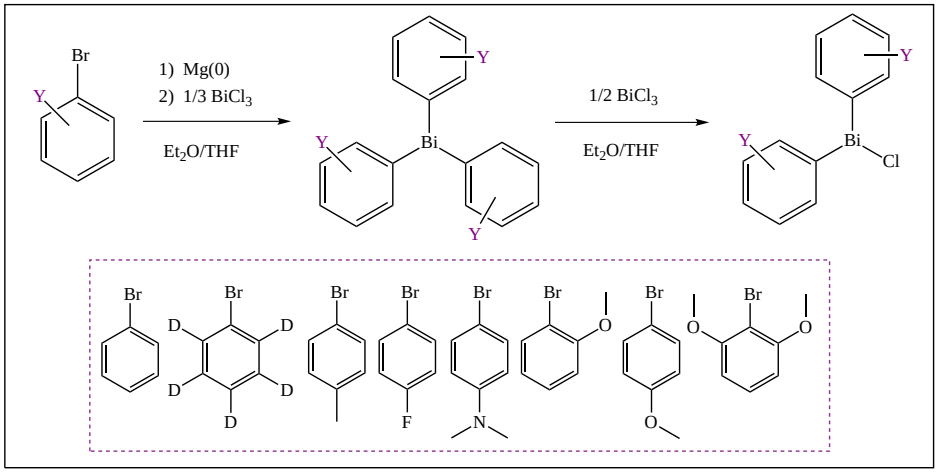

Fig. 2.1: Strategy to prepare triarylbismuth compounds via a Grignard reaction and subsequent conversion to the corresponding Ar_2BiCl species.

Once an arylbismuth-compound exhibiting the desired transition frequency has been identified, linking them to a more polar species becomes necessary, in order to make them soluble in water based environments (i.e. the human body).
To fulfil the defined task of connecting the NQR active bismuth compound to a water soluble species, different aspects have to be considered. A question of central importance is, which coupling partners comply with the requirements. Mono-, oligo- as

well as polysaccharides are very promising, further nano-particles could be auspicious coupling partners. Monosaccharides like glucose, galactose and xylose derivatives are intended coupling partners in the first attempts. In a further consequence the coupling concepts should be extended to oligo- and polysaccharides, such as for example cyclodextrins. Another promising approach could be the grafting of the bismuth compound onto nano-particles, e.g. SiO_2-NP's.
At this point, the most essential question of how to link the two species, as schematically displayed in Fig. 2.2, arises.

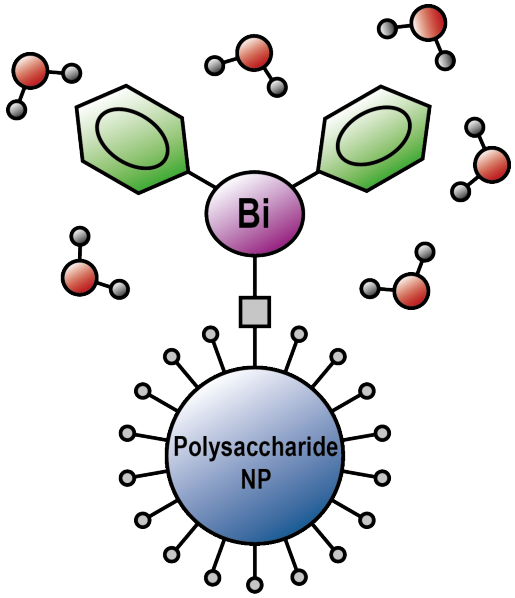

Fig. 2.2: Bio-compatible nano-particle carrying promising quadrupolar bismuth compound.

One of the most important aspects to consider is the stability and therefore the type of the linkage. To realize the coupling, different concepts have been developed (Fig. 2.3). The first concept, the "Amide Coupling", describes the reaction of Ar_2BiCl with different lithium-amides to obtain the corresponding Ar_2BiNR_2. These compounds represent very promising educts for further reactions with saccharides providing different functional groups like hydroxyl- sulfhydryl- or carboxyl-groups.
The second concept describes the copper-catalysed Huisgen 1,3-dipolar cycloaddition, to link a monosaccharide to the bismuth species. To perform described reaction a bismuthalkyne, which is synthesized via a Grignard or lithiation route, is combined with the corresponding sugar-azide forming a triazole ring.
In procedure 3, the "Ether Coupling" concept, the reaction between a bismuth providing a hydroxyl-group or a bromide and a saccharide is described.

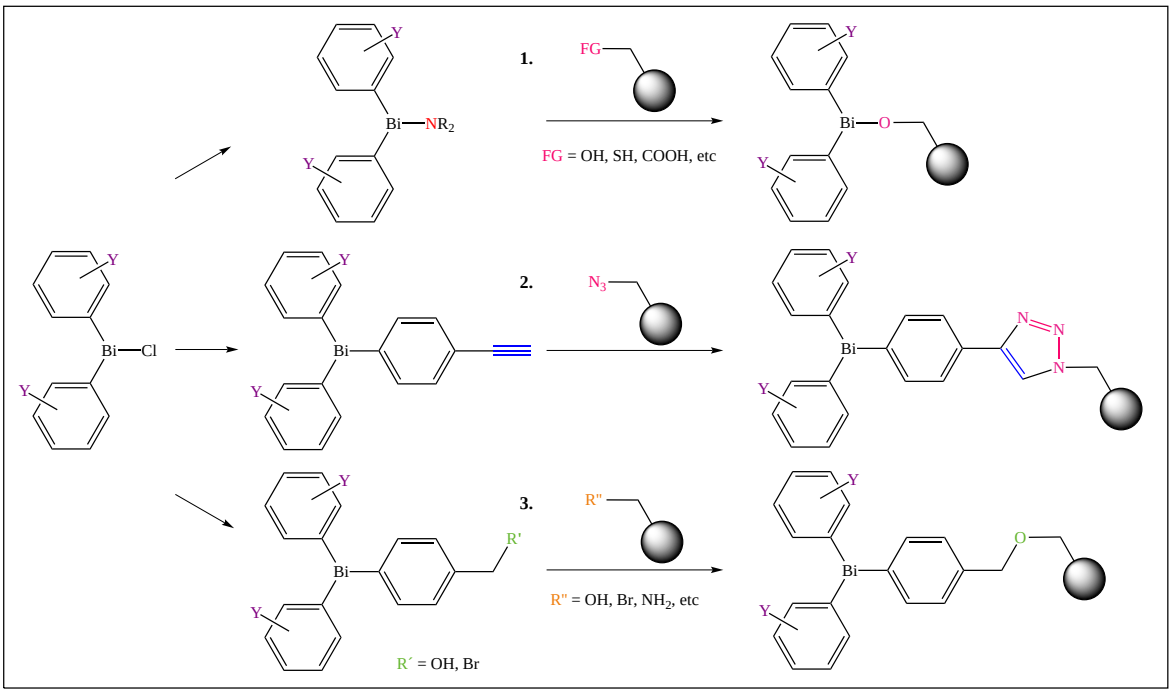

Fig. 2.3: General overview of the planed sythetic strategies

Following the reaction details for the three introduced synthetic strategies are described.

2.1 Amide Coupling

The amide concept describes connecting a bismuth amide with compounds exhibiting different functional groups (alcohols, thiols, carboxylic acids, etc.) For proof of concept, reactions connecting bismuth amides with bulky compounds alike 1-adamantanol, 1-adamanthane thiol and 1-adamantane carboxylic acid will be performed. The later step should involve reactions with protected and unprotected monosaccharides. An advantage of this concept is that there are not any complicated derivatization reactions of the carbohydrates needed. In Fig. 2.4 the synthetic concept is schematically displayed:

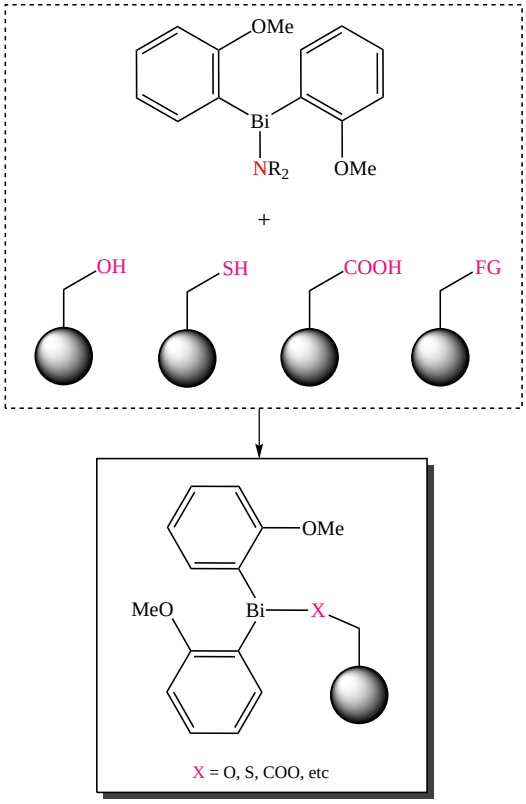

Fig. 2.4: Intended approach towards bismuth-containing saccharides.

The reactions will have to be carried out under an inert atmosphere, since the stability of the bismuth-educts in air is limited, due to the high reactivity of the bismuth-nitrogen bond. In addition, the question of air- and moisture stability of the products arises. However, a great advantage of this salt free route is the omission of formation of salts and insoluble Bi-salt adducts.

2.2 Huisgen 1,3-dipolar Cycloaddition

Additionally, an approach involving Huisgen 1,3-dipolar cycloaddition has been developed. As shown in Fig. 2.5 the reaction path intends to link a bismuth-alkyne species to a carbohydrate modified with an azide-moiety via formation of a stable triazole ring. Synthesis and modification of bismuth and saccharide species is supposed to be more complicated, however both are assumed to be air stable.

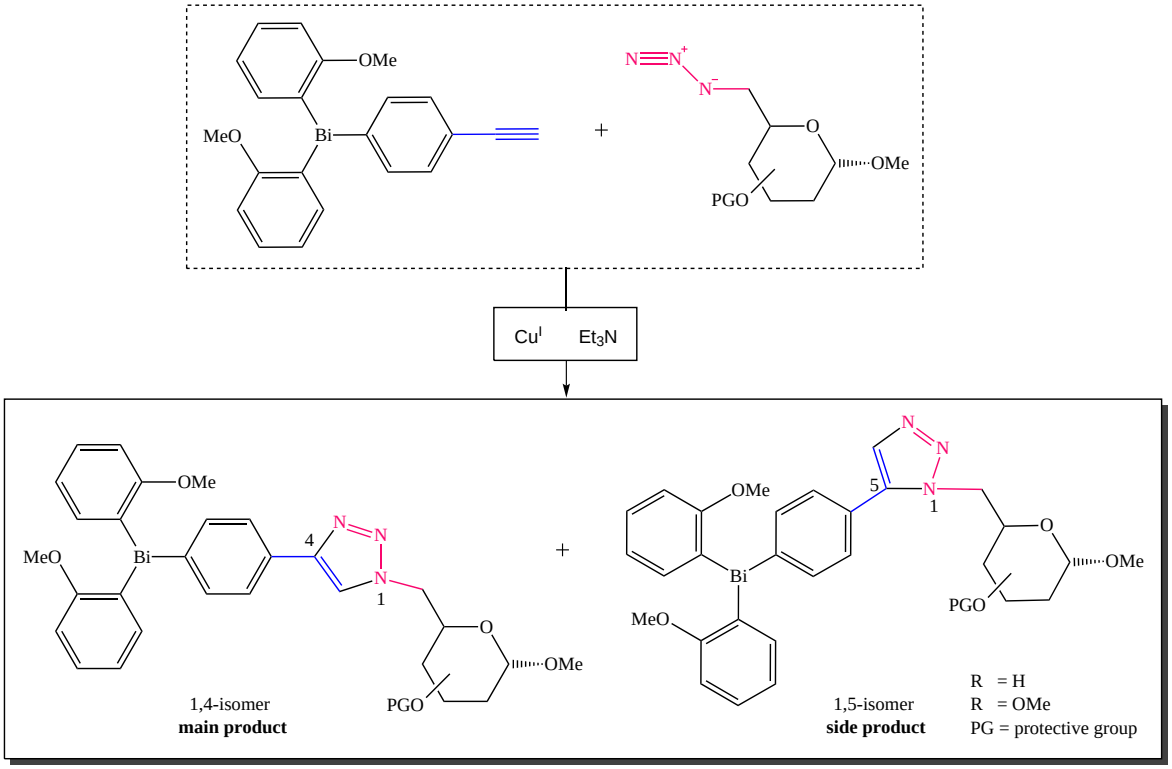

Fig. 2.5: General overview of the planned Huisgen 1,3-dipolar cycloaddition.

The reaction between the bismuth-alkyne and the saccharide-azide in presence of Cu^{I} and Et_3N leads to formation of two different click-reaction products. The 1,4-isomer represents the main product, whereas for this particular reaction the 1,5-isomer can be regarded as a side product. In comparison to other coupling concepts, this one represents the most limited concerning reaction partners, since it is restricted to the use of an alkyne and an azide carrying compound. In section 3.5 and 5.3.6 reaction details are presented.

2.3 Ether Coupling

A further concept to synthesize robust and stable bismuth-monosaccharide compounds has been developed and investigated, as displayed in Fig. 2.6. The main advantage of this concept is the possibility to provide the involved reactants, bismuth and carbohydrate, as either nucleophile or electrophile.

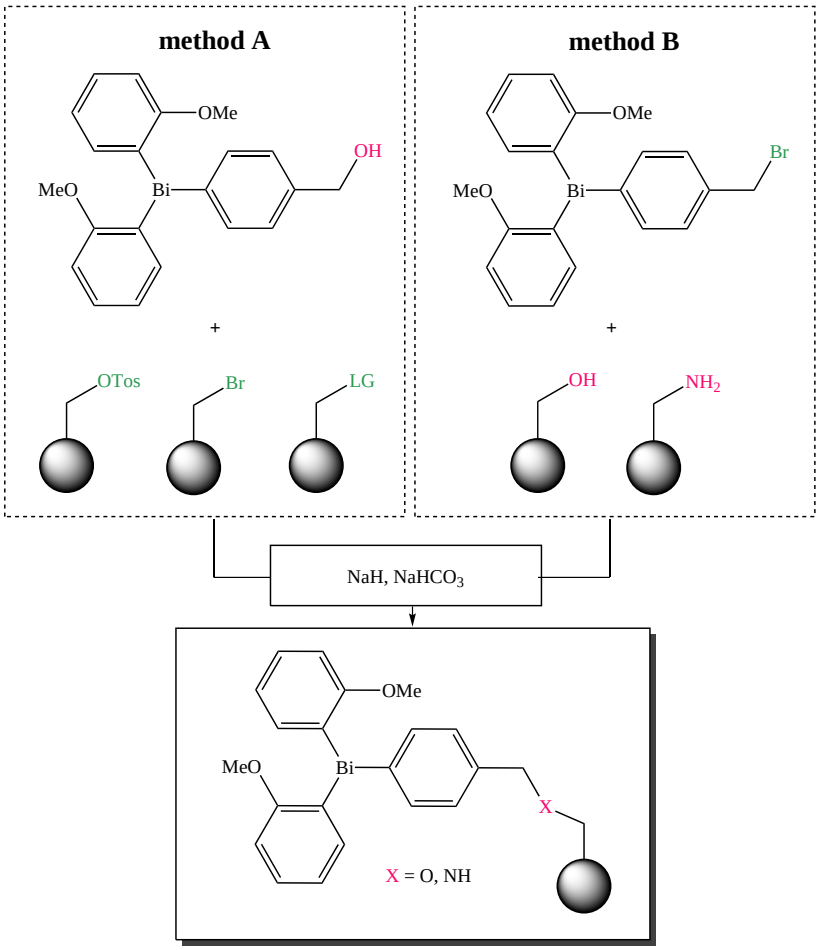

Fig. 2.6: Intended approach to bismuth-containing carbohydrates.

Method A describes the reaction between an "bismuth-alcohol" (nucleophile) and a monosaccharide having electrophilic character. Vice versa to A, for the second way (method B) the bismuth compound acts as the electrophile while the saccharide represents the nucleophile. In an appropriate solvent (THF, DMF), NaH or $NaHCO_3$ is used to deprotonate the nucleophile and therefore start the S_N2 reaction. The exact reaction details are described in section 3.6 and 5.3.6.

3 Results and Discussion

This section describes the originally scheduled synthetic routes to afford the desired organobismuth compounds. The synthetic approaches and results are presented and discussed in detail.

3.1 Triarylbismuth compounds - Ar_3Bi

3.1.1 Synthesis of symmetrical triarylbismuth compounds

The first part of this thesis focuses on the synthesis and characterization of triarylbismuth compounds, the determination of the corresponding NQR-transition frequencies (accomplished by the cooperation partners) and the subsequent selection of promising bismuth compounds to perform presented coupling concepts with saccharides.
The synthesis of triarylbismuth compounds Ar_3Bi is widely known and reported in literature.[5], [12], [18], [19], [24], [25], [35], [39], [74] In general, the bismuth species are synthesized by reaction of the corresponding starting material with Mg, following the Grignard procedure. However, alternative methods using *n*-BuLi are applied and reported. The triarylbismuth compounds shown in Fig. 3.1 are synthesized by a Grignard reaction as described in detail in section 5.3.1.1 on page 68, starting with the conversion of the respective commercially available bromobenzene species **1** - **8** and metallic magnesium to the Grignard reagent. After addition of the corresponding amounts of $BiCl_3$ in the second step, the desired triarylbismuth compound is afforded. This Grignard procedure was utilized to synthesize compounds **9** - **16** obtaining pure triarylbismuth species in high yields ranging from 77 - 90 %.[18]

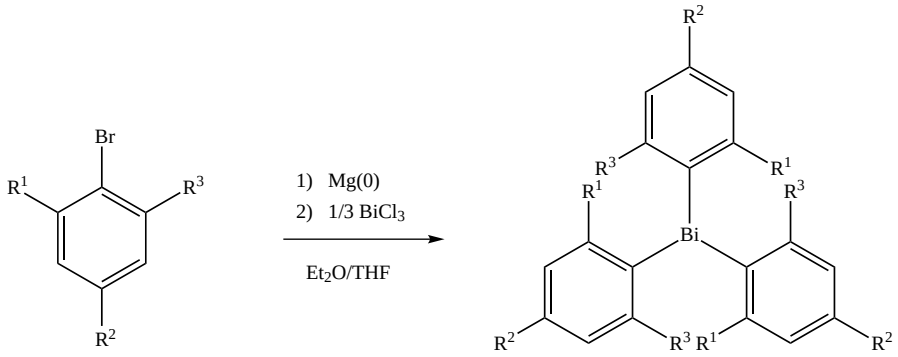

1	R^1 = H	R^2 = H	R^3 = H
2	R^1 = D	R^2 = D	R^3 = D
3	R^1 = H	R^2 = Me	R^3 = H
4	R^1 = H	R^2 = F	R^3 = H
5	R^1 = H	R^2 = NMe_2	R^3 = H
6	R^1 = H	R^2 = OMe	R^3 = H
7	R^1 = OMe	R^2 = H	R^3 = H
8	R^1 = OMe	R^2 = H	R^3 = OMe

9	R^1 = H	R^2 = H	R^3 = H
10	R^1 = D	R^2 = D	R^3 = D
11	R^1 = H	R^2 = Me	R^3 = H
12	R^1 = H	R^2 = F	R^3 = H
13	R^1 = H	R^2 = NMe_2	R^3 = H
14	R^1 = H	R^2 = OMe	R^3 = H
15	R^1 = OMe	R^2 = H	R^3 = H
16	R^1 = OMe	R^2 = H	R^3 = OMe

Fig. 3.1: Synthesis of triarylbismuth compounds **9** - **16** via a Grignard reaction

The synthesis of triphenylbismuthine $BiPh_3$ **9** and the deuterated analogues $BiPh_3$(d) **10** follows the standard Grignard procedure. The bromobenzene species was reacted with Mg in Et_2O and kept at reflux for approx 3 h. Afterwards the reaction mixture was cooled to 0 °C and added to a $BiCl_3$ suspension. After washing with H_2O, to eliminate formed Mg-salts, the organic phases were dried over Na_2SO_4, concentrated and recrystallized from EtOH. Both species were obtained as colourless crystals in yields of 90 %.

The crystalstructure of $BiPh_3$ has been studied frequently and Bi-C bond lengths (2.237, 2.268, 2.273 Å) as well as C-Bi-C bond angles (92.7, 94.3, 94.7 °) are published.[30] For compound **10** similar Bi-C bond lengths (2.260, 2.271, 2.252 Å) and C-Bi-C bond angles (94.4, 94.2, 94.1 °) were determined.

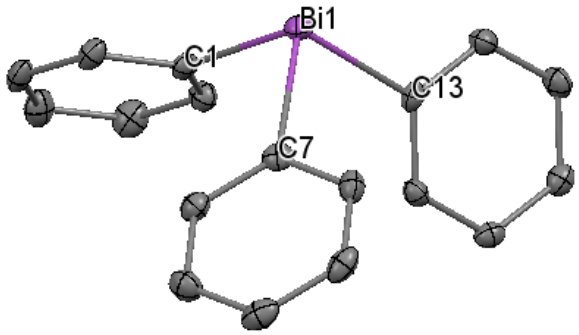

Fig. 3.2: Crystal structure of compound **10**. Hydrogen atoms are omitted for clarity. Selected distances [Å] and angles [°]: Bi1-C1 2.260(4), Bi1-C7 2.271(4), Bi1-C13 2.252(3), C1-Bi1-C7 94.4(1), C1-Bi-C13 94.2(1), C7-Bi1-C13 94.3(1).

Compound **11** was synthesized in a equal manner to $BiPh_3$ compounds, as described in section 5.3.1.1. XRD results confirm small differences in Bi-C bond lengths (2.261, 2.243, 2.256 Å) and C-Bi-C bond angles (93.48, 94.28, 95.01 °) as described in Fig. 3.3. Compared to $BiPh_3$ the bond lengths and angles do not differ immense, thus $BiTol_3$ crystallizes in the same pyramidal geometry.

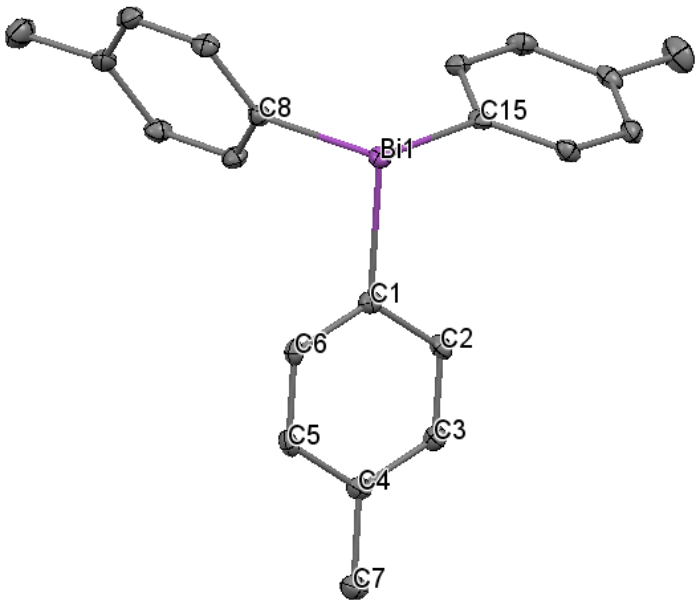

Fig. 3.3: Crystal structure of compound **11**. Hydrogen atoms are omitted for clarity. Selected distances [Å] and angles [°]: Bi1-C1 2.261(3), Bi1-C8 2.243(2), Bi1-C15 2.256(2), C4-C7 1,504(4), C1-Bi1-C8 93.48(8), C1-Bi-C15 94.28(8), C8-Bi1-C15 95.01(8), Bi1-C1-C2 122.9(2), C3-C4-C7 121.4(2).

Synthesis of compound **12** resembles to previously mentioned. After recrystallized from EtOH, the compound was obtained as colourless needles in a yield of 90 %. NMR as well as IR data validate the formation of desired compound **12**.

In an analogues manner the *p*-dimethylamino-phenyl derivative **13** was obtained. The Grignard reaction is performed as described, however a further purification step is necessary. After washing the reaction mixture with H_2O, drying the organic phases over Na_2SO_4 and removal of the solvent, the crude product was redissolved in toluene. The hot product solution was filtrated over Celite® 512 and recrystallized in toluene to afford compound **13** as colourless needles in 78 % yield.
It is of utmost importance to perform the washing step with H_2O at a neutral to slightly basic pH, since an acidic environment will break the Bi-C bonds and the compound decomposes in its educts, respectively N,N-dimethylanilin (a precursor for synthesis of azo-dyes) and elemental bismuth.

XRD data confirmed the pyramidal structure and comparing the Bi-C bond lenghts (2.240, 2.230, 2.247 Å) and C-Bi-C bond angles (93.4, 94.7, 95.6 °) to para-substituted $BiTol_3$ no drastic changes are observable.

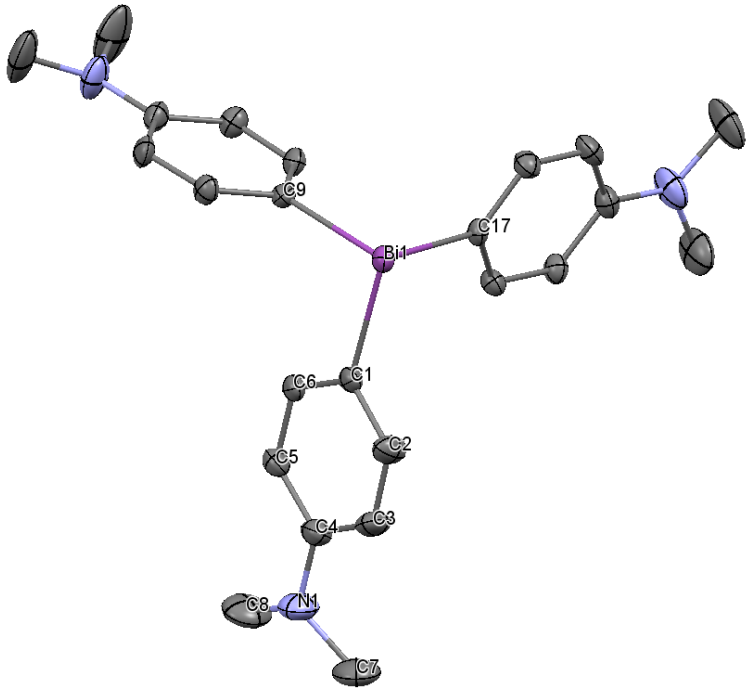

Fig. 3.4: Crystal structure of compound **13**. Hydrogen atoms are omitted for clarity. Selected distances [Å] and angles [°]: Bi1-C1 2.240(5), Bi1-C9 2.230(5), Bi1-C17 2.247(3), C4-N1 1.384(9), N1-C7 1.46(1), C1-Bi1-C9 93.4(2), C1-Bi1-C17 94.7(2), C9-Bi1-C17 95.6(2), Bi1-C1-C2 121.1(4), Bi1-C1-C6 121.9(3), C3-C4-N1 122.2(6), C5-C4-N1 120.7(5), C4-N1-C7 118.2(6), C7-N1-C8 116.8(7).

Further an additional para-substituted compound, namely the tris-*p*-anisyl-bismtuhine **14** was synthesized. The Grignard route is applied and the crude product obtained. Hot Celite® 512 filtration and subsequent recrystallization steps in EtOH respectively toluene afforded compound **14** in 77 % yield as colourless crystals.
Crystallographic experiments (see Fig. 3.5) confirmed the expected pyramidal structure and indicates similar C-Bi bond lengths (in average 2.252 Å) and C-Bi-C bong angles (93.8 ° in average) as described for other para-substituted compounds.

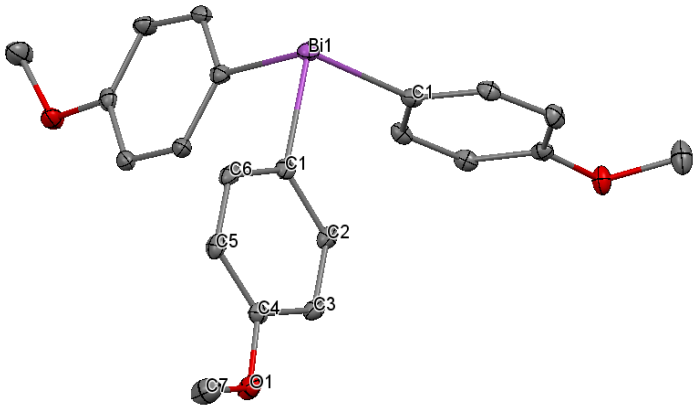

Fig. 3.5: Crystal structure of compound **14**. Hydrogen atoms are omitted for clarity. Selected distances [Å] and angles [°]: Bi1-C1 2.252, Bi-C8 2.252, Bi1-C15 2.252, O1-C4 1.377(4), O1-C7 1.439(4), C1-Bi1-C8 93.8, Bi1-C1-C2 121.6, Bi1-C1-C6 120.5, C4-O1-C7 116.6(3), O1-C4-C3 114.7(3), O1-C4-C5 124.7(3)

Crude compound **15** was obtained following General Procedure A as described in the experimental section. Recrystallisation in toluene afforded bismuth compound **15** as colourless crystals in yields up to 88 %.

Structural analysis of the compound again verified the pyramidal structure of the trivalent bismuth species. C-Bi bond lengths (2.247, 2.250, 2.251 Å) and C-Bi-C bond angles (95.8, 93.1, 93.4 °) resemble to those of the *p*-phenyl-compounds, however the Bi-C bonds are slightly elongated.

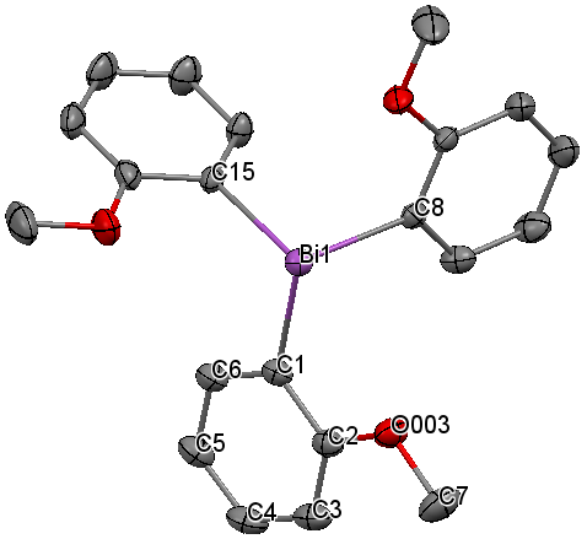

Fig. 3.6: Crystal structure of compound **15**. Hydrogen atoms are omitted for clarity. Selected distances [Å] and angles [°]: Bi1-C1 2.247(3), Bi1-C8 2.250(2), Bi1-C15 2.251(4), C1-C2 1.403(5), C2-O3 1.371(4), O3-C7 1.424(5), C1-Bi1-C8 95.8(1), C1-Bi-C15 93.1(1), C8-Bi1-C15 93.4(1), Bi1-C1-C2 117.3(2), C1-C2-O3 114.7(3), C2-O3-C7 117.6(3).

Noteworthly is the potential ability of the ortho-functionalized ligands for additional intramolecular interactions. This secondary intramolecular Bi $\cdots$ O interactions, ranging from 3.059 - 3.140 Å, are observed between all three pendant oxygen groups and the bismuth center - a similar phenomenon was reported by Breunig and Althaus.[68]

The more sterically demanding [2,6−$(MeO)_2C_6H_3]_3$Bi complex (**16**) was synthesized just as it's homologues.[51] The bromobenzene educt **8** was reacted with metallic magnesium, kept at reflux for 6 h and the reaction mixture was added to a suspension of $BiCl_3$ and stirred for several hours. After washing with H_2O, the organic phases were dried and concentrated to obtain the crude product. Filtration of the product solution (in toluene) over hot Celite® 512 and recrystallization from THF/toluene afforded compound **16** as colourless needles in 89 % yield (see 5.3.1.1).
Compared to compound **15** the Bi-C bond lengths are noticeably longer, ranging from 2.257 to 2.277 Å. The C-Bi-C bond angles (97.6, 99.5, 99.6 °) however, indicate significant distortion from the original pyramidal symmetry of Ar_3Bi compounds. The six oxygen atoms exhibit intramolecular through-space interactions to the Bi-center - the Bi $\cdots$ O distances are found in a range of 3.008 to 3.422,Å (being inside the van der Waals border of 3.9 Å).[68]

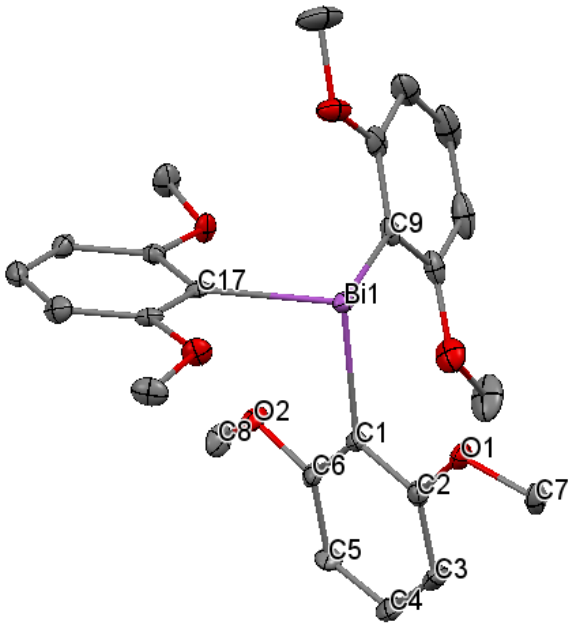

Fig. 3.7: Crystal structure of compound **16**. Hydrogen atoms are omitted for clarity. Selected distances [Å] and angles [°]: Bi1-C1 2.257(4), Bi1-C9 2.277(4), Bi1-C17 2.262(5), C1-C2 1.394(6), C2-O1 1.382(8), O1-C7 1.415(5), C1-C6 1.392(9), C6-O2 1.362(5), O2-C8 1.430(8), C1-Bi1-C9 99.6(2), C1-Bi-C17 97.6(2), C9-Bi1-C17 99.5(2), Bi1-C1-C2 117.9(3), Bi1-C1-C6 123.6(3), C1-C2-O1 115.6(4), C2-O1-C7 117.9(4), C1-C6-O2 114.8(4), C6-O2-C8 118.7(4).

Following table shortly sums up discussed crystallographic characteristics of selected triarylbismuth compounds.

Table 3.1: XRD results of selected Ar_3Bi compounds. Bi-C bond lengths in [Å] , C-Bi-C angles and $\sum \measuredangle$ C-Bi-C in [°].

Nr.	**compound**	**space group**	**Bi-C** [Å]	**C-Bi-C** [°]	$\sum \measuredangle$ **C-Bi-C** [°]
9	$BiPh_3$	C 2/c	2.237 - 2.273	92.7 - 94.7	281.7
10	$BiPh_3$(d)	C 2/c	2.252 - 2.271	94.2 - 94.4	280.9
11	$BiTol_3$	P-1	2.243 - 2.610	93.5 - 95.0	282.8
13	$Bi(p-NMePh_2)_3$	P-1	2.230 - 2.247	93.4 - 95.6	283.7
14	$Bi(p-OMePh)_3$	R-3	2.252	93.8	281.4
15	$Bi(o-OMePh)_3$	P 2_1/c	2.247 - 2.251	93.1 - 95.8	282.3
16	$Bi(di-o-OMePh)_3$	P 2_1/c	2.257 - 2.277	97.6 - 99.6	296.7

All para-substituted arybismuth compounds are found to have Bi-C bond length and C-Bi-C bong angles in similar ranges. Also for compound **15** similar values are calculated, however intramolecular $Bi\cdots O$ interactions between the oxygen atoms and the bismuth center are observed. The biggest deviation from the "normal" pyramidal geometry of Ar_3Bi compounds was ascertained for the sterically demanding $[2,6-(OMe)_2C_6H_3]_3Bi$ compound. Here the bismuth center interacts intramolecularly with the six oxygen atoms of the methoxygroups. The effects of this interactions are indicated by longer Bi-C bonds and especially the increasingly C-Bi-C bond angles.

3.1.1.1 NQR-Results

The synthesized arylbismuth compounds **9** - **16** were investigated by our project partners at the TU Graz (Institute of Biomedical Engineering) and at the University of Olsztyn (Faculty of Mathematics and Computer Science) regarding their NQR transition frequencies. Since a MRT operates at 3 T ($\sim$ 120 MHz) a suitable bismuth compound should exhibit a transition frequencies close to this predefined.
The NQR spectroscopic characteristics of the bismuth compounds were determined at 310 K, at room temperature and at 77 K (liquid nitrogen). Following table lists measured transition frequencies at 310 K.

Table 3.3: Measured NQR-trasition frequencies (TF) in MHz, the derived NQR parameter Q_{cc} [MHz] and the asymmetry factor η (at 310 K) of synthesized Bi-compounds

Nr.	**compound**	**TF 1** [MHz]	**TF 2** [MHz]	**TF 3** [MHz]	**TF 4** [MHz]	$\mathbf{Q_{cc}}$ [MHz]	η [1]
9	$BiPh_3$	29.67	55.14	83.42	111.32	668.3	0.087
10	$BiPh_3$(d)	29.68	55.20	83.49	111.40	668.8	0.086
12	$Bi(p-FPh)_3$	28.60	54.51	82.11	109.54	657.5	0.071
13	$Bi(p-NMePh_2)_3$	28.34	54.94	82.52	110.06	660.6	0.058
14	$Bi(p-OMePh)_3$	28.49	56.88	85.34	113.77	682.5	0.000
15	$Bi(o-OMePh)_3$	29.82	59.64	89.47	119.27	715.2	0.000
16	$Bi(di-o-OMePh)_3$	30.14	54.40	82.45	110.06	660.9	0.105

As indicated in Table 3.3, the influence of the different ligands can clearly be seen. As described in previous sections, the EFG is effected in two ways: at first, by influencing the electron density distribution through the whole molecule with change of substituents on the corresponding ligand - what considerably effects the quadrupolar coupling strength - if the changes influence the closer surrounding of the Bi nucleus. Second, by introducing different substituents, the crystal structure may change, what in turn has a significant impact onto the EFG, as reported in detail by Gösweiner.[22]

According to these results, the most promising TF's, in respect to the predefined frequency of the MRT, were obtained for compound **15** with a 9/2 - 7/2 transition frequency at 119.27 MHz. Thus, further synthetic concepts are constructed, beside other influencing factors, using $Bi(o-OMePh)_3$ as well as the reference substance $BiPh_3$, as chemical backbone for further modifications on the molecule.

3.1.2 Synthesis of unsymmetrical triarylbismuth compounds

3.1.2.1 Synthesis of bismuth styrene compounds

As described in Fig. 3.8, bromo-4-vinylbenzene was reacted with Mg in THF at -20 °C to avoid starting the polymerization reaction. After completed conversion with ((*o*−OMePh)$_2$BiCl) **19** at 0 °C, the reaction mixture was diluted and washed with HCl (6 %) and $NaHCO_3$. The organic layers were dried over Na_2SO_4, filtrated and concentrated. TLC and NMR measurements indicated, the formation of a product mixture of Bi(*o*−OMePh)$_3$ **15**, compound **22**, distyrylbismuth and tristyrylbismuth compounds. To separate the desired product **22**, the obtained crude product mixture was purified by column chromatography. By silica gel purification the trialrybismuth species **15** could be separated for the most part, however separation of the three styrene species turned out to be difficult. Modifying the reaction conditions, like reversing addition of the reactants or varying the reation times, does not seem to have an influence on the product distribution.

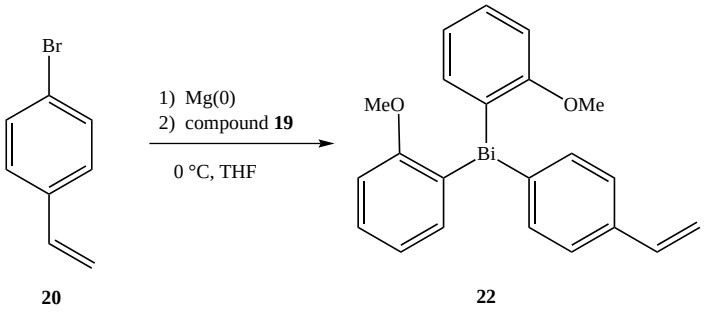

Fig. 3.8: Synthesis of bis(2-methoxyphenyl)(4-vinylphenyl)bismuthine **22** via Grignard route

These described redistribution problems arising during synthesis of asymmetrical bismuth compounds were reported by Freedman and Doak,[18] Ignatious,[28], [29] Tamber[76] and co-workers. Beside redistribution reactions, Wurtz-coupling and incidentally formed polymerization products; further are reaction of the monomer **22** with the Grignard-compound of **20** may occur, forming the distyrylbismuth compound and compound **15**, as reported by Ignatious and co-workers.[28]

Due to this obstacles, an additional synthetic route using *n*-BuLi was chosen, as depicted in Fig. 3.9. The exact reaction details are presented in section 5.3.1.2 on page 76.

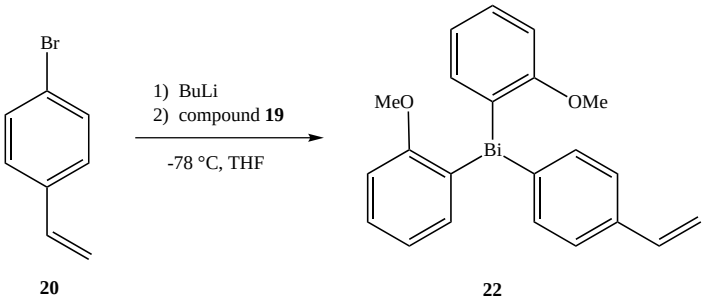

Fig. 3.9: Synthesis of bis(2-methoxyphenyl)(4-vinylphenyl)bismuthine **22** using *n*-BuLi

Unfortunately, no significant changes in product distribution compared to Grignard route were observed. However, through elimination of Wurtz-reaction an increase in yield was noticed. Column chromatography of the product mixture enabled separation of **22** including just small amounts of the distyrylbismuth compound. After recrystallization from toluene, slightly yellowish crystals were obtained and compound **22** can be used for polymerization reactions as described in section 3.7 on page 60.

For compound **22**, carbon-bismuth bond lengths ranging from 2.255 to 2.26 Å and C-Bi-C bond angles at approximately 93.45 ° were determined by XRD analysis. The calculated/measured C-C bond lengths of the vinyl group at the para-position of the phenyl ring are C18-C21 1.49 Å and C21-C22 1.293 Å for the double bond. Further, the C18-C21-C22 bond angle is 126.8 ° (see Fig. 3.10).

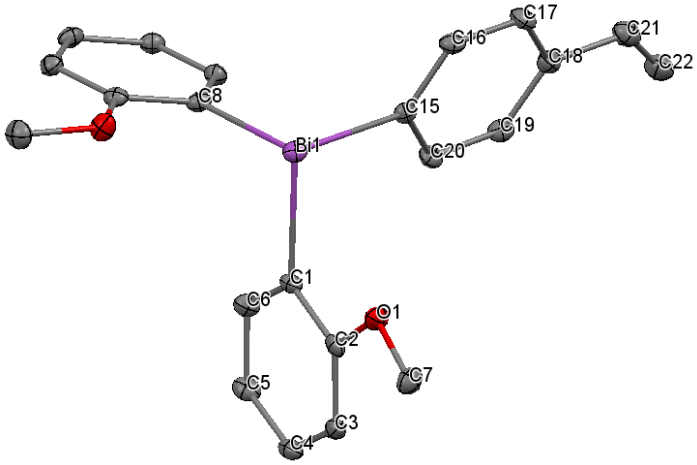

Fig. 3.10: Crystal structure of compound **22**. Hydrogen atoms are omitted for clarity. Selected distances [Å] and angles [°]: Bi1-C1 2.258(5), Bi1-C8 2.255(4), Bi1-C15 2.261(4), C2-O1 1.385(6), O1-C7 1.419(6), C18-C21 1.490(7), C21-C22 1.293(8), C1-Bi1-C8 93.5(2), C1-Bi1-C15 93.4(2), C8-Bi1-C15 93.4(2), Bi1-C1-C2 117.0(3), Bi1-C1-C6 123.6(3), Bi1-C15-C16 117.6(3), Bi1-C15-C20 123.7(3), C1-C2-O1 115.4(4), C2-O1-C7 117.6(4), C19-C18-C21 123.4(4), C17-C18-C21 119.3(4), C22-C21-C18 126.8(5).

3.1.2.2 Synthesis of bismuth alkyne compounds

As described in chapter 2, one of the key objectives is the coupling of a bismuth species to a monosaccharide. Similar to synthesis of compound **22**, the bismuth-alkyne species **25** and **26** are prepared.
In a first approach, compounds **25** and **26** are synthesized as displayed in Fig. 3.11. Synthesis applying Grignard concept (see section 5.3.1.2) and subsequent splitting of the protective $SiMe_3$ group, again yielded a product mixture of the respective Ar_3Bi, the di- and trialkynebismuth species and the desired monoalkynebismuth compound. After purification on silica gel, compounds **25** and **26** are obtained as slightly yellowish syrup in a yield of about 50 %.

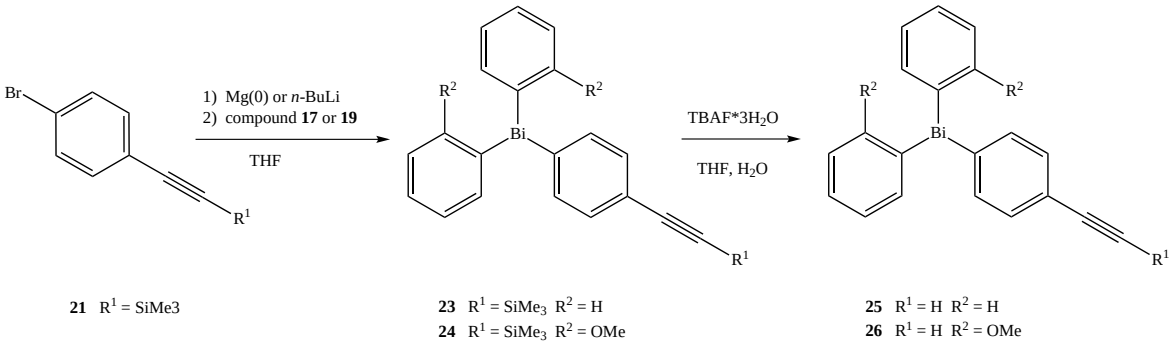

Fig. 3.11: Synthesis of (4-ethynylphenyl)diphenylbismuthine **25** and (4-ethynylphenyl)bis(2-methoxyphenyl)bismuthine **26**.

A change of reaction conditions - like solvent, time, temperature or reversed addition of precursors - does not have a significant effect on product distribution, similar as discussed for compound **22**. Lobez and Swager [37] reported about the synthesis of compound **25** using *n*-BuLi. They described the synthesis by lithiation of **21** with *n*-BuLi at -78 °C, addition of the Ar_2BiCl species and subsequent splitting of the protective group using TBAF · $3H_2O$. After purification on silica gel, they obtained bismuth species **25** as a colourless oil in a yield of 59 %.[37]

In section 5.3.1.2, the synthesis using *n*-BuLi for compounds **25** and **26** is described as Method B. Compared to the products obtained applying Grignard route, the *n*-BuLi approach yields after column chromatography and recrystallization compounds **25** and **26** in higher yields (about 55 %). Significant differences in synthesis of the two different bismuth species were not observed.

The attempts using monochloride species **17** and **19** for described synthetic strategies, always yielded discussed product mixtures due to redistribution reactions (see

3.2). Therefore compound **28** - the trialkyne - was additionally prepared to avoid redistribution reactions to the greates possible extent:

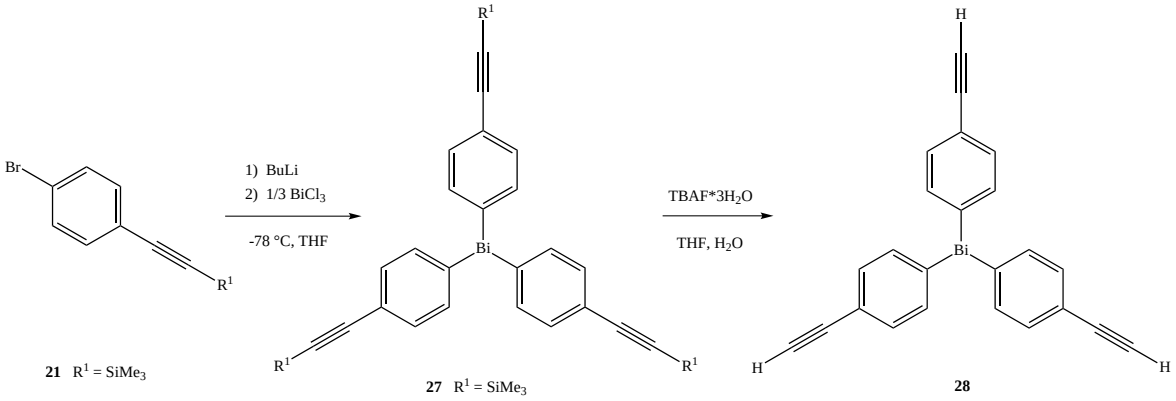

Fig. 3.12: Synthesis of compound **28**.

Alike compounds **25** and **26**, synthesis of compound **28** just differs in use of $BiCl_3$ instead of a monochloride species, as described in detail on page 73. After column chromatography and recrystallization from toluene **28** was obtained in a yield of 55 % as colourless crystals.

XRD analysis of compound **28** determined Bi-C bond lengths ranging from 2.258 to 2.261 Å and C-Bi-C bond angles between 91.31 and 95.63 °. The para-standing alkyne group shows a C4-C7-C8 bond angle of 178.1 ° and bond lengths of 1.439 Å (C4-C7) and 1.188 Å(C7-C8) for the triple bond.

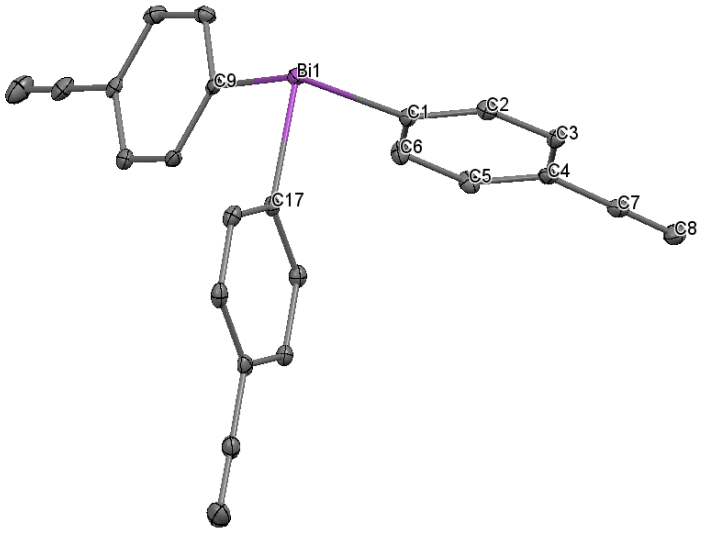

Fig. 3.13: Crystal structure of compound **28**. Hydrogen atoms are omitted for clarity. Selected distances [Å] and angles [°]: Bi1-C1 2.258(2), Bi1-C9 2.261(3), Bi1-C17 2.260(2), C3-C4 1.399(3), C4-C7 1.439(3), C7-C8 1.188(4), C1-Bi1-C9 91.31(8), C1-Bi1-C17 92.47(8), C9-Bi1-C17 95.63(9), Bi1-C1-C2 119.7(2), Bi1-C1-C6 122.2(2), C3-C4-C7 121.9(2), C5-C4-C7 119.6(2), C4-C7-C8 178.1(3)

3.2 Diarylbismuth chlorides - Ar_2BiCl

Chloro-diphenyl-bismuthine **17**, chloro-bis(*p*-methylphenyl)-bismuthine **18** and chloro-bis(2-methoxyphenyl)-bismuthine **19** are synthesized starting from the respective Ar_3Bi as described in section 5.3.2 on page 78.

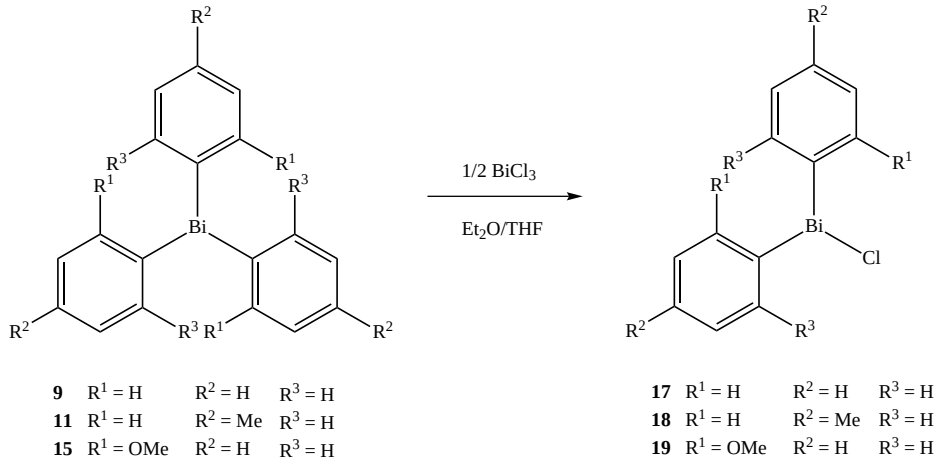

9 R^1 = H R^2 = H R^3 = H
11 R^1 = H R^2 = Me R^3 = H
15 R^1 = OMe R^2 = H R^3 = H

17 R^1 = H R^2 = H R^3 = H
18 R^1 = H R^2 = Me R^3 = H
19 R^1 = OMe R^2 = H R^3 = H

Fig. 3.14: Synthesis of Ar_2BiCl compounds **17** - **19**

In classic organometallic chemistry of main group elements, e.g. tin, various mixed chlorides can be obtained by redistribution reactions (in organotin chemistry Kocheshkov comproportionation) of the aryl-derivatives with the corresponding chloride species. In the case of bismuth, these are obtained by redistribution reaction of 2 equiv. of the corresponding Ar_3Bi with 1 equiv. of $BiCl_3$. The reactions are proceeding in good yields (88 - 90 %), though considerable amounts of $ArBiCl_2$ are formed. Separation of the two chloride species turns out to be difficult, however a change of solvent from Et_2O to THF relieved the separation procedure and reduced the portion of the yellow $ArBiCl_2$ to < 5 %. However, redistribution reactions will occure with time and $ArBiCl_2$, Ar_2BiCl, $BiCl_3$ as well as Ar_3Bi species will form.[9], [18], [20], [50]

XRD measurements reveals the arrangement of ligands of compound **19**. Bi-C bond lengths of 2.23 - 2.24 Å and a Bi-Cl bond length of 2.509 Å were determined. The C-Bi-C and C-Bi-Cl bond angles rage from 92.1 to 92.2 °.

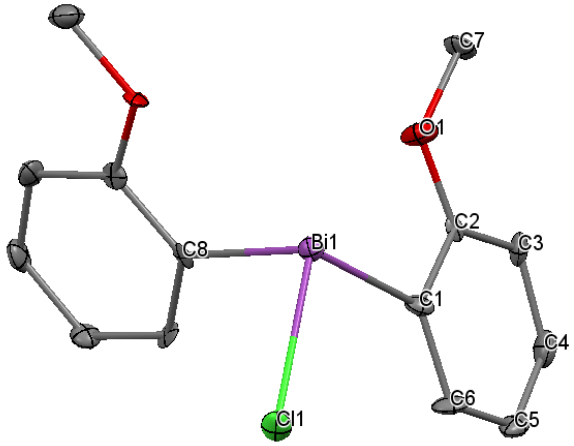

Fig. 3.15: Crystal structure of compound **19**. Hydrogen atoms are omitted for clarity. Selected distances [Å] and angles [°]: Bi1-C1 2.23(1), Bi1-C8 2.24(1), Bi1-Cl1 2.509(4), C2-O1 1.37(2), O1-C7 1.44(2), C1-Bi1-C8 91.2(5), C1-Bi1-Cl1 91.7(3), C8-Bi1-Cl1 92.2(4), Bi1-C1-C2 112.8(9), Bi1-C1-C6 128(1), C1-C2-O1 114(1), C3-C2-O1 125(1), C2-O1-C7 119(1).

Fig. 3.16 displays the packing of bismuth-chloride **17** on the left and compound **19** on the right side. In Ph_2BiCl the chloride atoms are forming Bi-Cl-Bi bridges - leading to the polymeric form of a four-fold bismuth species. In exact, the structure consists of zigzag chains with bent chloro-bridges (Bi-Cl-Bi 100.6 °)[68] between the bismuth atoms. Regarding the Bi-Cl bong lengths, any large differences were not found, within the chain they are almost equal. Breunig and Althaus observed similar bridging phenomena involved in different organobismuth halide compounds.[68]
Compound **19** however, exists as the normal pyramidal mononuclear compound with a Bi-Bi distance of 8.569 Å.

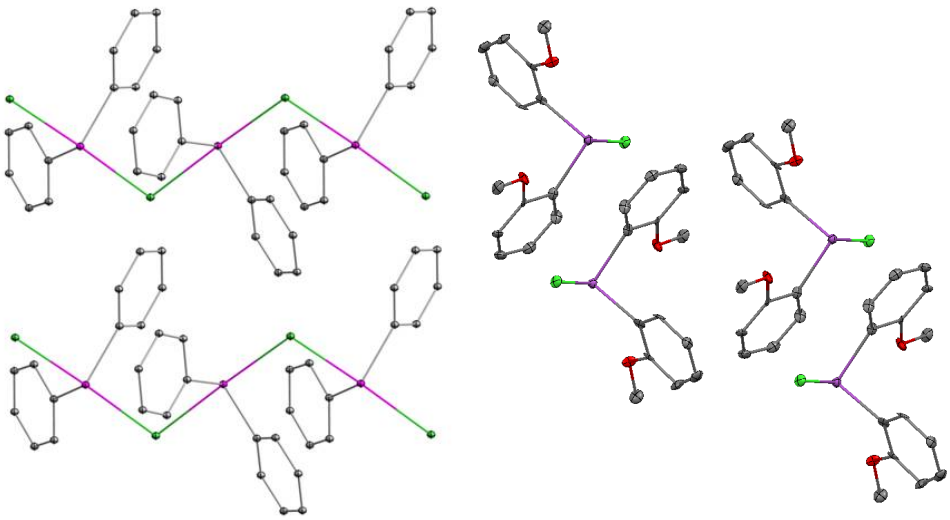

Fig. 3.16: Packing of compounds **17** (left) and **19** (right).

On the basis of these facts, the very poor solubility in almost all organic solvents of compound **17** can be explained. The solubility is influenced in a quite negative manner, due to the four-fold coordination of the bismuth atom and the associated formation of Bi-Cl chains. The solubility of species **19** either can not be described as very good however, it dissolves in most organic solvents. Beside the NQR results, it was decided at this point to perform further synthesis focusing on ortho-anisyl bismuth derivatives. Additionally subsequent chemistry is constructed on bismuth monochloride derivatives. The formation of $ArBiR_2$ species, beside the desired Ar_2BiR compounds can not be excluded, due to discussed redistribution reactions.

3.3 Diarylbismuth amides - Ar_2BiNR_2

Similar to the synthesis of bismuth amides reported in literature,[23], [57], [75], [74] the Ar_2BiNR_2 focusing on this thesis were prepared. As briefly shown in Fig. 3.17, to a -78 °C cooled solution of the corresponding lithium amide (**29** - **32**) in THF, a cooled suspension of freshly prepared compound **19** was added dropwise. After stirring the reaction mixture for approximately 4 h, the solvent was changed to *n*-pentane and the resulting mixture was filtrated, as described in section 5.3.3 on page 80. The solvent was removed and products **33** - **36** stored at - 30 °C in an inert atmosphere. Compounds **33** - **36** were obtained in acceptable yields ranging from 57 to 78 %.

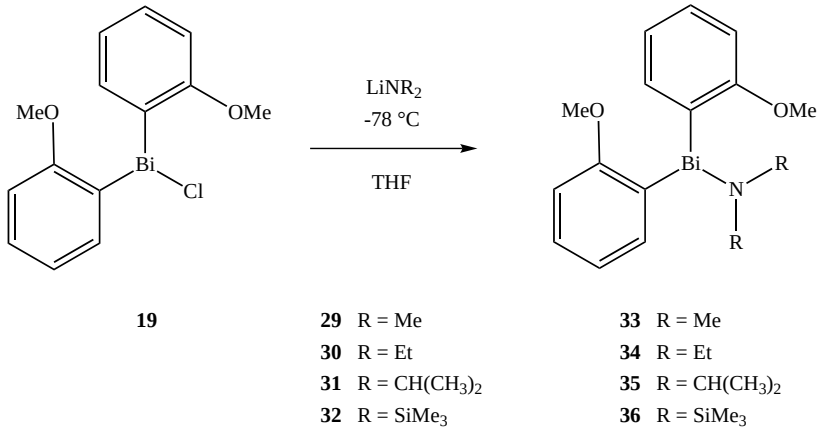

19

29 R = Me
30 R = Et
31 R = $CH(CH_3)_2$
32 R = $SiMe_3$

33 R = Me
34 R = Et
35 R = $CH(CH_3)_2$
36 R = $SiMe_3$

Fig. 3.17: Synthesis of diarylbismuth amides Ar_2BiNR_2 **33** - **36**

As described in chapter 2, the different bismuth amides were synthesized in order to investigate their reaction potential with compounds bearing different functional groups.

Compound **33** seems to be the most reactive or more precisely, the least stable compound of these four, therefore no XRD measurements could be performed. Compound **34** behaves similarly, which in addition could only be obtained in maximum 57 % yield. The stability of compounds **35** and **36** stored under the same cooled inert conditions was found to be acceptable and they were used for described coupling reactions discussed in section 3.4.

Compound **34** was synthesized following General Procedure D and was afforded after filtration over Celite® 512 as orange oil in 57 % yield. Structural investigations determined Bi-C bond lengths of 2.252 - 2.258 Å, a Bi-N bond length of 2.198 Å and C-Bi-C respectively C-Bi-N bond angles between 90.8 and 93.1 °.

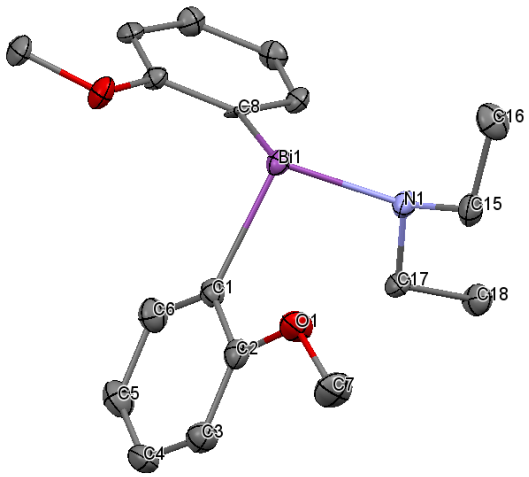

Fig. 3.18: Crystal structure of compound **34**. Hydrogen atoms are omitted for clarity. Selected distances [Å] and angles [°]: Bi1-C1 2.258(6), Bi1-C8 2.252(5), Bi1-N1 2.198(5), C2-O1 1.379(6), O1-C7 1.431(7), N1-C15 1.463(6), C15-C16 1.523(9), N1-C17 1.469(8), C17-C18 1.530(8), C1-Bi1-C8 96.1(2), C1-Bi1-N1 96.0(2), N1-Bi1-C8 90.8(2), Bi1-C1-C2 1155.4(4), Bi1-C1-C6 125.6(4), C1-C2-O1 115.3(5), C3-C2-O1 123.7(5), C2-O1-C7 118.1(5), Bi1-N1-C15 112.0(3), Bi1-N1-C17 112.4(3), N1-C15-C16 112.9(5), N1-C17-C18 112.4(5), C15-N1-C17 112.1(4).

Synthesis of compound **35** resembles to that of **34** and afforded the bismuth *iso*-propylamide as a yellowish powder in yields up to 78 %.

X-ray analysis results Bi-C and Bi-N bond lengths in range of 2.171 Å (Bi-N) to 2.244 - 2.259 Å. C-Bi-C bond has an angle of 94.5 ° and the C-Bi-N bonds show angles between 91.7 - 99.3 °. The notably enlarged angle between one C-Bi-N bond can be explained by the nitrogen's substituents orientating in the most sterically favoured position.

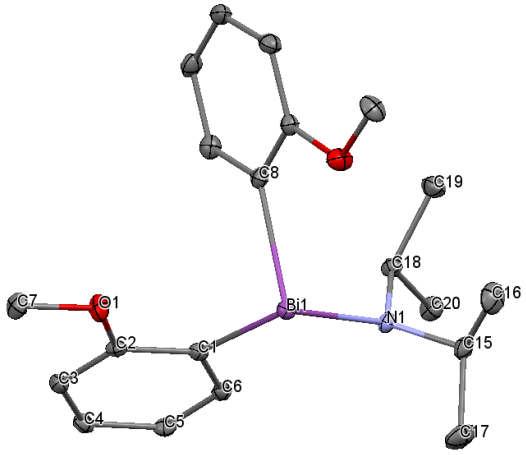

Fig. 3.19: Crystal structure of compound **35**. Hydrogen atoms are omitted for clarity. Selected distances [Å] and angles [°]: Bi1-C1 2.244(3), Bi1-C8 2.259(3), Bi1-N1 2.171(2), C2-O1 1.375(3), O1-C7 1.424(3), N1-C15 1.472(4), C15-C16 1.533(5), C15-C17 1.525(4), N1-C18 1.475(4), C18-C19 1.529(4), C18-C20 1.535(4), C1-Bi1-C8 94.5(1), N1-Bi1-C1 91.7(1), N1-Bi1-C8 99.3(1), Bi1-C1-C2 117.8(2), Bi1-C1-C6 123.1(2), C1-C2-O1 114.3(2), C3-C2-O1 124.3(3), C2-O1-C7 117.3(2), Bi1-N1-C15 115.9(2), Bi1-N1-C18 118.7(2), N1-C15-C16 115.9(3), N1-C15-C17 110.2(3), C16-C15-C17 109.5(3) N1-C18-C19 115.3(2), N1-C18-C20 111.3(2), C19-C18-C20 109.6(3), C15-N1-C18 116.3(2)

Compound **36** was synthesized by reaction of lithium bis(trimethylsilyl)amide with **19**. The product was obtained as a colourless powder in a yield of 78 %.
The Bi-C bonds have lengths between 2.240 - 2.250 Å, the Bi-N bond however, is somewhat smaller having 2.215 Å. A bond angle of 95.7 ° for the C-Bi-C bond and angles of 94.7 ° respectively 101.5 ° for C-Bi-N bonds were measured. This difference of 6.8 ° between the two C-Bi-N bond angles, can be explained by the orientation of the TMS-groups on the nitrogen ligand.

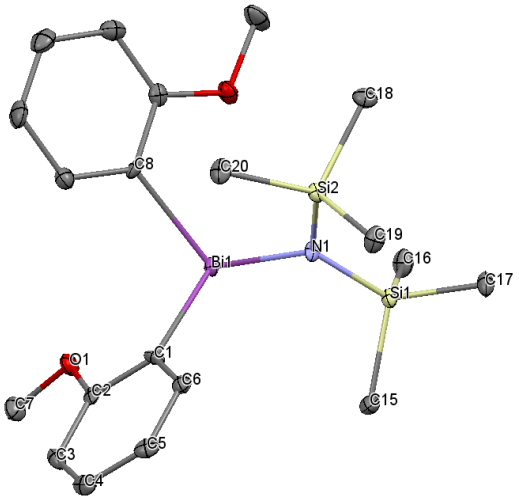

Fig. 3.20: Crystal structure of compound **36**. Hydrogen atoms are omitted for clarity. Selected distances [Å] and angles [°]: Bi1-C1 2.250(4), Bi1-C8 2.240(4), Bi1-N1 2.215(3), C2-O1 1.387(5), O1-C7 1.442(5), N1-Si1 1.733(4), Si1-C15 1.970(5), Si1-C16 1.878(5), Si1-C17 1.873(4), N1-Si2 1.725(4), Si2-C18 1.869(5), Si2-C19 1.882(4), Si2-C20 1.875(5), Ci-Bi1-C8 95.7(2), N1-Bi1-C1 94.7(1), N1-Bi1-C8 101.5(1), Bi1-C1-C2 115.1(3), Bi1-C1-C6 125.9(3), C1-C2-O1 114.1(4), C3-C2-O1 124.4(), C2-O1-C7 117.5(3), Bi1-N1-Si1 106.5(2), N1-Si1-C15 109.4(2), N1-Si1-C16 111.0(2), N1-Si1-C17 115.0(2), C15-Si1-C16 108.1(2), C15-Si1-C17 107.5(2), C16-Si1-C17 105.6(2), Bi1-N1-Si2 126.6(2), Si1-N1-Si2 126.4(2)

Table 3.5: XRD results of selected Bi(o−OMePh)$_2$NR$_2$ compounds. Bi-C and Bi-N bond lengths in [Å], C-Bi-C and C-Bi-N angles in [°].

Nr.	**compound**	**Bi-C** [Å]	**Bi-N** [Å]	**C-Bi-C** [°]	**C-Bi-N** [°]
34	Bi(o−OMePh)$_2$NEt$_2$	2.257	2.199	96.2	91.0/95.8
35	Bi(o−OMePh)$_2$NiPr$_2$	2.252	2.171	94.5	91.7/99.3
36	Bi(o−OMePh)$_2$N(TMS)$_2$	2.245	2.215	95.7	94.7/101.5

Table 3.5 illustrates the affect of different ligands on the C-Bi and Bi-N bond lengths as well as on the C-Bi-C and C-Bi-N bond angles, respectively.
With increasing bulkiness of the nitrogen's substituents, the Bi-C bonds shorten from averaged 2.257 Å to 2.245 Å, while the Bi-N bond lengths are weaving between 2.171 Å and 2.215 Å. The C-Bi-C bond angles diminish with sterically more demanding ligands from 96.2 ° to 95.7 °, whereas as expected the C-Bi-N bonding angles are expanding from 91 ° - 94.7 ° respectively 95.8 ° - 101.5 °. A concept developed to couple a bismuth compound to a saccharide is performed using described bismuth amides. Since compounds **36** and **35** seem to be the more stable ones and are obtained as solids these are the compounds of choice, in exact compound **35**, performing follow up chemistry.

3.4 Diarylbismuth-Monosaccharides: Amide Coupling

Suzuki et al.[74] describe reactions of Ar_2BiNR_2 with alcohols and thiols, Kou and co-workers[33] reported about the synthesis of bismuth aryloxides from $Bi(NR_2)_3$ and the appropriate phenol.

Compounds **40** - **42** were synthesized in a similar manner, as described in detail in section 5.3.4 on page 83. Fig. 3.21 displays the reaction path starting from compound **35**, dissolved in THF where the corresponding adamantyl-species was added. After completed conversion, the solvent was removed and replaced by *n*-pentane or toluene. Compounds **40** - **42** were obtained as colourless to slightly yellowish oils and were stored at -30 °C in the glove box.

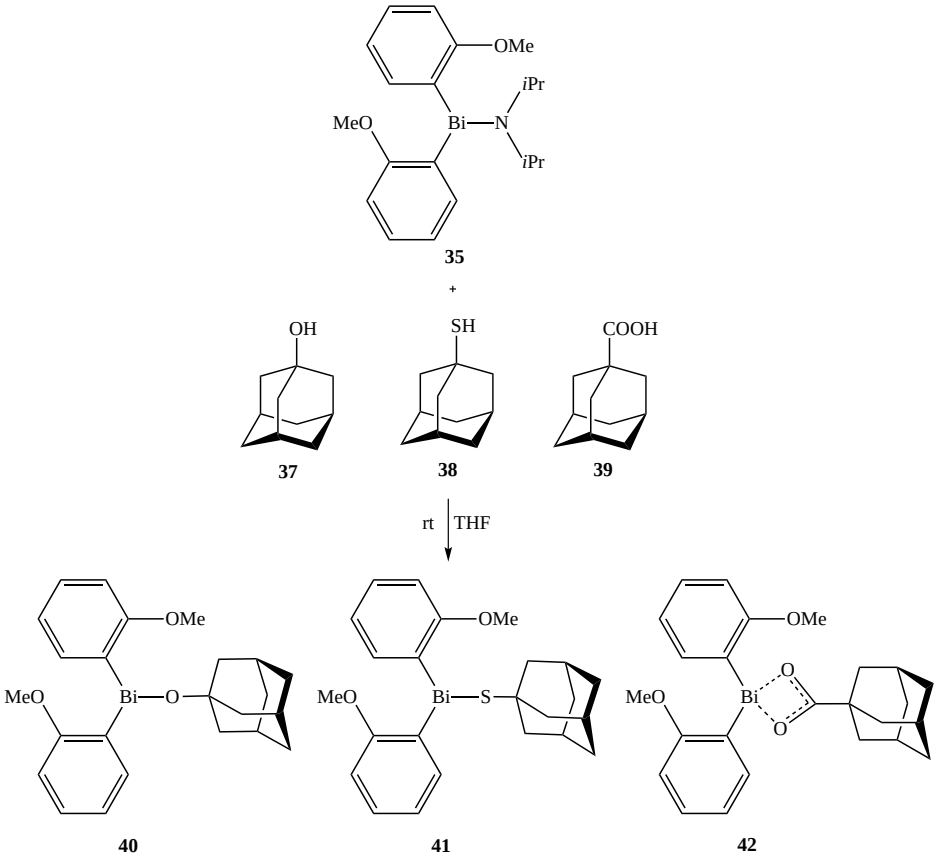

Fig. 3.21: Synthesis of compounds **40** - **42**

One of the key factors in synthesis of bismuth aryloxides is how to favour the product formation.[33] By selecting an appropriate solvent, the reactions can be driven towards completion and in the best case the products precipitate.

For compounds **40** to **42** yields are ranging from 62 % to 84 %.

Compound **40**, synthesized as described in section 5.3.4, for example hardly crystal-

lizes, after all a change to a solvent-mixture of toluene/pentan/THF yielded crystals at -30 °C. However, X-ray measurements showed, that beside **40** also a $Ar_2Bi-O-BiAr_2$ species has formed. The most interesting bond lengths and angles for this compound are probably those between Bi1, the oxygen and Bi2. The Bi1-O bond has a length of 2.097 Å and for Bi2-O a length of 2.07 Å was found. A Bi1-O-Bi2 bond angle of 127.5 ° was determined.
The formation of this oxygen bridged di-bismuthine compound is most likely related to presence of O_2, respectively moisture - probably from not completely dry precursors or solvents.

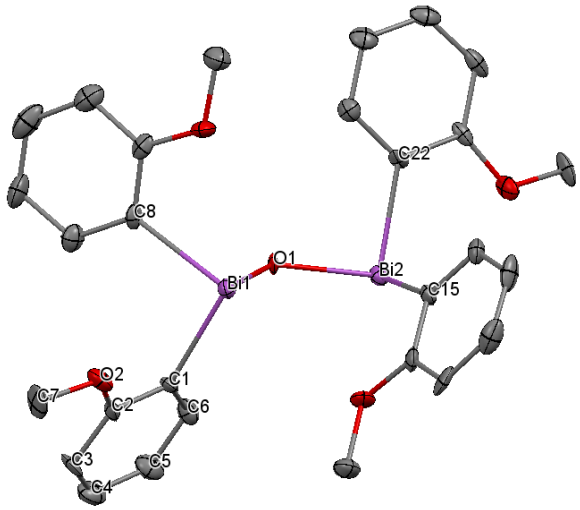

Fig. 3.22: Crystal structure of $Ar_2BiOBiAr_2$. Hydrogen atoms are omitted for clarity. Selected distances [Å] and angles [°]: Bi1-C1 2.27(2), Bi1-C8 2.25(2), Bi1-O1 2.097(9), O1-Bi2 2.07(1), Bi2-C15 2.25(2), Bi2-C22 2.23(2), C1-C2 1.37(2), C2-O2 1.38(2), O2-C7 1.45(3), O1-Bi2 2.07(1), C1-Bi1-C8 91.8(6), C1-Bi1-O1 92.1(5), C8-Bi1-O1 90.9(5), Bi1-C1-C2 118(1), C1-C2-O2 115(1), C3-C2-O2 124(2), C2-O2-C7 118(1), Bi1-O1-Bi2 127.5(5), O1-Bi2-C15 100.2(5), O1-Bi2-C22 92.4(5), C15-Bi2-C22 92.1(6)

However, compound **40** was obtained as a colourless oil in 62 % yield. Crystallographic data describe the structure as a P-1 space group with average Bi-C bond lengths of 2.242 Å and a Bi-O bond of 2.106 Å length (see Fig. 3.23). The C-Bi-C bond angle lies at 90.4 °, whereas one C-Bi-O angle is quite small (86.1 °) compared to the second (93.1 °). This differences in bonding angles can be explained by the orientation of the bulky adamantyl ligand, same as for the bismuth amide compounds described previously.

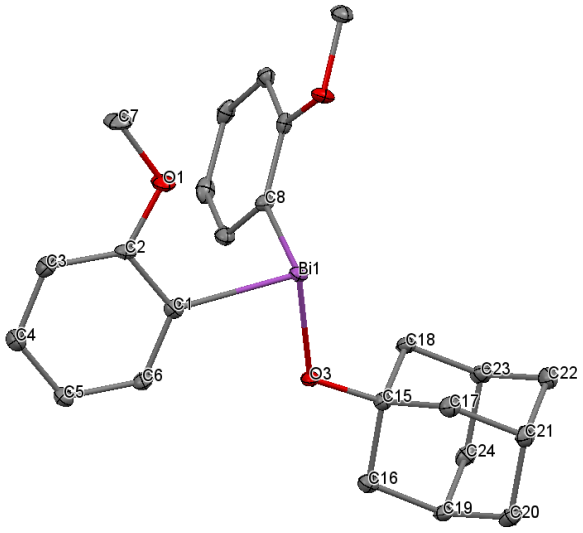

Fig. 3.23: Crystal structure of compound **40**. Hydrogen atoms are omitted for clarity. Selected distances [Å] and angles [°]: Bi1-C1 2.23(3), Bi1-C8 2.253(3), Bi1-O3 2.106(3), C1-C2 1.398(5), C2-O2 1.372(6), O2-C7 1.429(5), O3-C15 1.424(4), C15-C16 1.526(5), C15-C17 1.532(5), C15-C18 1.529(3), C16-C19 1.538(6), C17-C21 1.541(6), C18-C23 1.540(6), C19-C20 1.530(5), C19-C24 1.532(4), C20-C21 1.524(5), C21-C22 1.534(4), C22-C23 1.533(5), C23-C24 1.530(5), C1-Bi1-C8 90.4(1), C1-Bi1-O3 86.1(1), C8-Bi1-O3 93.1(1), Bi1-C1-C2 115.3(2), C1-C2-O1 114.3(3), C3-C2-O1 124.8(3), C2-O1-C7 117.8(3), Bi1-O3-C15 122.0(2), O3-C15-C16 106.0(2), O3-C15-C17 112.9(3), O3-C15-C18 111.5(2), C16-C15-C17 108.7(3), C16-C15-C18 108.5(3), C17-C15-C18 109.1(3).

Synthesis of compound **41** was accomplished by reaction of **35** with 1-adamantanethiol (**38**) at 45 °C. The crude product was obtained as slightly yellowish oil. Crystals were obtained by recrystallization in a mixture of *n*-pentane/THF and storing at - 30 °C under inert conditions. Formed crystals were characterized by XRD measurement.
In Fig. 3.24 the crystal structure is depicted. The Bi-S bond length is markedly longer (2.541 Å) compared to the Bi-C bond lengths (2.250 Å, 2.251 Å). C-Bi-S bond angles (93.5 ° and 89.3 °) and an angle of 92.0 ° for C-Bi-C bond strongly resemble to those of compound **40** and can be explained in a similar way.

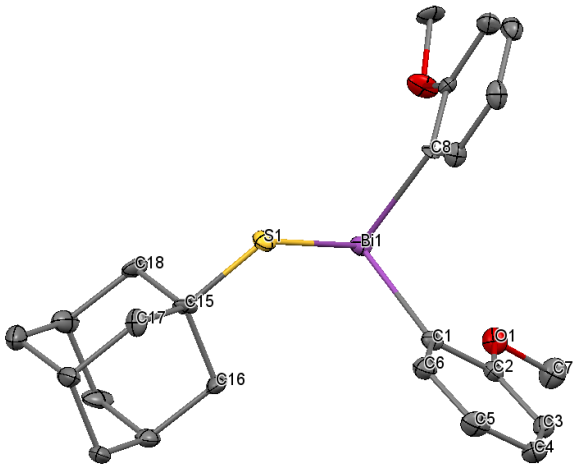

Fig. 3.24: Crystal structure of compound **41**. Hydrogen atoms are omitted for clarity. Selected distances [Å] and angles [°]: Bi1-C1 2.25(9), Bi1-C8 2.251(8), Bi1-S1 2.541(2), C1-C2 1.42(1), C2-O2 1.37(1), O2-C7 1.44(1), S1-C15 1.854(9), C15-C16 1.54(1), C15-C17 1.55(1), C15-C18 1.51(1), C1-Bi1-C8 92.0(3), C1-Bi1-S1 93.5(2), C8-Bi1-S1 89.3(2), Bi1-C1-C2 115.9(6), C1-C2-O1 112.9(8), C3-C2-O1 126.2(8), C2-O1-C7 115.7(7), Bi1-S1-C15 102.9(3), S13-C15-C16 112.5(6), S1-C15-C17 104.3(6), S1-C15-C18 111.7(6), C16-C15-C17 108.8(7), C16-C15-C18 109.7(7), C17-C15-C18 109.7(7).

Compound **42** was synthesized following General Procedure D. Therefore compound **35** and **39** were stirred a 45 ° for 48 h. After several purification steps the desired compound was obtained as colourless syrup in yields up to 69 %. Recrystallization of the product in *n*-pentane at - 30°C almost immediately yielded crystals appropriate to perform crystallographic measurements.

X-ray analysis has clarified the bonding situation of compound **42** as presented in Fig. 3.25. The Bi-C bond lengths as well as the C-Bi-C bond angle do not strongly differ from the other bismuth-adamantyl compounds (2.222 Å, 2.243 Å respectively 95 °). However, regarding this adamantyl ligand the bonding situation has remarkably changed. The crystal structure confirms the formation of a four fold coordinated Bi-atom. Each oxygen atom of the carboxylic acid ligand forms a bond to the bismuth atom, showing bond lengths of 2.193 Å (Bi-O3) and 2.902 Å(Bi-O4). Bond angles of 92 ° (C1-Bi-O3) and 82.2 ° (C1-Bi-O4) respectively 87 ° (C8-Bi-O3) and 135.8 ° (C8-Bi-O4) describe the distortion of the regular pyramidal structure. As presumed, these results confirm the delocalized behavior of the double bond of the COO(H) group. Associated to the bismuth the oxygen's electron forms an additive bond of a 2.902 Å (Bi-O4) length, describing a dative character.

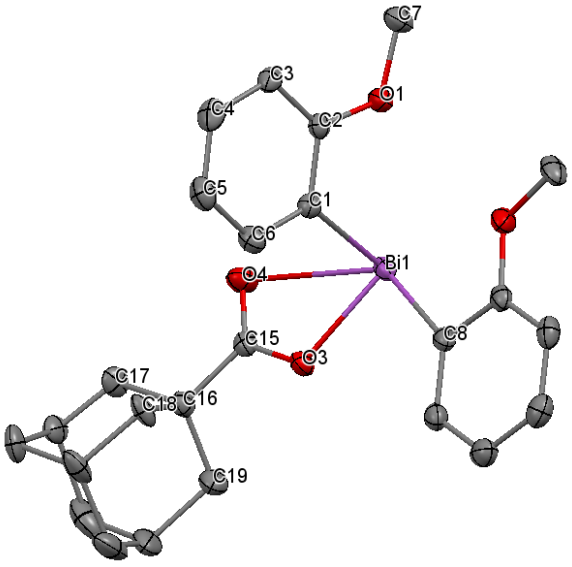

Fig. 3.25: Crystal structure of compound **42**. Hydrogen atoms are omitted for clarity. Selected distances [Å] and angles [°]: Bi1-C1 2.222(5), Bi1-C8 2.243(5), Bi1-O3 2.193(3), Bi1-O4 2.902(3), C1-C2 1.389(4), C2-O2 1.380(5), O2-C7 1.427(4), O3-C15 1.304(4), O4-C15 1.233(5) C15-C16 1.511(5), C16-C17 1.58(2), C16-C18 1.65(2), C16-C19 1.47(2), C1-Bi1-C8 95.0(1), C1-Bi1-O4 82.2(1), C1-Bi1-O3 92(1), C8-Bi1-O3 87.0(1), C8-Bi1-O4 135.8(1), O3-Bi1-O4 49.31(9), Bi1-C1-C2 115.5(3), C1-C2-O1 114.0(3), C3-C2-O1 124.9(3), C2-O1-C7 116.6(3), Bi1-O3-C15 110.3(2), Bi-O4-C15 78.3(2), O3-C15-O4 122.1(4), O3-C15-C16 114.9(3), O4-C15-C16 123.0(4), C15-C16-C17 115(1), C15-C16-C18 104.5(7), C15-C16-C19 113.2(8).

Following reaction scheme describes the first attempt of coupling a bismuth compound to a monosaccharide. To a solution of compound **35** in Et_2O, **43** was added in small portions as described in section 5.3.4. After completed conversion and purification compound **44** was afforded as colourless oil.

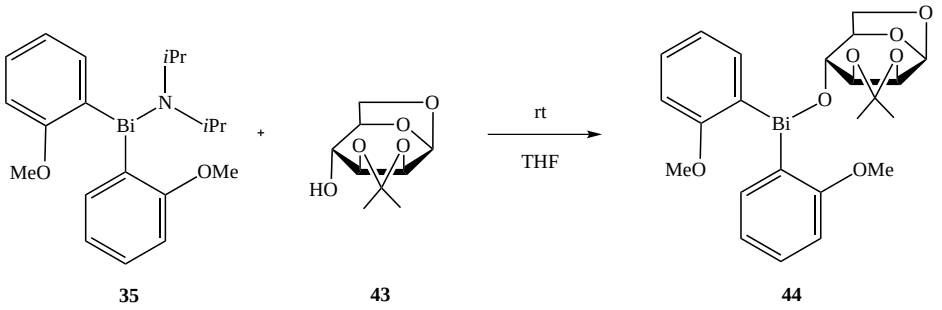

Fig. 3.26: Planned synthesis of compound **44**

NMR spectroscopic investigations of the compound confirmed the formation of the corresponding bismuth containing carbohydrate. However, the NMR data (see appendix Fig. 6.7 - Fig. 6.12) show that two species have formed. Comparing H-1

peaks (in the partial view spectra), it can clearly be seen that with time one species depletes and more of the second is formed. According to the formation of two compounds, a possible explanation might be the evolution of different conformers. A further explanation would be the decomposition of the compound when exposed to air, respectively moisture, similar to the bismuth amides/adamantyl. In this case the carbohydrate species might be split and a bismuth species, similar as described for synthesis of compound **40**, could be formed.

As compound **44** assumes to hydrolyse when exposed to moisture, this coupling concept using a bismuth amide and a monosaccharide species - forming a direct bond between bismuth and saccharide - is most likely not applicable for the design of NQR-CA's.

3.5 Diarylbismuth-Monosaccharides: Huisgen 1,3-dipolar cycloaddition

Connecting a bismuth compound with a monosaccharide, making use of Huisgen 1,3-dipolar cycloaddition is rarely reported in literature. Lobez and Swager reported about the synthesis of the Bi-precursor, as discussed in section 3.1.2, and reactions with different polymers.[37]

To perform the "click reaction" two bismuth precursors, compound **25** and **26** were synthesized. Further five different sugar azides, involving protected and free xylose (**45**), glucose (**47**, **48**) and galactose (**46**, **49**) derivatives were used.

Fig. 3.27 schematically describes the synthesis of compound **50**. Therefore the bismuth compound (**25**) dissolved in THF was added dropwise to a solution of the "xylosefuranose-azide" (**45**). CuI and Et_3N were added to catalyse the reaction and stirring at 30 °C for about 24 h completed the cycloaddition. After purification on silica gel the desired compound was afforded as a colourless solid in yields at about 50 %.

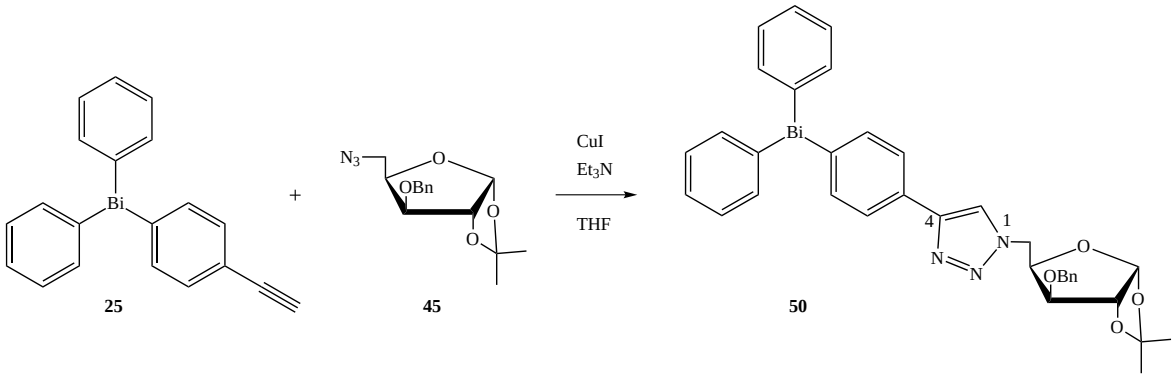

Fig. 3.27: Synthesis of compound **50** applying click-chemistry approach.

Compound **50** was characterized using IR- and NMR spectroscopy. The IR data in Fig. 3.28 clearly confirm that a conversion of the reactants took place. The alkyne vibration of the bismuth precursor (blue) at about 3280 cm^{-1} is no longer apparent in the product spectrum (green). This is also true for the azide vibration at about 2100 cm^{-1} of the saccharide species (pink). In the product spectrum neither the alkyne nor the azide vibration is present what confirms the conversion of the educts and consequently the formation of the bismuth-saccharide.

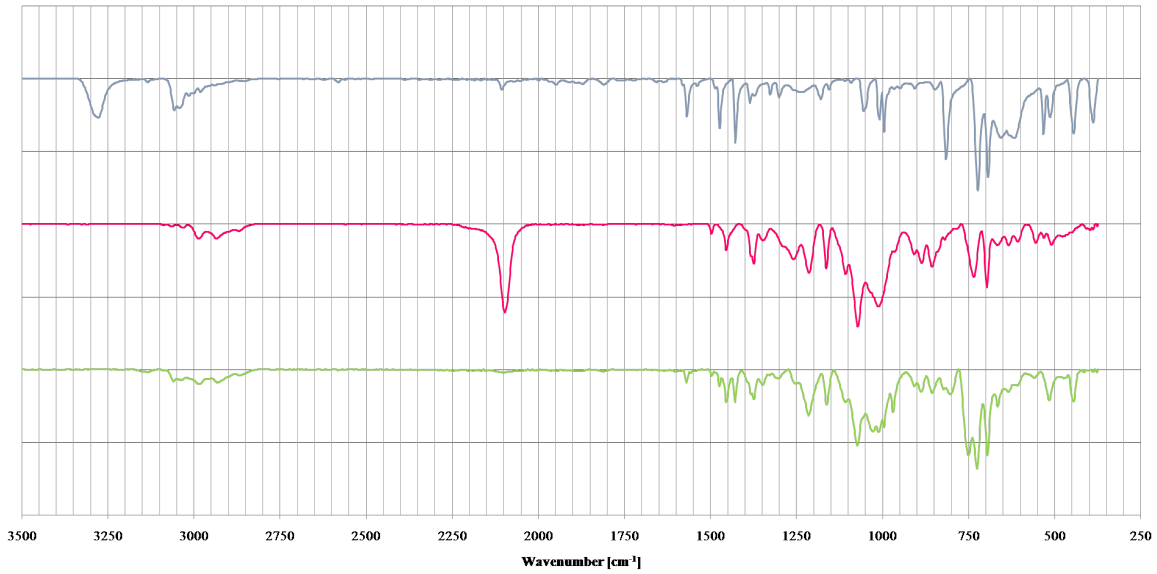

Fig. 3.28: IR data of bismuth compound **25** (blue), the xylose derivative **45** (pink) and product **50** (green).

^{1}H NMR and ^{13}C NMR data could further display the formation of a bismuth-saccharide species.

Synthesis of compound **51** was performed in a similar manner, as depicted in Fig. 3.29. The N_3-modified galactose derivative was reacted with the bismuth compound **25** in presence of CuI and Et_3N to yield the triazole-compound **51** as a colourless solid.

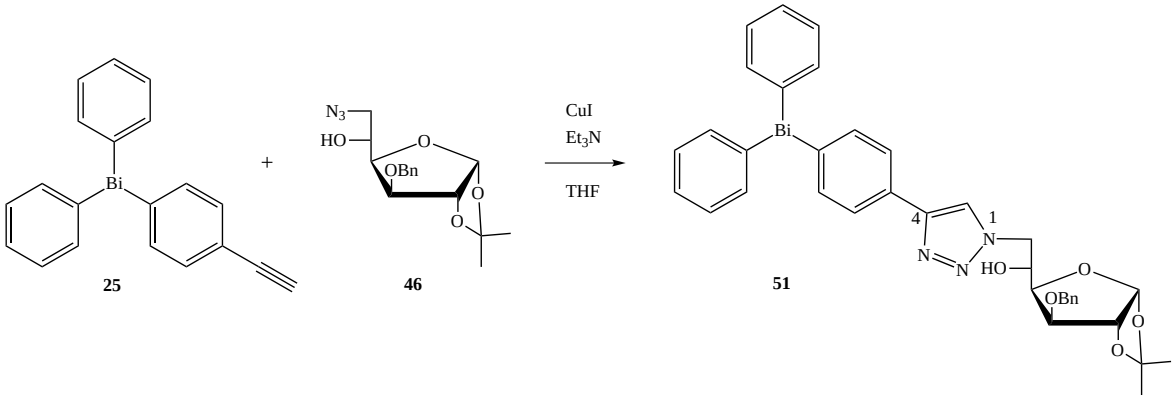

Fig. 3.29: Synthesis of compound **51** via click-chemistry reaction

A control of product formation for compound **51** was in addition performed using IR spectroscopy. Fig. 3.30 shows the bismuth compound **25** in blue with the characteristic vibration of the alkyne species at 3280 cm^{-1}. The vibration of the azide functionality of the monosaccharide species **46** (pink)is observed at 2100 cm^{-1}. The product spectrum

(green) clearly indicates a product formation, since the alkyne- and azide vibrations are no longer apparent.

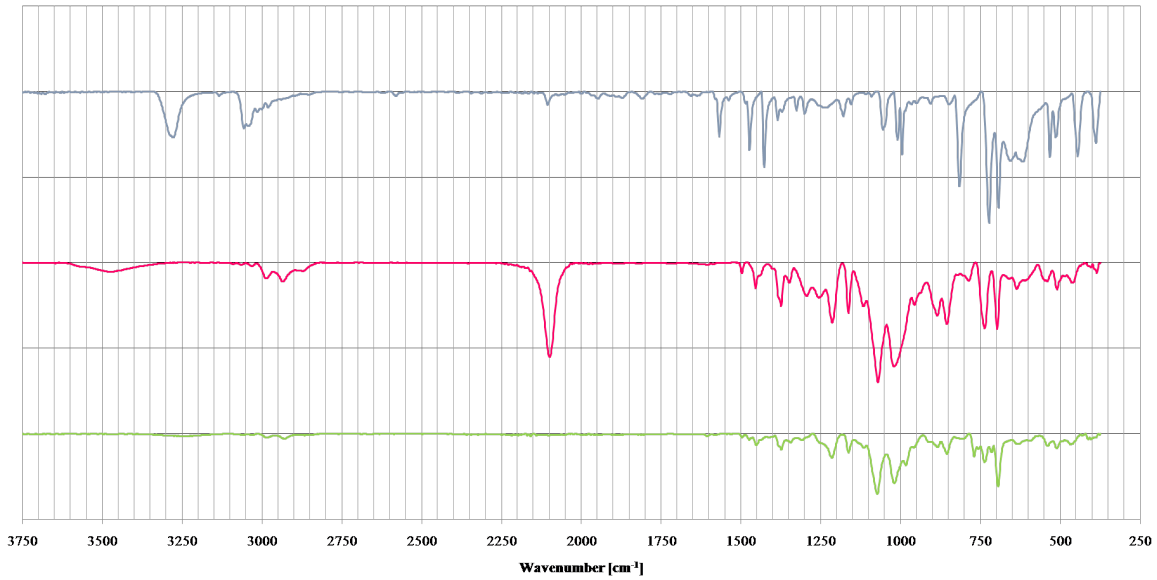

Fig. 3.30: IR data of bismuth compound **25** (blue), the galactose derivative **46** (pink) and product **51** (green)

Collected NMR data (see Fig. 6.13 and Fig. 6.14 in the appendix) further signify the formation of the bismuth containing carbohydrate.

The third "click-product", compound **52** (see Fig. 3.31) was obtained by reaction of bismuth compound **26** with the azide functionalized Bn-protected glucose derivative **47** as described in detain in section 5.3.5. Compound **52** was obtained after purification on silica gel as a colourless solid.

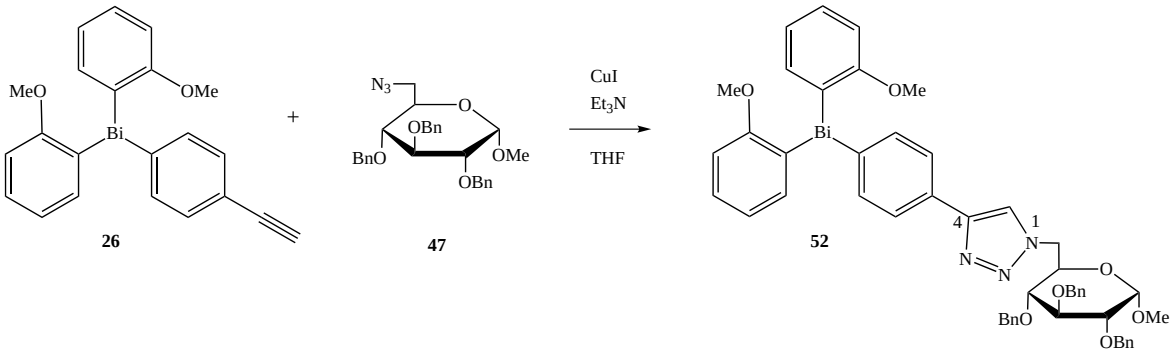

Fig. 3.31: Synthesis of compound **52** via click-chemistry reaction

Conversion of educts and product formation of compound **52** were controlled by IR

and NMR spectroscopy. ^{1}H NMR and ^{13}C NMR spectra express the formation of the bismuth containing carbohydrate (see Fig. 6.15 and Fig. 6.16 in the appendix).

For compounds **53** and **54** the bismuth precursor was varied. Fig. 3.32 again displays the synthetic strategy using a glucose derivative as the azide carrier. Triazole-compound **53** was afforded after column chromatography as a pale yellowish syrup, quite similar to compound **54**.

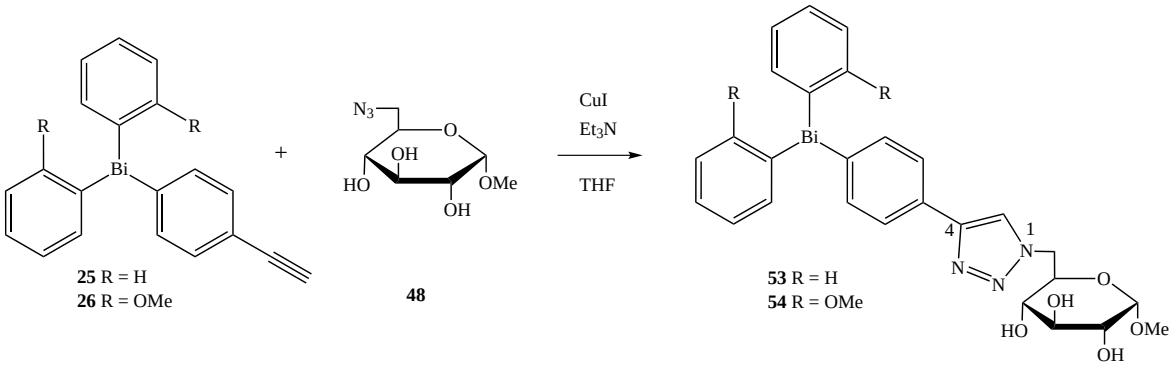

Fig. 3.32: Synthesis of compounds **53 - 54** via Huisgen cycloaddition.

For both compounds (**53-54**) IR spectra were recorded. In Fig. 3.33 those of compound **54** and its precursors are shown. The green spectrum (product spectrum) illustrates the formation of the product species, as the characteristic vibration for the azide ($\sim 2100\,\mathrm{cm^{-1}}$) and the alkyne ($\sim 3280\,\mathrm{cm^{-1}}$) species are not observable.

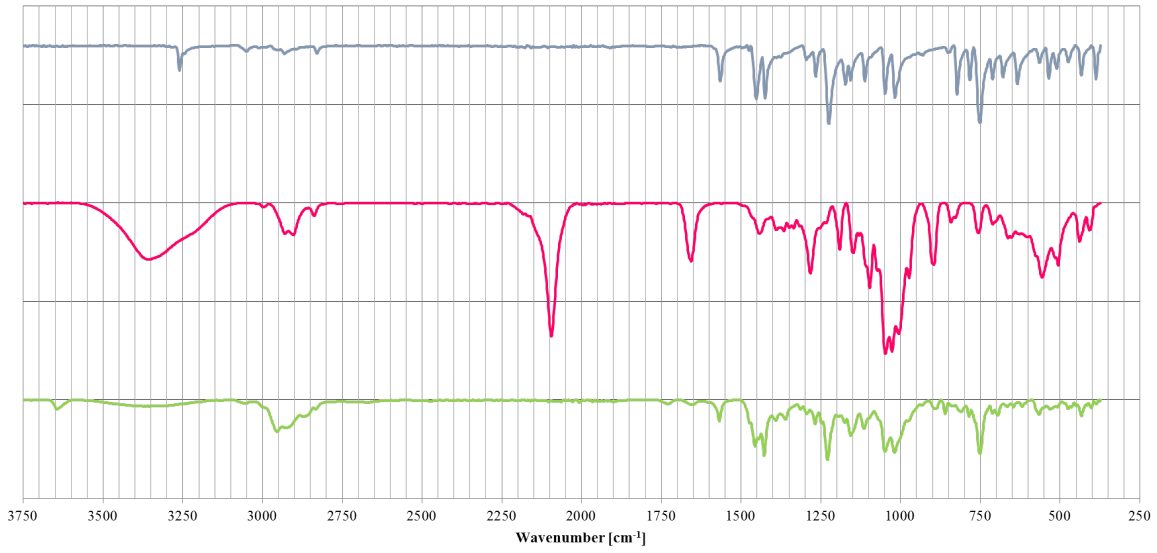

Fig. 3.33: IR data of bismuth compound **26** (blue), the glucose derivative **48** (pink) and product **54** (green)

The NMR spectra of the two species confirm the formation of a bismuth containing

monosaccharide as arising peaks in the aromatic (8.5 - 7.0 ppm) as well as in the corresponding saccharide area express. Fig. 6.17 - Fig. 6.20 in the appendix should provide further detailed information.

Another cycloaddition was performed by reaction of bismuth compound **26** with N_3-modified isopropyl-protected galactose derivative **49** in presence of CuI and Et_3N. Purification on silica gel provided a colourless solid in 56 % yield.

NMR-characterization of the obtained product indicated the formation of a triazole-compound however, excluding the aromatic bismuth species as shown in Fig. 3.34. Beside the desired click product (**55a**), reaction of compounds **26** and **49** yield a cross-coupling product. For both species **55a** and **55b** however, the cycloaddition works, since a triazole cycle is obtained. Nevertheless, this click reaction illustrates, that bismuth compounds can act as cross-coupling reagents and explain the formation of compound **55b**.

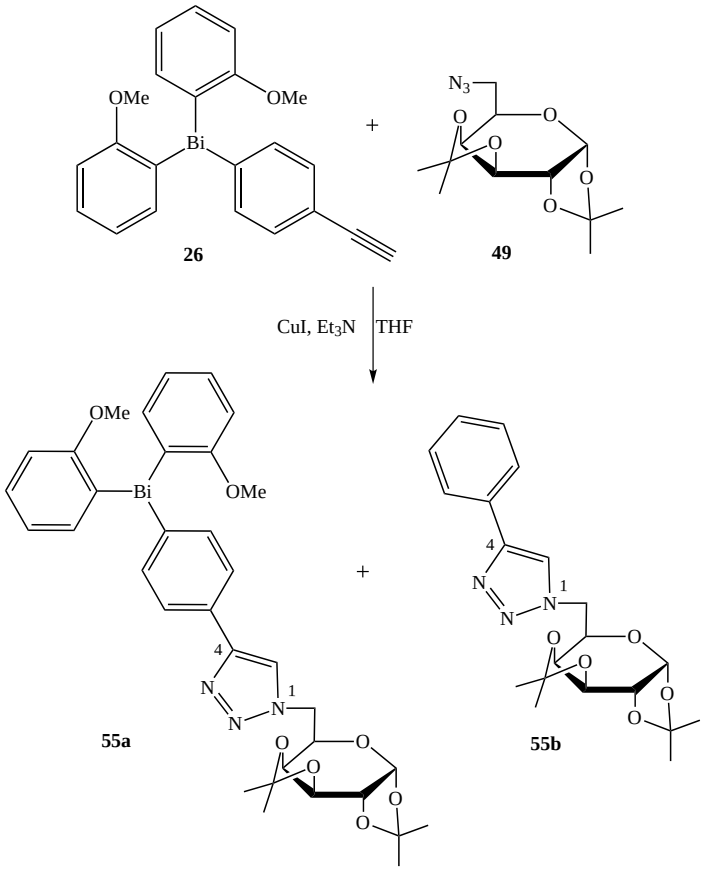

Fig. 3.34: Reaction scheme synthesis of compound **55** and cross-coupling product applying click-chemistry concept.

Literature[12], [13], [25], [55] reports about use of organobismuth reagents in palladium/copper-catalysed cross-coupling reactions as donors for different aryl-groups. This cross-coupling reactions are frequently used in organic synthesis, since triarylbismuthines can be synthesized in an inexpensive way, are easy to handle (air and moisture stable) as well as are obtained in high yields and purities and further, bismuth salts are considered as non-toxic.[25] Codon et al. presented a catalytic cycle of mentioned cross-coupling reactions in their work.[12], [55]

This result may also explain the product distribution, i.e. the yields, of desired bismuth-carbohydrates introduced above. Nevertheless, for all reactions a conversion of the azide- and the alkyne-compound and therefore a formation of a triazole species could be observed. The desired bismuth-monosaccharide compounds however, are formed in unsatisfying yields. Further, both the 1,4- and 1,5-isomer of compounds **50** to **55** may be formed.
Unfortunately, due to the not satisfying yields concerning our applications, the very promising Huisgen 1,3-dipolar cycloaddition, will not be used for further synthetic strategies.

3.6 Diarylbismuth-Monosaccharides: Ether Coupling

Following the synthetic concept introduced in section 2.3, robust and stable bismuth-monosaccharide compounds can be obtained. Therefore, the bismuth compounds **15** and **19** were synthesized as described in section 3.1.1 and 3.2. The alcohol **56** was silylated using tert-butyldimethylsilyl chloride in presence of imidazole in CH_2Cl_2 to provide protected compound **57** in excellent yields.
After treatment of compound **19** with *n*-BuLi in THF at -78 ° under an inert atmosphere, dropwise addition of compound **57** afforded the protected bismuth derivative **58**. An equal linkage employing a Grignard reaction was not as successful as the described one, particularly due to poor yields caused by purification problems. Compound **59** was provided by cleavage of silylether **58** with TBAF $\cdot 3H_2O$ in THF. Subsequently treatment with Hünig's base and triphenylphosphonium dibromide provided the desired compound **60** in excellent yields.

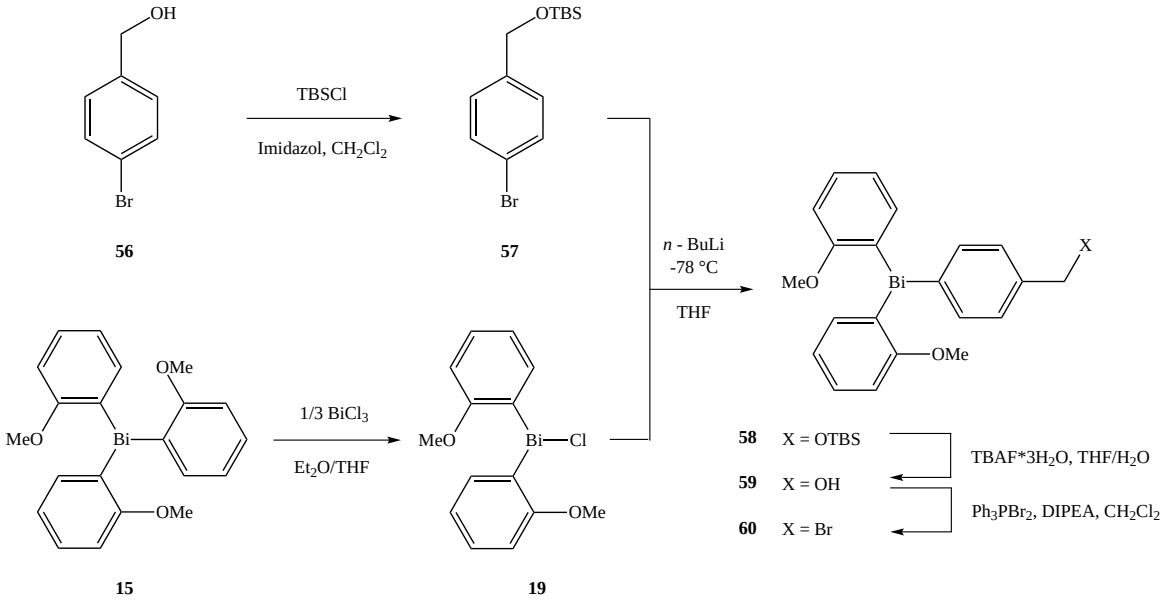

Fig. 3.35: Overview of the synthesis strategy.

Recrystallization of compound **59** afforded the Bi-benzyl-alcohol as colourless crystals whereby a crystal structure determination by XRD become possible (see Fig. 3.36). The Bi-C bonds reveal lengths ranging from 2.195 to 2.248 Å and C-Bi-C bond angles between 92.9 and 96.2 ° were determined. The C18-C21 bond (1.51 Å) and C21-O3 bond lengths (1.46 Å) as well as the C18-C21-O3 bond angle of 113 ° perfectly describe the alcohol group in para-position.

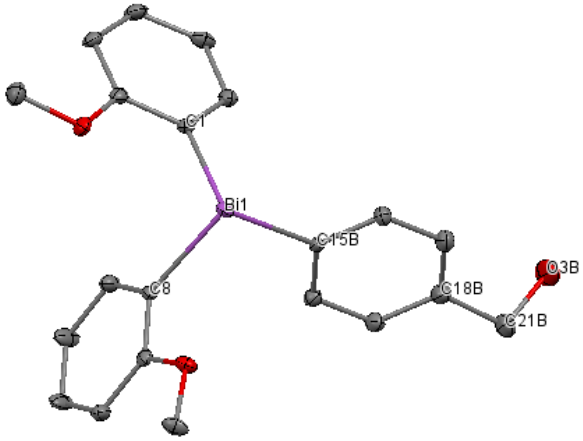

Fig. 3.36: Crystal structure of compound **59**. Hydrogen atoms are omitted for clarity. Selected distances [Å] and angles [C]: Bi1-C1 2.248(7), Bi1-C8 2.248(7), Bi1-C15 2.195(7), C1-C2 1.40(1), C2-O2 1.375(9), O2-C7 1.43(1), C15-C16 1.39(1), C16-C17 1.39(1), C17-C18 1.39(2), C18-C21 1.51(2), C21-O3 1.46(1), C1-Bi1-C8 92.9(2), C1-Bi1-C15 96.2(3), C8-Bi1-C15 95.2(3), Bi1-C1-C2 117.1(5), C1-C2-O1 114.7(6), C3-C2-O1 123.6(7), C2-O1-C7 117.3(6), Bi1-C15-C16 116.3(5), C17-C18-C21 124(1), C19-C18-C21 116(1), C18-C21-O3 113(1).

The Bi-C bond lengths (2.250 - 2.254 Å) and C-Bi-C bond angles (92.2 - 95.9 °) of compound **60** resemble to those of the alcoholic bismuth species. The C-C-Br bond angle (110.8 °) however is a little smaller whereas the C-Br bond length is elongated (1.962 Å).

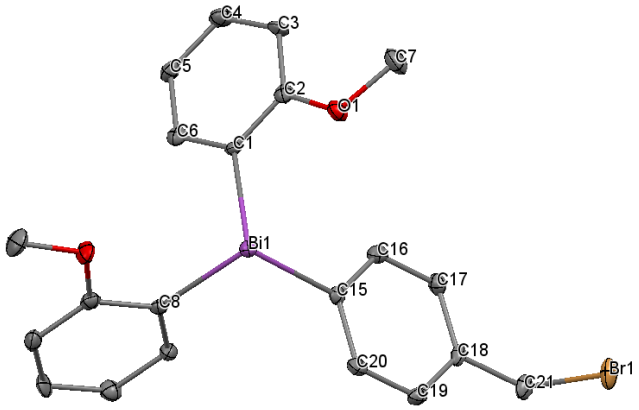

Fig. 3.37: Crystal structure of compound **60**. Hydrogen atoms are omitted for clarity. Selected distances [Å] and angles [°]: Bi1-C1 2.252(5), Bi1-C8 2.254(5), Bi1-C15 2.250(5), C1-C2 1.399(7), C2-O2 1.376(6), O2-C7 1.424(6), C15-C16 1.395(7), C16-C17 1.392(7), C17-C18 1.396(7), C18-C21 1.500(7), C21-Br1 1.962(6), C1-Bi1-C8 92.9(2), C1-Bi1-C15 95.9(2), C8-Bi1-C15 95.2(2), Bi1-C1-C2 115.8(3), C1-C2-O1 114.6(4), C3-C2-O1 124.7(4), C2-O1-C7 117.6(4), Bi1-C15-C16 122.9(3), C17-C18-C21 121.4(4), C19-C18-C21 119.8(4), C18-C21-Br1 110.8(4).

The figure below indicates the two methods of the planned synthesis of bismuth containing carbohydrates. Therefore, different monosaccharides, like D-galactose

derivatives, D-mannose derivatives and D-glucose derivatives like meglumine were intended as potential starting materials. To constitute the described synthesis, Fig. 3.38 depicts the two methods, using the D-galactose derivatives **61** and **62** for conversion with the bismuth compounds **59** and **60**. Accordingly, 1,2:3,4-di-*O*-isopropylidene-α-D-galactose **61** was treated with tosyl chloride in presence of pyridine and CH_2Cl_2 providing electrophile **62**.

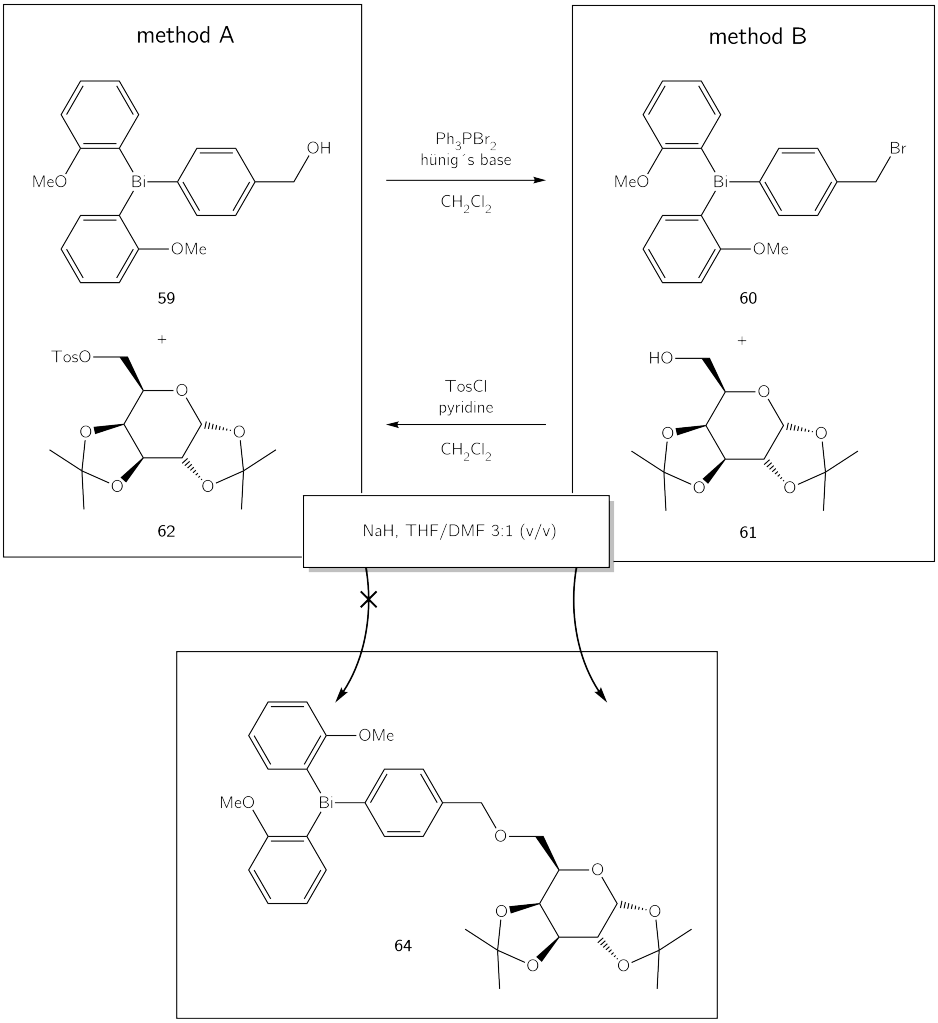

Fig. 3.38: Planned synthesis of bismuth containing carbohydrate **64**.

Following method B, compound **61** was treated with NaH in a mixture of THF and DMF providing the corresponding alkoxide, which was further reacted by addition of **60** to the desired product **64** in yields up to 95 %. Unfortunately, the inversed reaction (method A) of the deprotonated bismuth compound **59** with the tosylated carbohydrate derivative **62** was not successful. Regrettably this reaction yielded a $Ar_2BiBz-O-BzBiAr_2$ species.

To take advantage of this novel proposed strategy, conversions using a secondary alcohol - 1,6-anhydro-2,3-O-isopropylidene-β-D-mannopyranose **43** - as well as meglumine **63** with the bismuth bromide **60** were performed.

The synthesis of compound **65** was performed in a similar manner to **64**. Therefore, compound **43** is treated with NaH in THF/DME 3:1 at 0 °C, where bismuth compound **60** is added dropwise. After completed conversion and several purification steps, as described in detail in section 5.3.6, desired compound **65** is obtained in excellent yields up to 83 %.

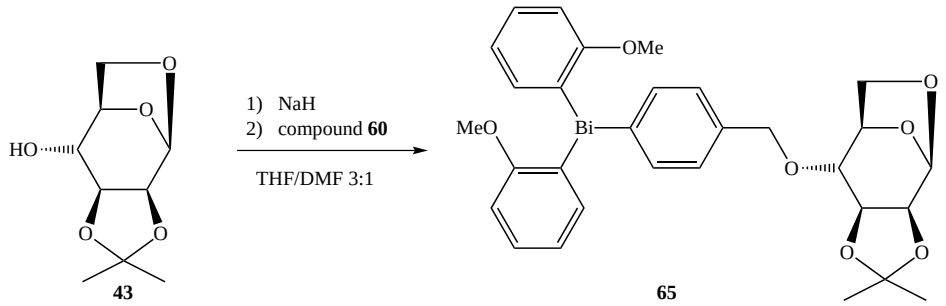

Fig. 3.39: Synthesis of bismuth-monosaccharide **65**.

In addition Fig. 3.40 presents the synthesis of compound **66**. In contrast to previous reactions, here the weaker base, $NaHCO_3$, is used to selectively deprotonate the NH group of meglumine. After addition of the bismuth compound **60** and purification compound **66** was obtained as a white wax (see 5.3.6).

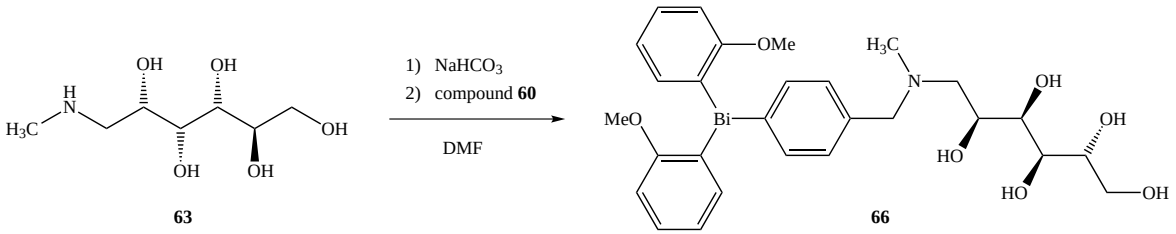

Fig. 3.40: Synthesis of bismuth-monosaccharide **66**.

This bismuth-monosaccharide was obtained in a yield of 79 % and confirms, that beside synthesis of O-benzylic bismuth containing carbohydrates, this concept also enables synthesis of N-benzylic bismuth-saccharides (**66**).

The ether strategy, in comparison to the amide approach and the Huisgen 1,3-dipolar cycloaddition, therefore represents the most promising concept to synthesize bismuth-carbohydrates. The main advantage of the "ether-approach" is, that no complicated

derivatizations of the carbohydrate, as introducing an azide-moiety, are needed and in turn each compound or material providing free hydroxyl-groups (or free amine groups) is intended as a potential partner in this S_N2 reaction. Furthermore, this bismuth containing carbohydrates are air and moisture stable and obtained in high yields ranging from 79 - 89 %.

Applying this concept, a coupling of the NQR-active bismuth to more complex and sterically demanding structures like oligo- and polysaccharides - e.g. cyclodextrins - should become possible.

Fig. 3.41 describes the coupling reaction of bismuth compound **60** and a protected β-cyclodextrin (**67**) yielding compound **68**. The exact reaction details are discussed in the experimental section 5.3.6 on page 95. The bismuth containing oligosaccharide is obtained in 88 % yield as a white solid.

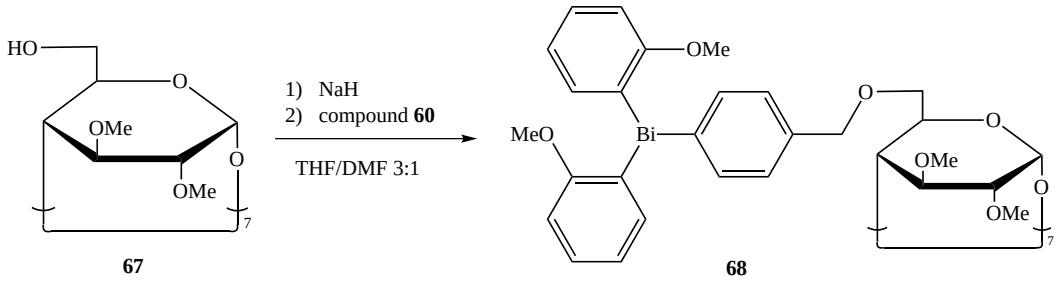

67 **68**

Fig. 3.41: Synthesis of bismuth-oligosaccharide **68**.

Applying the ether concept, linking of the NQR-active bismuth compound to an oligosaccharide in very satisfying yields became possible for the first time. NMR results clearly confirm the formation of the desired bismuth-cyclodextrin.
According to these excellent results, further coupling reaction will be based on this synthetic strategy.

3.7 Polymerization of bismuth compounds

The synthesis of polystyrene compounds bearing diarylbismuthine groups was reported in 2001 by Matano et al.[42] In a similar manner a polystyrene species, containing organobismuth compound **22** was synthesized. The radicalic polymerization of styrene and Bi(*o*–OMePh)$_3$ in a ratio of 8:1 was initiated using AIBN. After stirring the reaction for 48 h at 80 °C, the solvent (toluene) was removed and the residue dissolved in THF. Precipitation of the polymer in cold methanol afforded compound **70** as a colourless powder.

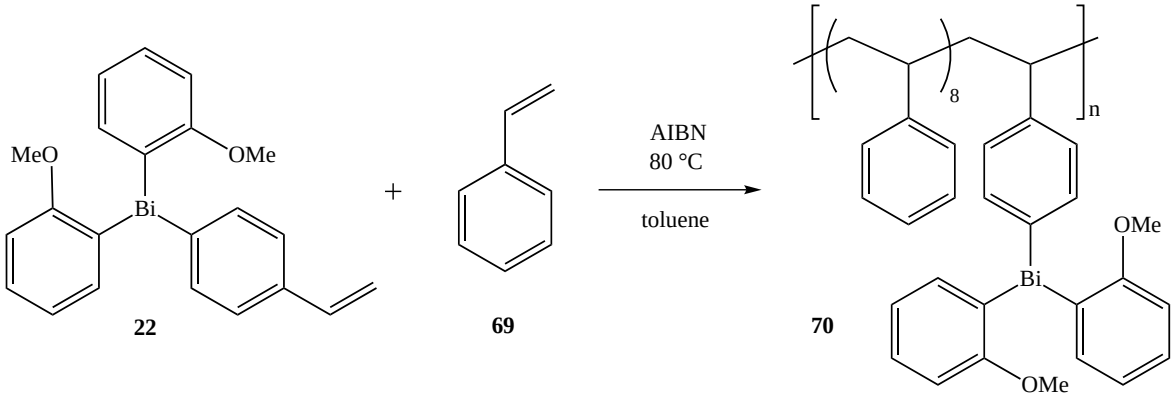

Fig. 3.42: Synthesis of compound **70**.

In Fig. 3.43 the IR spectra of the corresponding precursors **22** (blue) and **69** (pink), the product spectra (green) as well as those of polystyrene (orange) are shown. For styrene and the bismuth precursor the probably most important vibration is the vinyl vibration at $\sim$1630 cm^{-1} (C=C str. vibr.) Regarding the product spectra (green) this vibration is no longer apparent what indicates the product formation.
Vibrations of **22** and **70** at around 1430 and 1223 cm^{-1} (sym. CH_3 deformation and rocking vibr.) correspond to the bismuth's $-OCH_3$ groups of the anisyl ligands. Symmetrical and asymmetrical $-OCH_3$ vibrations and aromatic CH stretching vibrations are determined between 3080 and 2785 cm^{-1}. Further comparing polystyrene and polymer **70**, a broad band at 2928 cm^{-1} (CH_2 asym. stretching vibr.), 1494 cm^{-1} (CH_2 def. vibr.) and 752 and 696 cm^{-1} (CH_2 rocking vibr.) can be assigned to the aliphatic main chain of the polymers. Aromatic stretching vibrations at 3080 - 2980 cm^{-1} and 1453 cm^{-1} are found for polystyrene, styrene and compound **70**.

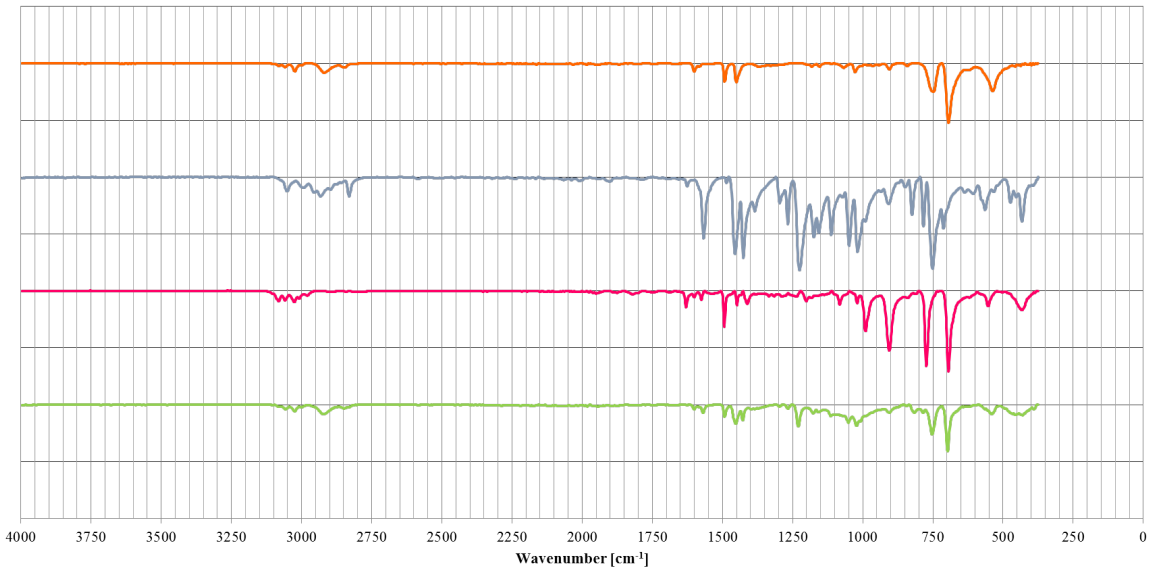

Fig. 3.43: IR data of polystyrene (orange), bismuth compound **22** (blue), styrene **67** (pink) and the polymer **70** (green)

Overall the IR spectra confirm the formation of a polystyrene species including the bismuth compound. Further ^{1}H NMR (Fig. 6.21) and ^{13}C NMR (Fig. 6.22 in the appendix) indicate the polymer formation. The polystyrene environment of compound **70** can be used as a substrate/carrier for the NQR-active bismuth compound. However, the solubility problem - especially for this polystyrene compounds - in H_2O remains. Even though NQR experiments can be performed and would provide suitable results, this specific bismuth polymer **70** would not be applicable without further modifications.

4 Conclusion and Outlook

The synthetic approaches developed in this thesis enabled the synthesis of trivalent NQR-active symmetrical organobismuth compounds and derivatives as well as connecting them to different saccharide species.

Starting from $BiCl_3$, different triarylbismuth compounds were synthesized and extensively investigated by means of nuclear quadrupole resonance spectroscopy. For compound **15**, tris(2-methoxyphenyl)bismuthine, a quadrupole transition, intersecting the protons Larmor frequency, close at the desired frequency of 121 MHz was detected. This result identifies compound **15**, beside the model substrate $BiPh_3$ (**9**), as the most promising bismuth compound for further synthesis of QRE-based contrast agents.

To fulfil the task of linking the NQR-active bismuth compound to more polar species like saccharides, different concepts were developed and investigated (see section Fig. 2.3).
The amide approach describes connecting a bismuth-amide to compounds functionalized with different groups (-OH, -SH, -COOH etc.), forming a direct bismuth-carbohydrate bond. Unfortunately, experiments revealed the relatively low air and moisture stability of these compounds. For this reason the amide approach is not applicable for synthesis of Bi-containing CA's.

Applying the click-chemistry concept (Huisgen 1,3-dipolar cycloaddition), a N_3-functionalized monosaccharide can be linked to a Ar_2Bi-alkyne. Since both precursors are air and moisture stable, this feature should also be valid for the product species. Various experiments confirmed the formation of a bismuth containing carbohydrate linked via a triazole ring. However, the desired bismuth containing carbohydrates are not obtained in satisfying yields.

The third concept, the ether-coupling approach, links a bismuthyl-benzyl-bromide species to a carbohydrate. Finally, experiments confirmed the successful coupling of the bismuth species to different "nucleophilic" saccharides. Applying this method, the bismuth compound **15** was connected to various monosaccharides, providing O-benzylic and N-benzylic bismuth containing carbohydrates. The main advantage of

this concept is, that no complicated derivatizations of the saccharides are needed and every compound providing, e.g. free hydroxyl-groups, is a potential partner. Consequently the next step aims at reactions involving oligo- and polysaccharides. Using the ether concept, connecting the NQR-active bismuth compound to a cyclodextrin was enabled for the first time.

Further experiments to link the bismuth species to mono-, oligo- and polysaccharides as well as to nano-particles, e.g. SiO_2 NP's, will be accomplished. In a further consequence the deprotection of the coupled saccharides, without splitting the bismuth species, will become a complex task. These bismuth containing carbohydrate species will be investigated regarding their NQR-spectroscopic properties and integrated into medicinal studies.

5 Experimental

5.1 Materials and General Analytic Methods

All reaction procedures involving usage of air and moisture sensitive compounds were either performed under an atmosphere of nitrogen using standard Schlenk tube techniques or were carried out in a nitrogen flushed Govebox UNILAB supplied by M.Braun. Involved deoxygenated and dried solvents were sustained from an Innovative Technology solvent drying system. Except for THF, which was in addition dried over $LiAlH_4$ and freshly distilled prior use, all other solvents were used without any further purification steps. All used commercial chemicals have been used purchased from chemical suppliers.

5.1.1 Chromatography

Analytical thin-layer chromatography was accomplished on aluminum plates precoated with silica gel 60 F_{254} (E. Merck 5554). For staining the TLC plates were treated with one of the below mentioned solutions and developed by employment of a heat gun. In addition the compounds were detected using UV light (254 nm).

VAN	Vanillin/sulfuric acid: vanillin (9 g) in H_2O (950 mL), H_2SO_4 (120 mL) and EtOH (750 mL)
CAM	Ceric ammonium molybdate: ammonium heptamolybdate tetrahydrate (100 g) in 10 % H_2SO_4 (1000 mL) and ceric sulfate (8 g) in 10 % H_2SO_4 (80mL)

5.1.2 NMR - Nuclear Magnetic Resonance Spectroscopy

NMR spectra were recorded on a Varian Mercury 300 MHz spectrometer operation at 300.22 MHz (^{1}H) and at 75.5 MHz (^{13}C). Chemical shifts δ (in ppm) are listed relative to TMS and the spectra were referenced to solvent residual signals. The corresponding

coupling constants are reported in Hertz (Hz).

s	singlet	dd	double doublet
d	doublet	ddd	double double doublet
t	triplet	bm	broad multiplet
m	multiplet	bs	broad singlet

5.1.3 XRD - X-Ray Diffraction Analysis

Single crystal X-Ray diffractometry was performed on a Bruker APEX II diffractometer with use of Mo Kα radiation ($\lambda = 0.71073$ Å) and a CCD area detector. For single crystal X-Ray measurements all suitable crystals were covered with a layer of silicon oil. A selected crystal is mounted on a glass rod on a copper pin and placed in the N_2 stream supplied by an Oxford Cryosystems cryometer (T = 100 K, if not stated alternatively). Empirical absorption corrections were applied using SADABS.[6], [65]. Structures were solved either using the Patterson option in SHELXS or direct methods and further refined by full-matrix least-squares precedures in SHELXL.[66], [64] The space group assignments and structural solutions were evaluated using PLATON. [71, 72] Anisotropically refining was applied for refining non-hydrogen atoms. All other hydrogen atoms were located in calculated positions corresponding to standard bond lengths and angles.

5.1.4 ATR-FTIR - Infrared Spectroscopy

All IR measurements were performed on an *ALPHA-P* device from Bruker under ambient conditions using the transition modus. The IR-abbreviations "s" (strong), "m" (medium), and "w" (weak) were used to signify the intensity of the measured transmission bands.

5.2 General Procedures

5.2.1 General Procedure A: Grignard Reaction

Metallic magnesium (3.8 equiv.) was reacted with the corresponding aryl halide (3.6 equiv.) at reflux of dry ether or dry THF under an atmosphere of nitrogen. After complete addition of the halide the reaction mixture was kept at reflux for 2-4 h. The reaction was allowed to reach ambient temperature and was added dropwise to an ice cooled solution of $BiCl_3$ (1 equiv.) in dry Et_2O or dry THF. After completed addition the reaction mixture was allowed to warm to room temperature and was stirred for 12 h. Further the reaction mixture was ice cooled and diluted with H_2O. After consecutively washing with H_2O and drying the combined organic phases over Na_2SO_4, the filtrate was concentrated under reduced pressure to provide the crude product. For further purification the residue was dissolved in EtOH or toluene, heated and filtrated over hot Celite® 512. The filtrate was again concentrated, heated and allowed to slowly cool to room temperature for crystallization.

5.2.2 General Procedure B: Lithiation Reaction - *n*-BuLi

To a solution of the respective aryl bromide in dry THF 1.6 M *n*-BuLi (1.1 equiv.) was added dropwise at -78 °C under an inert atmosphere of nitrogen. The reaction mixture was stirred for 2-4 h at -78 °C and further an ice cooled solution of the respective arylbismuthchloride compound in dry THF was added slowly. Another 2-5 h of stirring at -78 °C completed the conversion of the reactants and the mixture was allowed to warm to ambient temperature. The reaction mixture was carefully diluted with CH_2Cl_2, Et_2O or toluene and quenched with H_2O. The organic layers were dried over Na_2SO_4, filtrated and concentrated under reduced pressure.

5.2.3 General Procedure C: TMS/TBS Deprotection

The respective *O*-silylated compound dissolved in THF/H_2O (100:1 v/v) was stirred with TBAF · 3 H_2O (1 - 3.5 equiv.). After completed cleavage of the protecting group, the solvents were removed under reduced pressure yielding the free alcohol.

5.2.4 General Procedure D: Amide

A solution of the corresponding bismuthchloride compound in dry THF was added dropwise at -78 °C under an atmosphere of nitrogen to a suspension of the respective lithium amide. After stirring for 2 h at -78 °C the reaction mixture was allowed to warm

to ambient temperature. Following, the solvent was removed under reduced pressure in an inert atmosphere and further dissolved in dry pentane. Using a reverse frit the formed precipitate was filtrate off and the filtrate was concentrated under reduced pressure to provide the crude product.

5.2.5 General Procedure E: Amide Coupling

To a solution of the respective bismuthamide in dry THF, the respective coupling partner (adamantyl, saccharide) was added at room temperature under an inert atmosphere. After stirring at 50 °C for 12 - 14 h the solvent was removed under reduced pressure. The residue was dissolved in dry pentane/THF (20:1 v/v) and separated from the precipitate by transferring the product solution into another flask. Removal of the solvents under reduced pressure yielded the coupling product.

5.2.6 General Procedure F: Huisgen 1,3-dipolar cycloaddition

To a solution of the respective azide-saccharide in THF/H_2O (100:1 v/v), the corresponding bismuth alkyne was added in small portions. CuI and Et_3N are added and the reaction mixture was stirred at 30 °C. After completed conversion, the solvent was removed to afford the product.

5.2.7 General Procedure G: Ether Coupling

To a solution of the respective carbohydrate (1 equiv.) in a mixture of THF/DMF 3:1 (v/v), sodium hydride (60 % in mineral oil, 1.2 equiv. per OH-group) was added at 0 °C. After 30 min a solution of the respective bismuth-halide (1 equiv.) in THF was added dropwise and the reaction was allowed to warm to room temperature. After completed conversion of the starting material, the reaction was diluted with CH_2Cl_2 and successively washed with HCl (6 %) and saturated $NaHCO_3$. The combined organic layers were dried over Na_2SO_4, filtrated and concentrated in vacuum. The resulting residue was purified on silica gel to provide the corresponding product.

5.3 Synthesis

5.3.1 Triarylbismuth compounds - Ar_3Bi

5.3.1.1 Symmetrical triarylbismuth compounds

Triphenylbismuthine - $BiPh_3$

Following General Procedure A, metallic magnesium (8.32 g, 342.5 mmol) in dry Et_2O was reacted with bromobenzene **1** (44.81 g, 285.4 mmol) at reflux in an inert atmosphere of nitrogen. After completed addition of the halide the reaction mixture was kept at reflux for 2.5 h. The reaction was allowed to reach ambient temperature, stirred for 1 h and further added dropwise to an ice cooled solution of $BiCl_3$ (25 g, 79.28 mmol) in dry Et_2O. After addition, the reaction mixture was stirred at room temperature for another 12 hours and following diluted with H_2O at 0 °C. Washing with H_2O, drying the combined organic phases over Na_2SO_4 and concentrating the filtrate under reduced pressure, yielded the crude product. The residue was taken up in EtOH, filtrated over hot Celite® 512, concentrated and recrystallized from EtOH. $BiPh_3$ (31.54 g, 71.63 mmol, 90 %) was isolated as colourless crystals.

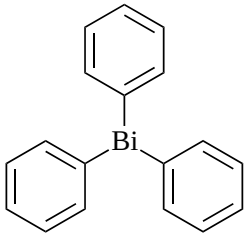

Compound: **9**
$C_{18}H_{15}Bi$
MW: 440.30 $\frac{g}{mol}$
mp: 78 - 79 °C

^{1}H NMR (300 MHz, $CDCl_3$) δ = 7.77 (dd, 6 H, J = 7.8, 1.4 Hz, H^{Ar}), 7.46 – 7.30 (m, 9 H, H^{Ar}) ppm.
^{13}C NMR (75.5 MHz, $CDCl_3$) δ = 155.3 (ipso C), 137.7, 130.7, 127.9 (CH^{Ar}) ppm.

Triphenylbismuthine deuterated - $BiPh_3$(d)

Following General Procedure A, a solution of freshly prepared PhMgBr [by dropwise addition of deuterated bromobenzene (15.5 g, 95.69 mmol) in dry Et_2O (120 mL) to metallic magnesium (2.79 g, 114.8 mmol) in dry Et_2O (50 mL) and refluxing for 2.5 h] was added dropwise at 0 °C under an atmosphere of nitrogen to a suspension of $BiCl_3$ (8.59 g, 26.58 mmol) in dry Et_2O (70 mL). After stirring at 0 °C for 1 h the reaction mixture was allowed to reach ambient temperature and was stirred for another 12 h. The reaction mixture was diluted and washed with H_2O. After drying the organic phase over Na_2SO_4, the filtrate was concentrated under reduced pressure. For

further purification the residue was recrystallized from EtOH and $BiPh_3$(d) (10.86 g, 23.85 mmol, 90 %) was isolated as colourless crystals.

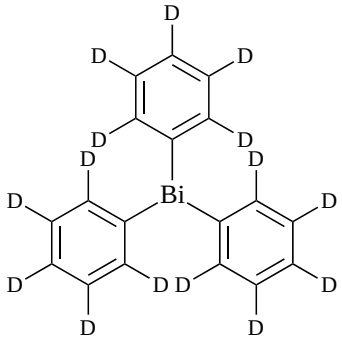

Compound: **10**
$C_{18}D_{15}Bi$
MW: 455.39 $\frac{g}{mol}$
mp: 69 °C

Tris(4-methylphenyl)bismuthine - Bi(p − Tol)$_3$

As described in General Procedure A, *p*-tolylbromide (29.29 g, 171.3 mmol) dissolved in dry Et_2O was added dropwise to a suspension of metallic magnesium (4.99 g, 205.5 mmol) under an inert atmosphere. After refluxing for 2.5 h and stirring for 1 h at room temperature the Grignard solution was added at 0 °C to a suspension of $BiCl_3$ (15 g, 47.57 mmol) in dry Et_2O. The reaction mixture was stirred for 12 h at ambient temperature and further quenched and washed with water. The organic layer was dried over Na_2SO_4 and the filtrate was concentrated under reduced pressure to provide the crude product. Recrystallization from EtOH yielded **11** (18.81 g, 39.01 mmol, 82 %) as colourless needles.

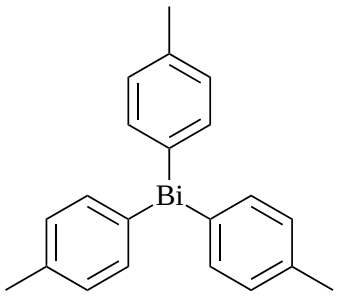

Compound: **11**
$C_{21}H_{21}Bi$
MW: 482.38 $\frac{g}{mol}$
mp: 119 - 121 °C

^{1}H NMR (300 MHz, $CDCl_3$) δ = 7.63 (d, 6 H, J = 7.7 Hz, H^{Ar}), 7.19 (d, 6 H, H^{Ar}), 2.33 (s, 9 H, 3 x CH_3) ppm.
^{13}C NMR (75.5 MHz, $CDCl_3$) δ = 162.2 (ipso C), 137.7 (CH^{Ar}), 137.3 (ipso C), 131.1 (CH^{Ar}), 21.6 (3 x CH_3) ppm.

Tris(4-fluorophenyl)bismuthine - Bi(p−FPh)$_3$

Following General Procedure A, to a suspension of $BiCl_3$ (10.29 g, 32.62 mmol) in 80 mL dry Et_2O a solution of 4-fluorophenylmagnesium bromide [prepared from **4** (20.55 g, 117.4 mmol) and metallic magnesium (3.43 g, 140.9 mmol) in dry Et_2O (230 mL)] was added in small portions at 0 °C. After addition the reaction mixture was stirred for 12 h at room temperature and was further diluted and washed with H_2O at 0 °C. The organic phase was dried over Na_2SO_4 and concentrated under reduced pressure to obtain the crude product. Recrystallization in EtOH afforded Bi(p−FPh)$_3$ (14.43 g, 29.19 mmol, 90 %) as colourless needles.

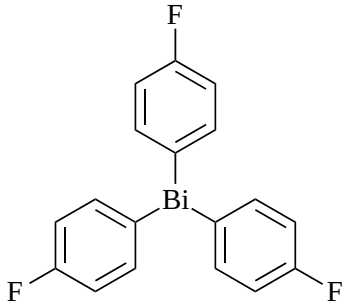

Compound: **12**
$C_{18}H_{12}BiF_3$
MW: 494.27 $\frac{g}{mol}$
mp: 95.7 °C

^{1}H NMR (300 MHz, $CDCl_3$) δ = 7.65 (dd, 6 H, J = 8.5, 6.2 Hz, H^{Ar}), 7.08 (ddd, 6 H, J = 8.5, 5.4, 2.3 Hz, H^{Ar}) ppm.
^{13}C NMR (75.5 MHz, $CDCl_3$) δ = 162.8 (d, J = 247.5 Hz, C^{Ar}), 139.1 (d, J = 7.0 Hz, CH^{Ar}), 118.0 (d, J = 19.8 Hz, CH^{Ar}) ppm.

Tris[4-(dimethylamino)phenyl]bismuthine - Bi(p−NMe$_2$Ph)$_3$

As described in General Procedure A, a solution of 4-dimethylaminophenylmagnesium bromide [prepared by dropwise addition of **5** (13.33 g, 66.59 mmol) in 110 ml dry THF to metallic magnesium (1.943 g, 79.92 mmol) in dry THF (40 mL)] was added to a suspension of $BiCl_3$ (6 g, 19.03 mmol) in 60 mL dry THF at 0 °C under an atmosphere of nitrogen. The reaction mixture was allowed to warm to ambient temperature and stirred for 12 h. After having been stirred for another 3 h at reflux, the reaction was diluted with toluene and washed with H_2O at 0 °C. Drying the organic phase over Na_2SO_4 and concentrating the filtrate under reduced pressure, provided the crude bismuth-compound. Hot Celite® 512 filtration and recrystallization in toluene afforded Bi(p−NMe_2Ph)$_3$ (8.44 g, 14.82 mmol, 78 %) as colourless crystals.

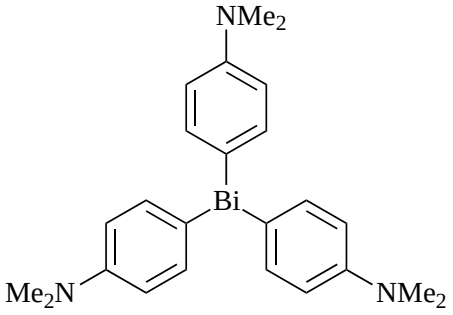

Compound: **13**
$C_{24}H_{30}BiN_3$
MW: 569.51 $\frac{g}{mol}$
mp: 199 - 202 °C

^{1}H NMR (300 MHz, $CDCl_3$) δ = 7.61 (d, 6 H, J = 8.3 Hz, H^{Ar}), 6.76 (d, 6 H, H^{Ar}), 2.94 (s, 18 H, 6 x CH_3) ppm.
^{13}C NMR (75.5 MHz, $CDCl_3$) δ = 150.0, 140.2 (ipso C), 138.6, 114.9 (CH^{Ar}), 40.6 (6 x CH_3) ppm.

Tris(4-methoxyphenyl)bismuthine - Bi(p−OMePh)$_3$

According to General Procedure A, bromo-4-methoxybenzene **6** (32.03 g, 171.3 mmol) was reacted with metallic magnesium (4.99 g, 205.5 mmol) in dry Et_2O at reflux under an inert atmosphere of nitrogen. After refluxing for 4 h and stirring for 1 h at room temperature, the Grignard solution was added dropwise at 0 °C to a suspension of $BiCl_3$ (15 g, 47.57 mmol) in dry Et_2O. The reaction was stirred for 12 h at ambient temperature, followed by refluxing for another 3 h. The ice cooled reaction mixture was further diluted and washed with H_2O at 0 °C. After drying over Na_2SO_4, the filtrate was concentrated under reduced pressure providing the crude product. Hot Celite® 512 filtration and further recrystallization steps in EtOH and toluene finally yielded **14** (19.47 g, 36.71 mmol, 77 %) as colourless crystals.

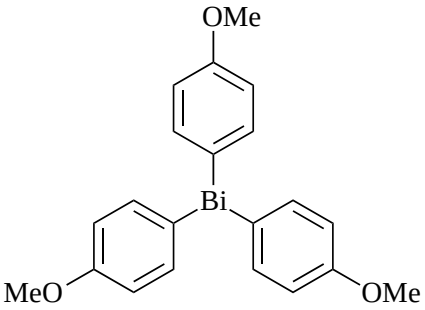

Compound: **14**
$C_{21}H_{21}BiO_3$
MW: 530.38 $\frac{g}{mol}$
mp: 190 - 192 °C

^{1}H NMR (300 MHz, $CDCl_3$) δ = 7.62 (d, 6 H, J = 8.1 Hz, H^{Ar}), 6.92 (d, 6 H, H^{Ar}), 3.79 (s, 9 H, 3 x CH_3) ppm.
^{13}C NMR (75.5 MHz, $CDCl_3$) δ = 165.6, 159.4 (ipso C), 138.9, 116.4 (CH^{Ar}), 55.2 (3 x CH_3) ppm.

Tris(2-methoxyphenyl)bismuthine - Bi(o−OMePh)$_3$

Following General Procedure A, 2-methoxyphenylmagnesium bromide was prepared by addition of **7** (44.88 g, 239.9 mmol) in 190 ml dry Et_2O to metallic magnesium (7 g, 287.9 mmol) in dry Et_2O (80 mL) under an atmosphere of nitrogen. After 2.5 h refluxing, the Grignard solution was stirred at ambient temperature for 1 h. The reaction mixture was added to a suspension of $BiCl_3$ (21.62 g, 68.56 mmol) in 100 ml dry Et_2O via a canula transfer at 0 °C. After stirring for 12 h at room temperature, the reaction mixture was diluted and quenched 0 °C with H_2O. The organic phases were combined, dried over Na_2SO_4 and the solvent removed under reduced pressure. Bi(*o*−OMePh)$_3$ (31.87 g, 60.09 mmol, 88 %) was recrystallized from toluene and isolated as colourless crystals.

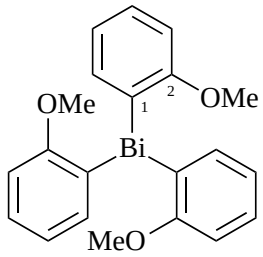

Compound: **15**
$C_{21}H_{21}BiO_3$
MW: 530.38 $\frac{g}{mol}$
mp: 163 °C

^{1}H NMR (300 MHz, $CDCl_3$) δ = 7.46 (dd, 3 H, J = 7.1, 1.5 Hz H^{Ar}), 7.38 - 7.28 (m, 3 H, H^{Ar}), 7.01 (d, 3 H, J = 8.0 Hz, H^{Ar}), 6.88 (dt, 3 H, J = 7.3, 0.7 Hz, H^{Ar}), 3.77 (s, 9 H, 3 x CH_3) ppm.
^{13}C NMR (75.5 MHz, $CDCl_3$) δ = 162.3 (ipso C-1), 139.2 (CH^{Ar}), 137.3 (ipso C-2), 129.3, 124.2, 109.9 (CH^{Ar}), 55.7 (3 x CH_3) ppm.

Tris(2,6-dimethoxyphenyl)bismuthine - Bi(di−o−OMePh)$_3$

Following General Procedure A, **8** (12.5 g, 57.60 mmol) dissolved in 100 mL dry Et_2O was added dropwise to metallic magnesium (1.68 g, 69.11 mmol) in dry THF (50 mL) under an atmosphere of nitrogen. After refluxing for 6 h, the reaction was stirred at ambient temperature for another 12 h. To a suspension of $BiCl_3$ (5.05 g, 15.99 mmol) in 50 mL dry Et_2O, the Grignard solution was added at 0 °C. The mixture was stirred for 12 h at ambient temperature, followed by refluxing for another 4 h. After completed conversion the reaction mixture was diluted and washed with H_2O at 0 °C, dried over Na_2SO_4 and concentrated under reduced pressure. Hot filtration using Celite® 512 and further recrystallization steps in Et_2O and toluene afforded **16** (8.84 g, 14.25 mmol, 89 %) as colourless needles.

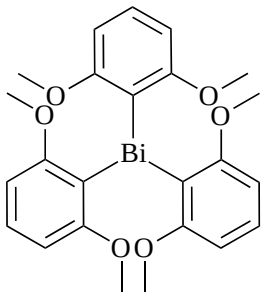

Compound: **16**
$C_{24}H_{27}BiO_6$
MW: 620.45 $\frac{g}{mol}$
mp: 185 °C

^{1}H NMR (300 MHz, $CDCl_3$) δ = 7.12 (t, 3 H, J = 8.1 Hz, H^{Ar}), 6.60 (d, 6 H, H^{Ar}), 3.46 (s, 18 H, 6 x CH_3) ppm.
^{13}C NMR (75.5 MHz, $CDCl_3$) δ = 164.5, 133.8 (ipso C), 129.0, 104.1 (CH^{Ar}), 55.6 (6 x CH_3) ppm.

Tris(4-ethynylphenyl)bismuthine

Following General Procedure B, ((4-bromophenyl)ethynyl)trimethylsilane (**21** (1.5 g, 5.93 mmol) dissolved in 60 mL dry THF is cooled to -78 °C under an inert atmosphere of nitrogen. *n*-BuLi (3.75 mL, 5.99 mmol) was added dropwise and the reaction mixture was stirred for 3 h at -78 °C. After slowly addition of a suspension of $BiCl_3$ (623 mg, 1.98 mmol) in 20 mL dry THF, the reaction was stirred for another 4 h at -78 °C. After completed conversion, the reaction mixture was allowed to warm to ambient temperature. Following General Procedure C, TBAF · 3 H_2O (1.99 g, 6.32 mmol) was added. After completed cleavage of the silyl-group, the solvents were removed under reduced pressure to provide the crude bismuthcompound. The residue was dissolved in CH_2Cl_2 and washed with H_2O. The combined organic layers were dried over Na_2SO_4, filtrated and the solvent was removed under reduced pressure. The residue was purified on silica gel (C/EA 20:1 v/v) to afford to product as a slightly brownish syrup. Recrystallization yielded the bismuthtrialkyne (0.557 g, 1.09 mmol, 55 %) as colourless crystals.

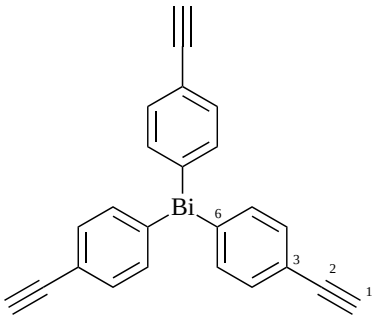

Compound: **28**
$C_{24}H_{15}Bi$
MW: 512.36 $\frac{g}{mol}$
mp: 149-151 °C

^{1}H NMR (300 MHz, $CDCl_3$) δ = 7.67 (d, 6 H, J = 7.7 Hz, H^{Ar}), 7.50 (d, 6 H, H^{Ar}), 3.09 (s, 3 H, 3 x CH) ppm.
^{13}C NMR (75.5 MHz, $CDCl_3$) δ = 156.7 (ipso C-6), 137.5, 134.1 (CH^{Ar}), 121.9 (ipso C-3), 83.7 (ipso C-2), 77.9 (ipso C-1) ppm.

5.3.1.2 Asymmetrical triarylbismuth compounds

(4-Ethynylphenyl)-diphenyl-bismuthine

Method A:

As described in General Procedure A, ((4-bromophenyl)ethynyl)trimethylsilane (**21**) (2 g, 7.89 mmol) dissolved in 50 mL dry THF was added dropwise to metallic magnesium (0.23 g 9.47 mmol) in dry THF (20 mL) under an atmosphere of nitrogen. After stirring for 3 h at reflux, the reaction mixture was stirred at ambient temperature for 1 h. The reaction was added dropwise to an ice cooled solution of $BiPh_2Cl$ (3.15 g, 7.89 mmol) in 40 mL dry THF. After having been stirred for 12 h at room temperature, the reaction mixture was kept at reflux for another 4 h. After completed conversion the mixture was diluted with Et_2O and washed with H_2O. Drying the organic layers over Na_2SO_4 and concentrating under reduced pressure provided the crude silylated product.
Following General Procedure C, the residue was dissolved in THF/H_2O (60 mL, 100:1 v/v) and stirred with TBAF · $3H_2O$ (3.70 g, 11.73 mmol) at ambient temperature. After completed deprotection, the solvents were removed under reduced pressure to give the free alkyne. Recrystallization in toluene and pentane gave a pale yellow syrup which was purified on silica gel (C/EA 20:1 v/v) to provide compound **25** (1.87 g, 4.02 mmol, 51 %) as a slightly yellowish syrup.

Method B:

Following General Procedure B, ((4-bromophenyl)ethynyl)trimethylsilane (2 g, 7.90 mmol) dissolved in 80 mL dry THF was treated with 1.6 M *n*-BuLi (5.13 mL, 8.22 mmol) under an inert atmosphere of nitrogen at -78 °C. After stirring for 120 min at -78 °C, an ice cooled solution of chlorodiphenylbismuthane $BiPh_2Cl$ (3.15 g, 7.90 mmol) in 50 mL dry THF was added dropwise. Another 4 h of stirring at -78 °C completed the conversion and the reaction mixture was allowed to warm to ambient temperature. Following General Procedure C, TBAF · 3 H_2O (3.07 g, 9.71 mmol) and 3 mL H_2O were added to split the protective silyl-group. After completed cleavage of the protecting group, the solvents were removed under reduced pressure to provide the deprotected crude product as a slightly brownish syrup. The residue was dissolved in CH_2Cl_2 and

washed with H_2O. The combined organic layers were dried over Na_2SO_4 and concentrated under reduced pressure. The residue was purified on silica gel (C/EA 20:1 v/v) to afford compound **25** (2.02 g, 4.35 mmol, 55 %) as a slightly yellowish syrup.

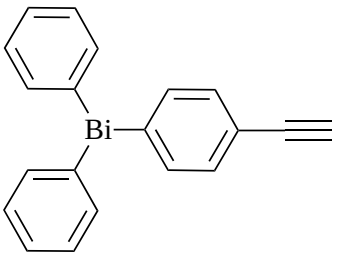

Compound: **25**
$C_{20}H_{15}Bi$
MW: 464.32 $\frac{g}{mol}$

The obtained NMR data were equivalent to those reported in literature.[37]

(4-Ethynylphenyl)-bis(o-methoxyphenyl)-bismuthine

Method A:
A solution of ((4-bromophenyl)ethynyl)trimethylsilane (2 g, 7.90 mmol) in dry THF (60 mL) was added dropwise to metallic magnesium (0.23 g, 9.48 mmol) in dry THF (20 mL) under an inert atmosphere of nitrogen. Following General Procedure A, the reaction mixture was stirred for 3 h at reflux and another hour at ambient temperature. The Grignard solution was cooled and slowly added to a suspension of chlorobis(2-methoxyphenyl)bismuthane (3.62 g, 7.88 mmol) in dry THF (40 mL) at 0 °C under a nitrogen atmosphere. After stirring for 12 hours at room temperature, the reaction mixture was additionally kept at reflux for another 3 h. Following the reaction was diluted with Et_2O and washed with H_2O three times. The combined organic layers were dried over Na_2SO_4, filtrated off and concentrated under reduced pressure.
Following General Procedure C, the crude product (yellow-brownisch syrup) was dissolved in THF/H_2O (55 mL, 100:1 v/v), TBAF · 3 H_2O (3.06 g, 9.71 mmol) was added and the reaction mixture stirred until completed cleavage. The reaction is concentrated under reduced pressure providing the crude product as a brownish syrup. Purification of the residue on silica gel (C/EA 20:1 v/v) provided compound **26** (2.04 g, 3.98 mmol, 48 %) as a slightly yellowish syrup.

Method B:
To a solution of ((4-bromophenyl)ethynyl)trimethylsilane (2 g, 7.90 mmol) in 70 mL dry THF, 1.6 M *n*-BuLi (5.13 mL, 8.22 mmol) was added dropwise at -78 °C under an inert atmosphere. After completed addition, the reaction mixture was stirred for further 3 h.

A cooled suspension of chlorobis(2-methoxyphenyl)bismuthane (3.62 g, 7.90 mmol) in 30 mL dry THF was added to the reaction and stirred for another 2 h at -78 °C. After completed conversion, the reaction mixture was allowed to warm to room temperature. Following General Procedure C, 1.5 ml H_2O and TBAF · 3 H_2O (3.07 g, 9.72 mmol) were added. After completed cleavage of the protecting group, the solvents were removed to afford the crude product. The residue was dissolved in CH_2Cl_2 and washed with H_2O. The combined organic layers were dried over Na_2SO_4, filtrated and concentrated under reduced pressure. The residue was purified on silica gel (C/EA 20:1 v/v) to provide **26** (2.37 g, 4.52 mmol, 57 %) as slightly yellow syrup.

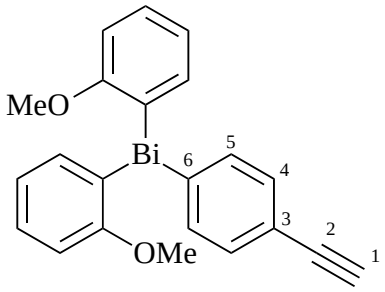

Compound: **26**
$C_{22}H_{19}BiO_2$
MW: 524.37 $\frac{g}{mol}$
mp: 157 - 158 °C

^{1}H NMR (300 MHz, $CDCl_3$) $\delta = 7.62$ (d, 2 H, $J = 7.7$ Hz, H-4), 7.50 (d, 2 H, $J = 7.2$ Hz, H^{Ar}), 7.42 (d, 2 H, H-5), 7.34 (d, 2 H, H^{Ar}), 7.02 (d, 2 H, $J = 7.9$ Hz, H^{Ar}), 6.89 (t, 2 H, H^{Ar}), 3.76 (s, 6 H, 2 x CH_3), 3.05 (s, 1 H, H-1) ppm.
^{13}C NMR (75.5 MHz, $CDCl_3$) δ = 162.1, 139.3 (ipso C), 138.9 (CH^{Ar}), 138.1 (C-4), 133.5 (C-5), 129.7 (CH^{Ar}), 129.3 (ipso C), 124.4, 110.2 (CH^{Ar}), 89.1, 84.3 (ipso C), 55.7 (2 x CH_3) ppm.

Bis(o-methoxyphenyl)-(4-vinylphenyl)-bismuthine

Method A:
Following General Procedure A, bromo-4-vinylbenzene (2.50 g, 13.66 mmol) was added dropwise to metallic magnesium (0.40 g, 16.39 mmol) in 50 mL dry THF at -20 °C under an inert atmosphere of nitrogen. After stirring for 4 h, the reaction mixture was allowed to warm to 0 °C. The Grignard solution was added dropwise to a suspension of chlorobis(2-methoxyphenyl)bismuthane (6.26 g, 13.65 mmol) dissolved in 40 mL dry THF at 0 °C. The reaction was stirred for 6 h and after slowly warming to room temperature, the reaction mixture was consecutively washed with HCl (6 %) and saturated $NaHCO_3$. After drying the organic layers over Na_2SO_4, the filtrate was concentrated under reduced pressure to afford compound **22** (3.76 g, 7.13 mmol, 52 %) as slightly yellowish crystals.

Method B:

As described in General Procedure B, to a solution of **20** (0.71 g, 3.85 mmol) in 60 mL dry THF under an inert atmosphere of nitrogen, *n*-BuLi (0.25 g, 3.85 mmol) was added dropwise at -78 °C. After completed addition, the reaction mixture was stirred for 3 h at -78 °C. A suspension of chlorobis(2-methoxyphenyl)bismuthane (1.77 g, 3.86 mmol) in 15 mL dry THF was added to the reaction and stirred for another 4 h at -78 °C. After completed conversion of the reactants, the reaction mixture was allowed to warm to ambient temperature. The solvent was removed under reduced pressure and the residue dissolved in Et_2O and quenched with H_2O. The combined organic phases were dried over Na_2SO_4, filtrated and concentrated under reduced pressure obtaining a brownish syrup. Purification on silica gel (C/EA 50:1 v/v) provided **22** (1.17 g, 2.22 mmol, 57.7 %) as slightly yellowish crystals.

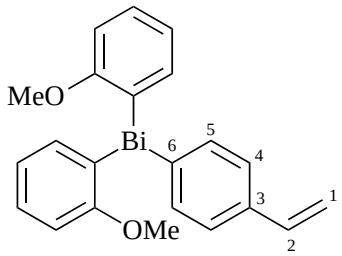

Compound:	**22**
$C_{22}H_{21}BiO_2$	
MW:	526.39 $\frac{g}{mol}$
mp:	150-151.5 °C

^{1}H NMR (300 MHz, $CDCl_3$) δ = 7.62 (d, 1 H, J = 7.6 Hz, H-4a), 7.55 (d, 1 H, J = 7.0 Hz, H-4b), 7.46 (d, 2 H, J = 7.1 Hz, H^{Ar}), 7.43 - 7.28 (m, 4 H, H-5, H^{Ar}), 7.08 - 6.84 (m, 4 H, H^{Ar}), 6.69 (dd, 1 H, $J_{2,1a}$ = 17.6 Hz, $J_{2,1b}$ = 10.9 Hz, H-2), 5.74 (d, 1 H, H-1a), 5.21 (dd, 1 H, $J_{1b,1a}$ = 5.4 Hz, H-1b), 3.77 (s, 6 H, 2 x CH_3) ppm.
^{13}C NMR (75.5 MHz, $CDCl_3$) δ = 162.3 (ipso C), 139.2 (CH^{Ar}), 139.0, 136.6, 129.6 (ipso C), 129.3 (CH^{Ar}), 127.9 (C-5), 124.3 (C-4), 124.2 (CH^{Ar}), 110.1 (ipso C), 109.9 (CH^{Ar}), 55.7 (2 x CH_3) ppm.

5.3.2 Diarylbismuth chlorides - Ar_2BiCl

Chloro-diphenyl-bismuthine - Ph_2BiCl

To a solution of $BiPh_3$ (10 g, 22.71 mmol) in 120 mL dry Et_2O, $BiCl_3$ (3.58 g, 11.36 mmol) was added in small portions at 0 °C under an inert atmosphere of nitrogen. After stirring for 2 h at 0 °C, the reaction was allowed to warm to ambient temperature and stirred for another 3 h. After completed conversion of the reactants the solvent was removed under reduced pressure. The residue was washed with Et_2O three times to yield **17** (11.95 g, 29.98 mmol, 88 %) as a colourless powder.

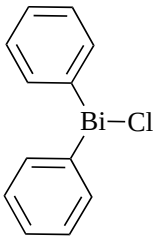

Compound: **17**
$C_{12}H_{10}BiCl$
MW: 398.64 $\frac{g}{mol}$
mp: 187 °C

^{1}H NMR (300 MHz, DMSO) $\delta = 8.31$ (d, 4 H, $J = 7.6$ Hz, H^{Ar}), 7.61 (t, 4 H, $J = 7.5$ Hz, H^{Ar}), 7.33 (t, 2 H, $J = 7.4$ Hz, H^{Ar}) ppm.
^{13}C NMR (75.5 MHz, DMSO) δ = 157.3 (ipso C), 137.1, 131.2, 127.7 (CH^{Ar}) ppm.

Chloro-bis(p-methylphenyl)-bismuthine - Tol_2BiCl

Dry $BiCl_3$ (1.63 g, 5.17 mmol) was added in small portions to **11** (5 g, 10.37 mmol) dissolved in 70 mL dry Et_2O at 0 °C under an atmosphere of nitrogen. The reaction mixture was stirred for 2 h at 0 °C, further allowed to warm to room temperature and additionally stirred for another 3 h. After completed conversion, the solvent was removed under reduced pressure and the residue was washed three times with Et_2O. Removing the solvent afforded **18** (5.77 g, 13.53 mmol, 87 %) as a colourless powder.

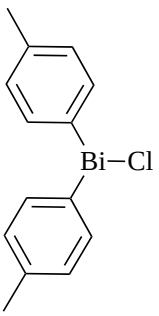

Compound: **18**
$C_{14}H_{14}BiCl$
MW: 426.70 $\frac{g}{mol}$
mp: 185 °C

^{1}H NMR (300 MHz, DMSO) δ = 8.17 (d, 4 H, J = 7.6 Hz, H^{Ar}), 7.42 (d, 4 H, H^{Ar}), 3.41 (s, 6 H, 2 x CH_3)) ppm.
^{13}C NMR (75.5 MHz, DMSO) δ = 162.6 (ipso C), 137.1 (CH^{Ar}), 137.0 (ipso C), 131.9 (CH^{Ar}), 21.3 (2 x CH_3) ppm.

Chloro-bis(o-methoxyphenyl)-bismuthine

To a solution of compound **15** (3.5 g, 6.59 mmol) in 60 ml dry Et_2O, $BiCl_3$ (1.04 g, 3.29 mmol) was added in small portions over a period of 30 min at 0 °C under an atmosphere of nitrogen. The reaction mixture was stirred at 0 °C for 2.5 h. After stirring for another 3 h at ambient temperature, the solvent was removed under reduced pressure and the residue washed with Et_2O. Removing the solvent gave **19** (4.08 g, 8.89 mmol, 90 %) as a colourless powder.

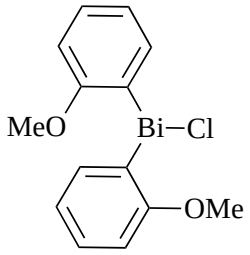

Compound: **19**
$C_{14}H_{14}BiClO_2$
MW: 458.69 $\frac{g}{mol}$
mp: 89 - 91 °C

^{1}H NMR (300 MHz, $CDCl_3$) δ = 8.55 (d, 2 H, J = 7.1 Hz, H^{Ar}), 7.41 (t, 2 H, J = 7.6 Hz, H^{Ar}), 7.30 (t, 2 H, J = 6.7 Hz, H^{Ar}), 7.19 (d, 2 H, J = 8.0 Hz, H^{Ar}), 3.83 (s, 6 H, 2 x CH_3) ppm.
^{13}C NMR (75.5 MHz, $CDCl_3$) δ = 161.5 (ipso C), 137.5 (CH^{Ar}), 136.3 (ipso C), 130.3, 126.5, 111.6 (CH^{Ar}), 55.8 (2 x CH_3) ppm.

5.3.3 Diarylbismuth amides - Ar_2BiNR_2

N,N-Dimethylamino-1,1-bis(o-methoxyphenyl)bismuthine

A suspension of **19** (2 g, 4.36 mmol) in dry THF (30 mL) was added dropwise at -78 °C to lithiumdimethylamide (**29**) (0.22 g, 4.36 mmol) dissolved in 30 ml dry THF under an atmosphere of nitrogen. After completed addition of the chloride, the reaction was stirred for 120 min at -78 °C. The reaction mixture was stirred for 3 h slowly warming to ambient temperature. The solvent was removed under reduced pressure and the residue dissolved in 50 mL of dry n-pentane. The reaction mixture was filtrated through Celite® 512 using a reverse frit. The resulting solution was evaporated to dryness under reduced pressure. Product **33** (1.43 g, 3.06 mmol, 70 %) was afforded as an orange syrup.

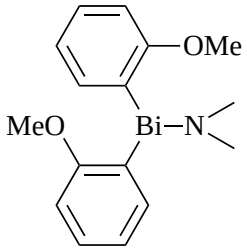

Compound: **33**
$C_{16}H_{20}BiNO_2$
MW: 467.32 $\frac{g}{mol}$

^{1}H NMR (300 MHz, C_6D_6) δ = 8.70 - 8.59 (m, 2 H, H^{Ar}), 7.24 - 7.05 (m, 4 H, H^{Ar}), 6.76 - 6.68 (m, 2 H, H^{Ar}), 3.17 (s, 6 H, 2 x CH_3), 2.32 - 2.10 (m, 6 H, 2 x CH_3) ppm.
^{13}C NMR (75.5 MHz, C_6D_6) δ = 162.4, 136.3 (ipso C), 136.2, 129.5, 124.7, 110.8 (CH^{Ar}), 54.8 (2 x CH_3), 38.9 (2 x CH_3) ppm.

N,N-Diethylamino-1,1-bis(o-methoxyphenyl)-bismuthine

To a solution of $LiNEt_2$ (0.73 g, 9.29 mmol) in 50 ml dry THF, **19** (4.26 g, 9.29 mmol) dissolved in dry THF (40 ml) was added dropwise over a period of 60 min at -78 °C under an inert atmosphere of nitrogen. After completed addition, the reaction was stirred for 2 h at -78 °C, slowly warmed to room temperature and stirred for another 2 h. The solvent was removed under reduced pressure and the slightly orange residue was suspended in 40 ml dry pentane. The resulting solution was filtered over Celite® 512 and the solvent was removed. Compound **34** (2.61 g, 5.27 mmol, 57 %) was obtained as an orange syrup.

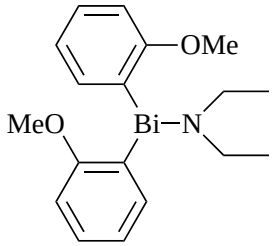

Compound: **34**
$C_{18}H_{24}BiNO_2$
MW: 495.38 $\frac{g}{mol}$

^{1}H NMR (300 MHz, C_6D_6) δ = 8.35 (d, 2 H, J = 6.9 Hz, H^{Ar}), 7.26 - 7.02 (m, 4 H, H^{Ar}), 6.74 (d, 2 H, J = 8.0 Hz, H^{Ar}), 3.66 (q, 4 H, J = 6.9 Hz, 2 x CH_2), 3.25 (s, 6 H, 2 x CH_3), 1.14 (t, 6 H, 2 x CH_3) ppm.
^{13}C NMR (75.5 MHz, C_6D_6) δ = 162.8 (ipso C), 137.8 (CH^{Ar}), 136.2 (ipso C), 129.9, 124.5, 110.5 , 54.9 (2 x CH_3), 50.0 (2 x CH_2), 18.9 (2 x CH_3) ppm.

N,N-Diisopropylamino-1,1-bis(o-methoxyphenyl)-bismuthine

Compound **19** (3.18 g, 6.94 mmol) in 40 ml dry THF was added dropwise to a cooled (-78 °C) solution of LiN(*i*Pr)$_2$ in THF (40 ml) over a period of 60 min under an atmosphere of nitrogen. Stirring for 2 h at -78 °C and further stirring for 3 h at ambient temperature afforded a yellow reaction mixture. Under reduced pressure the solvent was removed and the residue suspended in 40 ml dry pentane. Filtrating over Celite® 512 and removing of the solvent yielded **35** (2.82 g, 5.39 mmol, 78 %) as a slightly yellowish powder.

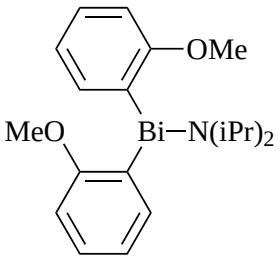

Compound: **35**
$C_{20}H_{28}BiNO_2$
MW: 523.43 $\frac{g}{mol}$
mp: 99 - 101 °C

^{1}H NMR (300 MHz, C_6D_6) δ = 8.30 (dd, 2 H, J = 7.1, 1.7 Hz, H^{Ar}), 7.28 - 7.03 (m, 4 H, H^{Ar}), 6.72 (d, 2 H, J = 7.5 Hz, H^{Ar}), 4.14 (hept, 2 H, J = 6.5 Hz, 2 x CH), 3.24 (s, 6 H, 2 x CH_3), 1.19 (t, 12 H, 4 x CH_3) ppm.
^{13}C NMR (75.5 MHz, C_6D_6) δ = 163.1 (ipso C), 138.2,(CH^{Ar}), 136.2 (ipso C), 129.8, 124.3, 110.2 (CH^{Ar}), 54.8 (2 x CH_3), 52.4 (2 x CH), 28.5 (4 x CH_3) ppm.

N,N-Bis(trimethylsilyl)amino-1,1-bis(o-methoxyphenyl)-bismuthine

To a solution of lithium bis(trimethylsilyl)amide (0.7 g, 4.14 mmol) in 20 ml dry THF, a suspension of **19** (1.9 g, 4.14 mmol) in THF (30 ml) was added dropwise at -78 °C under an inert atmosphere of nitrogen. The reaction mixture was stirred for 2 h at -78 °C and additionally 3 h at room temperature. The solvent was removed under reduced pressure and the residue dissolved in 20 ml dry pentane. The reaction was filtrated over Celite® 512, concentrated and afforded **36** (1.89 g, 3.24 mmol, 78 %) as a colourless powder.

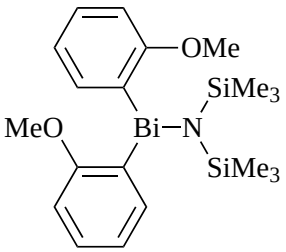

Compound: **36**
$C_{20}H_{32}BiNO_2Si_2$
MW: 583.63 $\frac{g}{mol}$
mp: 60 °C

^{1}H NMR (300 MHz, C_6D_6) δ = 8.45 (d, 2 H, J = 7.0 Hz, H^{Ar}), 7.26 - 7.02 (m, 4 H, H^{Ar}), 6.72 (d, 2 H, J = 8.2 Hz, H^{Ar}), 3.23 (s, 6 H, J = 6.9 Hz, 2 x CH_3), 0.29 (s, 18 H, 6 x CH_3) ppm.
^{13}C NMR (75.5 MHz, C_6D_6) δ = 162.8 (ipso C), 139.2 (CH^{Ar}), 136.4 (ipso C), 130.3, 124.5, 110.7 (CH^{Ar}), 54.8 (2 x CH_3), 6.6 (6 x CH_3) ppm.

5.3.4 Diarylbismuth-Monosaccharides: Amide Coupling

[(Adamantan-1-yl)oxy]-bis(o-methoxyphenyl)-bismuthine

To a solution of $Bi(o-OMePh)_2N(iPr)_2$ (100 mg, 0.19 mmol) in 15 ml dry THF was added 1-Adamantanol (**37**) (30 mg, 0.19 mmol) over a period of 30 min at ambient temperature. The reaction mixture was stirred for 48 h at 45 °C under an inert atmosphere. After completed conversion of the starting materials, the solvent was removed under reduced pressure. The residue was suspended in 10 ml of pentane and the product mixture was separated from the formed precipitate. Concentrating the solution yielded **40** (67.7 mg, 0.12 mmol, 62 %) as a colourless oil.

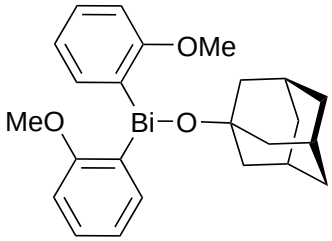

Compound: **40**
$C_{24}H_{29}BiO_3$
MW: 574.47 $\frac{g}{mol}$

^{1}H NMR (300 MHz, $CDCl_3$): see appendix (Fig. 6.1)
^{13}C NMR (75.5 MHz, $CDCl_3$): see appendix (Fig. 6.2)

[(Adamantan-1-yl)thio]-bis(o-methoxyphenyl)-bismuthine

1-Adamantanethiol (**38**) (32.2 mg, 0.19 mmol) was added slowly to a solution of **35** (100 mg, 0.19 mmol) in 15 ml dry THF under an inert atmosphere of nitrogen. After stirring the reaction mixture for 48 h at 45 °C, the reaction was concentrated and further suspended in 5 ml of pentane. The product solution was separated and concentrated in vacuum. Compound **41** (94.3 mg, 0.16 mmol, 84 %) was afforded as slightly yellowish syrup.

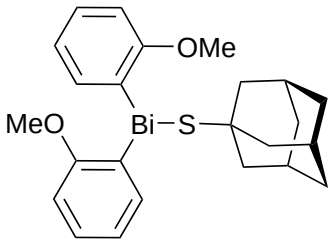

Compound: **41**
$C_{24}H_{29}BiO_2S$
MW: 590.53 $\frac{g}{mol}$

^{1}H NMR (300 MHz, $CDCl_3$): see appendix (Fig. 6.3)
^{13}C NMR (75.5 MHz, $CDCl_3$): see appendix (Fig. 6.4)

[(Adamantan-1-yl)carboxy]-bis(o-methoxyphenyl)-bismuthine

To a solution of **35** (100 mg, 0.19 mmol) in 15 ml dry THF was added 1-Adamantanecarboxylic acid (**39**) (34.4 mg, 0.19 mmol) over a period of 30 min under an inert atmosphere. Stirring the reaction mixture for 48 h at 45 °C and removing the solvent under reduced pressure yielded a slightly yellowish syrup. The syrup was dissolved in 5 ml pentane and the separated product solution was concentrated in vacuum. Compound **42** (79 mg, 0.13 mmol, 69 %) was obtained as colourless syrup.

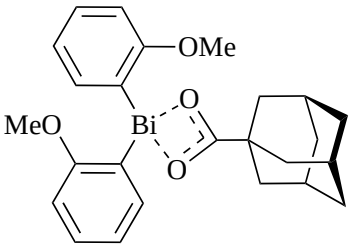

Compound: **42**
$C_{25}H_{29}BiO_4$
MW: 602.48 $\frac{g}{mol}$

^{1}H NMR (300 MHz, $CDCl_3$): see appendix (Fig. 6.5)
^{13}C NMR (75.5 MHz, $CDCl_3$): see appendix (Fig. 6.6)

1,6-Anhydro-4-O-[Bis(o-methoxy)phenyl]bismuthyl-2,3-O-isopropylidene-β-D-mannopyranose

A solution of **43** (38.6 mg, 0.19 mmol) in 5 ml dry THF was added to **35** (100 mg, 0.19 mmol) in 15 ml dry THF. After stirring the reaction mixture for 72 h at 45 °C, the solvent was removed under reduced pressure. The residue was suspended in 5 ml of dry pentane and the separated product solution was concentrated under vacuum. Compound **44** (85.4 mg, 0.14 mmol, 72 %) was obtained as a colourless syrup.

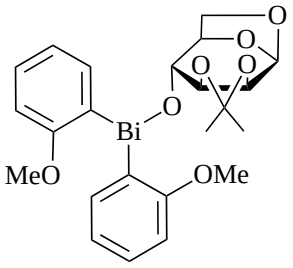

Compound: **44**
$C_{23}H_{27}BiO_7$
MW: 624.44 $\frac{g}{mol}$

^{1}H NMR (300 MHz, $CDCl_3$: see appendix (Fig. 6.7 - Fig. 6.10)
^{13}C NMR (75.5 MHz, $CDCl_3$): see appendix (Fig. 6.11 - Fig. 6.12)

5.3.5 Diarylbismuth-Monosaccharides: Huisgen 1,3-dipolar Cycloaddition

p-[1-(3-O-Benzyl-5-deoxy-1,2-O-isopropylidene-α-D-xylofuranos-5-yl)-1H-1,2,3-triazol-4-yl]-phenyl-di-phenyl-bismuthine

Following General Procedure F, to a solution of **45** (0.13 g, 0.43 mmol) in 15 ml dry THF, **25** (0.2 g, 0.43 mmol) was added dropwise. To perform the click reaction CuI (1.5 equiv) and Et_3N (1.5 equiv) were added. The reaction was warmed to 30 °C and stirred for 24 h. After completed conversion of the starting materials, the solvent was removed and the residue was purified on silica gel (C/EA 15:1 v/v) to afford compound **50** (153 mg, 0.20 mmol, 46 %) as a colourless solid.

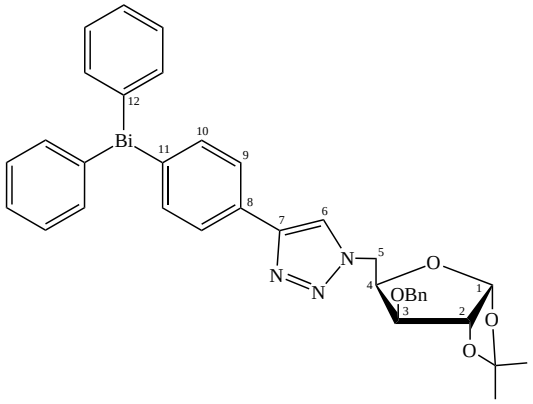

Compound: **50**
$C_{35}H_{34}BiN_3O_4$
MW: 769.65 $\frac{g}{mol}$

^{1}H NMR (300 MHz, $CDCl_3$) δ = 7.78 - 7.52 (m, 9 H, H^{Ar}), 7.36 - 7.12 (m, 11 H, H^{Ar}), 5.89 (d, 1 H, $J_{1,2}$ = 3.4 Hz, H-1), 4.69 - 4.32 (m, 6 H, H-2, H-3, H-5, CH_2), 3.90 (d, 1 H, $J_{4,3}$ = 1.8 Hz, H-4), 1.32, 1.20 (2s, 6 H, 2 x CH_3) ppm.
^{13}C NMR (75.5 MHz, $CDCl_3$) δ = 155.3 (ipso C-12), 147.9 (ipso C-11), 138.1, 137.6 (2 x CH^{Ar}), 136.9 (ipso C-Bn), 130.6 (CH^{Ar}), 130.1 (ipso C-8), 128.8, 128.4, 128.0, 127.8, 127.7, 121.0 (6 x CH^{Ar}), 112.2 (ipso C-7), 105.3 (C-1), 82.0 (C-2), 81.7 (C-4), 78.9 (C-3), 72.1 (CH_2), 49.3 (C-5), 26.8, 26.3 (2 x CH_3) ppm.

p-[1-(3-O-Benzyl-6-deoxy-1,2-O-isopropylidene-α-D-glucofuranos-6-yl)-1H-1,2,3-triazol-4-yl]-phenyl-diphenyl-bismuthine

A solution of **25** (0.29 g, 0.63 mmol) in 10 ml THF was added dropwise to **46** (0.21 g, 0.63 mmol) in 10 ml THF. CuI and Et_3N were added to the reaction mixture and stirred for 24 h at 30 °C. After completed conversion, the solvent was removed and the residue purified on silica gel (C/EA 15:1 v/v) to obtain compound **51** (220 mg, 0.27 mmol, 44 %) as a colourless solid.

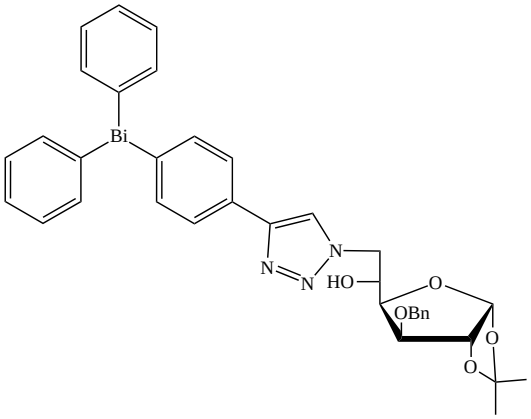

Compound: **51**
$C_{36}H_{36}BiN_3O_5$
MW: 769.65 $\frac{g}{mol}$

^{1}H NMR (300 MHz, $CDCl_3$): see appendix (Fig. 6.13)
^{13}C NMR (75.5 MHz, $CDCl_3$): see appendix (Fig. 6.14)

p-[1-(Methyl-2,3,4-Tri-O-benzyl-6-deoxy-α-D-glucopyranosid-6-yl)-1H-1,2,3-triazol-4-yl]-phenyl-di-(o-methoxyphenyl)-bismuthine

As described in General Procedure F, **26** (0.2 g, 0.38 mmol) dissolved in THF is added at room temperature to a solution of **47** (0.19 g, 0.38 mmol) in 15 ml THF. To accelerate the reaction CuI and Et_3N were added and the reaction stirred at elevated temperatures for 48 h. The reaction mixture was concentrated and the residue purified on silica gel (C/EA 15:1 v/v) to obtain compound **52** (53 mg, 0.05 mmol, 13 %).

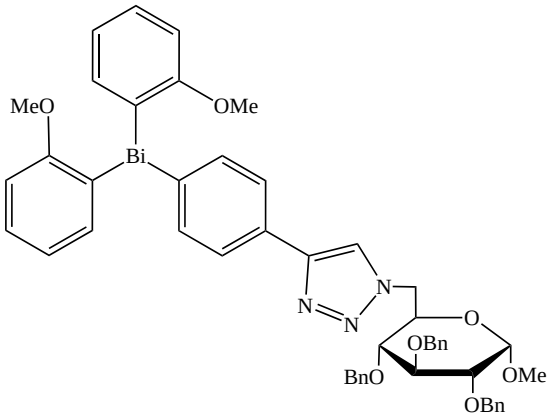

Compound: **52**
$C_{50}H_{50}BiN_3O_7$
MW: 1013.94 $\frac{g}{mol}$

^{1}H NMR (300 MHz, $CDCl_3$): see appendix (Fig. 6.15)
^{13}C NMR (75.5 MHz, $CDCl_3$): see appendix (Fig. 6.16)

p-[1-(Methyl-6-deoxy-α-D-glucopyranosid-6-yl)-1H-1,2,3-triazol-4-yl]-phenyl-diphenyl-bismuthine

To a solution of **48** (0.09 g, 0.43 mmol) in 15 ml dry THF, **25** (0.2 g, 0.43 mmol) was added dropwise. To perform the click reaction CuI and Et_3N were added. The reaction was warmed to 30 °C and stirred for 48 h. Following, the solvent was removed under vacuum and the crude product **53** (36 mg, 0.05 mmol, 12 %) as yellowish syrup obtained.

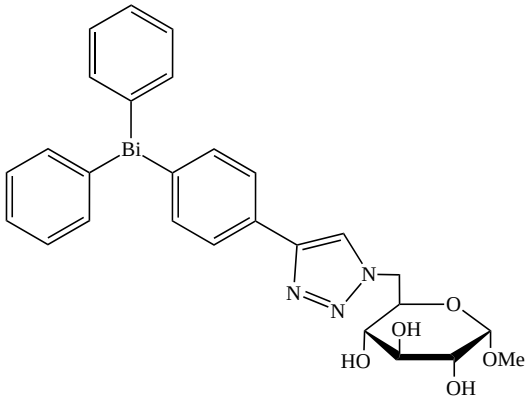

Compound: **53**
$C_{27}H_{28}BiN_3O_5$
MW: 683.52 $\frac{g}{mol}$

^{1}H NMR (300 MHz, $CDCl_3$): see appendix (Fig. 6.17)
^{13}C NMR (75.5 MHz, $CDCl_3$): see appendix (Fig. 6.18)

p-[1-(Methyl-6-deoxy-α-D-glucopyranosid-6-yl)-1H-1,2,3-triazol-4-yl]-phenyl-di-(o-methoxyphenyl)-bismuthine

According to General Procedure F, a solution of **26** (0.31 g, 0.59 mmol) in 10 ml THF was added dropwise to **48** (0.13 g, 0.59 mmol) in 10 ml THF. Et_3N and CuI were added to the reaction mixture and stirred for 48 h at 30 °C. Afterwards, the solvent was removed under reduced pressure and the residue purified on silica gel (C/EA 10:1 v/v) to obtain compound **54** (48 mg, 0.06 mmol, 11 %) as a pale yellow syrup.

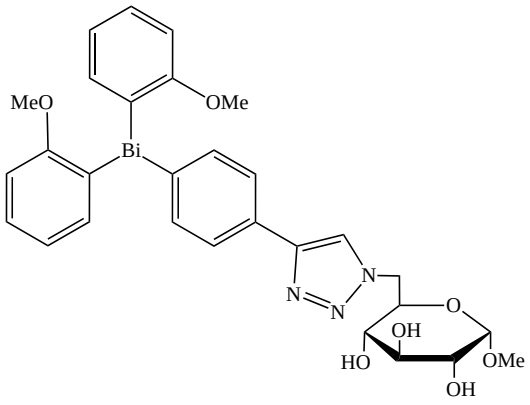

Compound: **54**
$C_{29}H_{32}BiN_3O_7$
MW: 743.57 $\frac{g}{mol}$

^{1}H NMR (300 MHz, $CDCl_3$): see appendix (Fig. 6.19)
^{13}C NMR (75.5 MHz, $CDCl_3$): see appendix (Fig. 6.20)

[1-(1,2:3,4-di-O-isopropylidene-α-D-galactopyranos-6-yl)-1H-1,2,3-triazol-4-yl]-benzene

A solution of **26** (0.2 g, 0.38 mmol) in 10 ml THF was added dropwise to **49** (0.11 g, 0.38 mmol) in 10 ml THF. CuI and Et_3N were added to the reaction mixture and stirred for 48 h at 30 °C. After conversion, the solvent was removed under reduced pressure and the residue purified on silica gel (C/EA 15:1 v/v) to obtain compound **55** (83 mg, 0.21 mmol, 56 %) as a colourless solid.

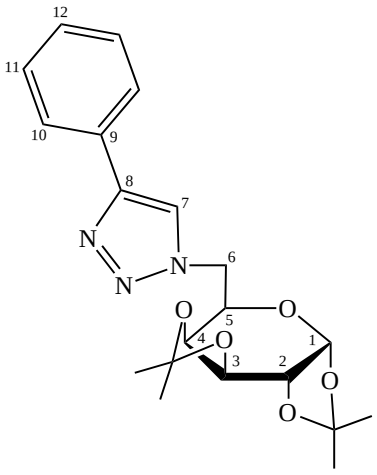

Compound: **55**
$C_{20}H_{25}N_3O_5$
MW: 387.44 $\frac{g}{mol}$

^{1}H NMR (300 MHz, $CDCl_3$) δ = 7.89 (s, 1 H, H-7), 7.77 (d, 2 H, H-10), 7.34 (t, 2 H, J = 7.5 Hz, H-11), 7.23 (d, 1 H, H-12), 5.47 (d, 1 H, $J_{1,2}$ = 5.0 Hz, H-1), 4.65 - 4.54 (m, 2 H, H-6a, H-3), 4.42 (dd, 1 H, $J_{6b,6a}$ = 14.2 Hz, $J_{6b,5}$ = 8.4 Hz, H-6b), 4.27 - 4.24 (m, 1 H, H-2), 4.21 - 4.11 (m, 2 H, H-4, H-5), 1.44, 1.33, 1.29, 1.21 (4 s, 3 H each, isoproylidene) ppm.
^{13}C NMR (75.5 MHz, $CDCl_3$) δ = 147.6 (C-8), 130.9 (C-9), 128.9 (C-11), 128.1 (C-12), 125.8 (C-10), 121.0 (C-7), 110.0, 109.2 (2 x isopropylidene), 96.4 (C-1), 71.3 (C-4), 70.9 (C-3), 70.5 (C-2), 67.4 (C-5), 50.7 (C-6), 26.1, 26.0, 25.0, 24.5 (2 x isopropylidene) ppm.

5.3.6 Diarylbismuth-Monosaccharides: Ether Coupling

p*-{*[(tert-butyldimethylsilyl)oxy]benzyl*}*di(o-methoxyphenyl)bismuthine

To a solution of (4-bromophenoxy)(tert-butyl)dimethylsilane (1.32 g, 4.36 mmol) in 100 ml dry THF, *n*-BuLi (2.73 ml, 4.36 mmol) was added dropwise at -78 °C under an atmosphere of nitrogen. After stirring the reaction mixture for 60 min at -78 °C, a cooled suspension of $Bi(o-OMePh)_2Cl$ was added dropwise and the mixture was stirred for 4 h at -78 °C. After completed conversion of the starting material, the reaction was diluted with CH_2Cl_2 and successively washed with HCl (6 %) and saturated $NaHCO_3$. The combined organic layers were dried over Na_2SO_4, filtrated and concentrated to dryness. The remaining residue was purified on silica gel (C/EA 20:1 v/v) to afford compound **58** (2.21 g, 3.43 mmol, 79 %) as colourless syrup.

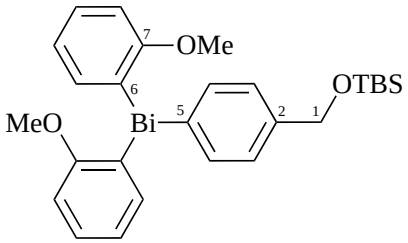

Compound: **58**
$C_{27}H_{35}BiO_3Si$
MW: 644.64 $\frac{g}{mol}$

^{1}H NMR (300 MHz, $CDCl_3$) δ = 7.80 (d, 2 H, J = 7.7 Hz, H^{Ar}), 7.54 - 7.42 (m, 4 H, H^{Ar}), 7.71 (d, 2 H, J = 7.0 Hz, H^{Ar}), 7.15 (d, 2 H, J = 8.0 Hz, H^{Ar}), 7.07 (t, 2 H, H^{Ar}), 4.91 (s, 2 H, CH_2), 3.89 (s, 6 H, 3 x CH_3), 1.13, 0.28 (2 s, 15 H, 5 x CH_3) ppm.
^{13}C NMR (75.5 MHz, $CDCl_3$) δ = 162.1 (ipso C-6), 152.4 (ipso C-5), 143.5 (ipso C-2), 140.5 (ipso C-7), 138.9, 137.9, 129.3, 128.0, 124.2, 110.0 (6 x CH^{Ar}), 65.3 (CH_2), 55.6 (2 x CH_3), 26.1, 18,5, -5.1 (5 x CH_3) ppm.

{p-[Bis(o-methoxy)phenyl]bismuthyl}phenyl)methanol

To a solution of **58** (2.21 g, 3.43 mmol) in 20 ml THF containing 3 ml H_2O, TBAF · 3 H_2O was added in catalytic amounts. After completed conversion of the starting materials, indicated by TLC, the reaction mixture was concentrated to dryness. The remaining residue was purified by column chromatography (C/EA 10:1 v/v) providing compound **59** (1.49 g, 2.81 mmol, 82 %) as white, crystalline powder.

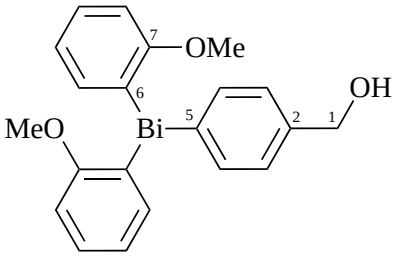

Compound: **59**
$C_{21}H_{21}BiO_3$
MW: 530.38 $\frac{g}{mol}$

^{1}H NMR (300 MHz, $CDCl_3$) δ = 7.53 (d, 2 H, J = 7.6 Hz, H^{Ar}), 7.42 (d, 2 H, J = 7.1 Hz, H^{Ar}), 7.26 - 7.12 (m, 4 H, H^{Ar}), 6.89 (d, 2 H, J = 8.1 Hz, H^{Ar}), 6.79 (t, 2 H, H^{Ar}), 4.47 (d, 2 H, J = 5.8 Hz, CH_2), 3.62 (s, 6 H, 2 x CH_3) ppm.
^{13}C NMR (75.5 MHz, $CDCl_3$) δ = 161.9 (ipso C-6), 153.1 (ipso C-5), 143.3 (ipso C-2), 139.7 (ipso C-7), 138.8, 138.3, 129.5, 128.9, 124.2, 110.0 (6 x CH^{Ar}), 65.5 (CH_2), 55.6 (2 x CH_3) ppm.

[p-(Bromomethyl)phenyl]di(o-methoxyphenyl)bismuthine

Compound **59** (1.49 g, 2.81 mmol) dissolved in 20 ml CH_2Cl_2 was treated with hünig's base (0.5 ml, 2.81 mmol) and triphenylphosphonium dibromide (1.19 g, 2.81 mmol). When TLC indicated full conversion of the starting materials, the reaction mixture was successively washed with HCl (6 %) and saturated $NaHCO_3$. After drying the combined organic layers over Na_2SO_4, the solvent was removed under reduced pressure. Purification on silica gel (C/EA 15:1 v/v) yielded **60** (1.53 mg, 2.58 mmol, 92 %) as colourless syrup.

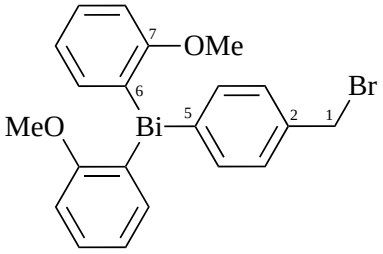

Compound: **60**
$C_{21}H_{20}BiBrO_2$
MW: 593.27 $\frac{g}{mol}$

^{1}H NMR (300 MHz, $CDCl_3$) δ = 7.53 (d, 2 H, J = 7.6 Hz, H^{Ar}), 7.43 (d, 2 H, J = 7.1 Hz, H^{Ar}), 7.27 - 7.13 (m, 4 H, H^{Ar}), 6.90 (d, 2 H, J = 8.1 Hz, H^{Ar}), 6.81 (t, 2 H, H^{Ar}), 4.34 (s, 2 H, CH_2), 3.63 (s, 6 H, 2 x CH_3) ppm.
^{13}C NMR (75.5 MHz, $CDCl_3$) δ = 162.1 (ipso C-6), 154.7 (ipso C-5), 143.7 (ipso C-2), 136.6 (ipso C-7), 138.9, 138.5, 130.6, 129.6, 124.3, 110.1 (6 x CH^{Ar}), 55.6 (2 x CH_3), 34.2 (CH_2), ppm.

6-O-{p-[Bis(o-methoxy)phenyl]bismuthyl}benzyl-1,2:3,4-di-O-isopropylidene-α-D-galactopyranose

Following General Procedure G, to a solution of **61** (50 mg, 0.19 mmol) in 15 ml of a mixture of THF/DMF 3:1 (v/v), NaH (60 % in mineral oil, 5.53 mg, 0.23 mmol) was added at 0 °C. After 30 min of stirring, a solution of **60** (114 mg, 0.19 mmol) in 10 ml THF was added dropwise. The reaction mixture was allowed to warm to ambient temperature and after completed conversion, the reaction was diluted with CH_2Cl_2 and successively washed with HCl (6 %) and saturated $NaHCO_3$. The combined organic layers were dried over Na_2SO_4, filtrated off and evaporated to dryness. The residue was purified on silica gel (C/EA 10:1 v/v) to provide compound **64** (132 mg, 0.17 mmol, 89 %) as white solid.

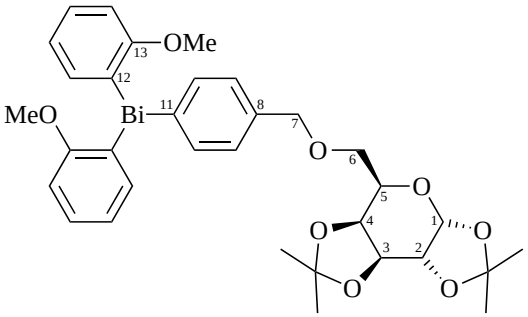

Compound: **64**
$C_{33}H_{39}BiO_8$
MW: 772.65 $\frac{g}{mol}$

^{1}H NMR (300 MHz, $CDCl_3$) δ = 7.53 (d, 2 H, J = 7.6 Hz, H^{Ar}), 7.44 (d, 2 H, J = 7.1 Hz, H^{Ar}), 7.30 - 7.16 (m, 4 H, H^{Ar}), 6.93 (d, 2 H, J = 8.1 Hz, H^{Ar}), 6.83 (t, 2 H, H^{Ar}), 5.46 (d, 1 H, $J_{1,2}$ = 4.9 Hz, H-1), 4.57 - 4.39 (m, 3 H, CH_2, H-3), 4.28 - 4.16 (m, 2 H, H-2, H-4), 3.98 - 3.88 (m, 1 H, H-5), 3.67 (s, 6 H, 2 x CH_3), 3.71 - 3.50 (m, 2 H, H-6a, H-6b), 1.45, 1.36, 1.25, 1.24 (4 s, 12 H, 2 x isopropylidene) ppm.
^{13}C NMR (75.5 MHz, $CDCl_3$) δ = 162.0 (ipso C-12), 153.2 (ipso C-11), 143.4 (ipso C-8), 138.8, 137.9 (2 x CH^{Ar}), 137.2 (ipso C-13), 129.4, 129.3, 124.1, 109.9 (4 x CH^{Ar}), 109.2, 108.5 (2 x isopropylidene), 96.3 (C-1), 73.5 (CH_2), 71.2 (C-4), 70.6 (C-3), 70.5 (C-2), 68.9 (C-6), 66.8 (C-5), 55.5 (2 x CH_3), 26.2, 26.0, 25.0, 24.5 (2 x isopropylidene) ppm.

1,6-Anhydro-4-O-{p-[Bis(o-methoxy)phenyl]bismuthyl}benzyl-2,3-O-isopropylidene-β-D-mannopyranose

According to General Procedure G, 50 mg of **62** (0.25 mmol) were treated with 7.12 mg NaH (60 % in mineral oil, 0.30 mmol) in 15 ml of a mixture of THF/DMF 3:1 (v/v) at 0 °C. After stirring the reaction for 30 min, the mixture was allowed to warm to room temperature and a solution of **60** (147 mg, 0.25 mmol) in 10 ml THF was added dropwise. After completed conversion of the starting materials, the reaction was diluted with CH_2Cl_2 and successively washed with HCl (6 %) and saturated $NaHCO_3$. The combined organic layers were dried over Na_2SO_4, filtrated off and the solvents are removed under reduced pressure. The crude product was purified on silica gel (C/EA 10:1 v/v) to obtain compound **65** (147 mg, 0.21 mmol, 83 %) as a white solid.

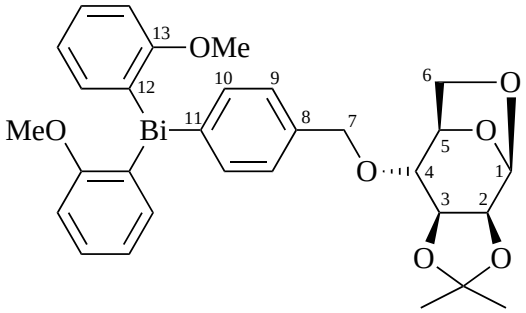

Compound: **65**
$C_{30}H_{33}BiO_7$
MW: 714.57 $\frac{g}{mol}$

^{1}H NMR (300 MHz, $CDCl_3$) δ = 7.57 (d, 2 H, J = 7.6 Hz, H^{Ar}), 7.43 (dd, 2 H, J = 7.2 Hz, 1.7 Hz, H^{Ar}), 7.31 - 7.13 (m, 4 H, H^{Ar}), 6.93 (d, 2 H, J = 8.1 Hz, H^{Ar}), 6.83 (t, 2 H, H^{Ar}), 5.28 (d, 1 H, $J_{1,2}$ = 3.1 Hz, H-1), 4.64 - 4.47 (m, 3 H, H−7, H-5), 4.19 (d, 1 H, $J_{3,2}$ = 6.5 Hz, H-3), 4.02 (dd, 1 H, H-2), 3.83 (d, 1 H, $J_{6,5}$ = 7.3 Hz, H-6a), 3.77 - 3.54 (m, 8 H, 2 x CH_3, H-6b, H-4), 1.45, 1.24 (2 s, 6 H, isopropylidene) ppm.
^{13}C NMR (75.5 MHz, $CDCl_3$) δ = 162.1 (ipso C-12), 153.9 (ipso C-11), 143.6 (ipso C-8), 138.9, 138.3 (2 x CH^{Ar}), 136.4 (ipso C-13), 129.7, 129.6, 124.2, 110.1 (4 x CH^{Ar}), 109.9 (isopropylidene), 99.3 (C-1), 76.4 (C-4), 73.9 (C-3), 73.6 (C-5), 72.5 (C-2), 72.0 (C-7), 64.7 (C-6), 55.6 (2 x CH_3), 26.1, 26.0 (isopropylidene) ppm.

N-{p-[Bis(o-methoxy)phenyl]bismuthyl}benzyl-1-deoxy-1-(methylamino)-D-glucitol

To a 10 % solution of **63** (50 mg, 0.26 mmol) in dry DMF, $NaHCO_3$ (25.8 mg, 0.31 mmol) and compound **60** (152 mg, 0.26 mmol) were added. When TLC indicated full conversion of **60**, the reaction mixture was evaporated to dryness. Purification of the remaining residue on silica gel (C/EA 3:1 v/v to EE) provided compound **66** (143 mg, 0.20 mmol, 79 %) as a white wax.

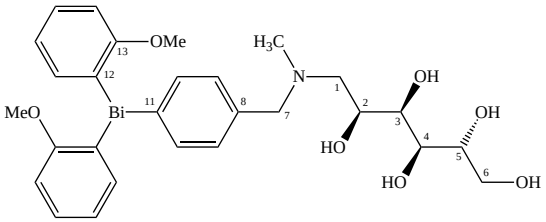

Compound: **66**
$C_{28}H_{36}BiNO_7$
MW: 707.58 $\frac{g}{mol}$

^{1}H NMR (300 MHz, $CDCl_3$) δ = 7.58 (d, 2 H, J = 7.5 Hz, H^{Ar}), 7.38 (d, 2 H, J = 7.1 Hz, H^{Ar}), 7.34 - 7.22 (m, 4 H, H^{Ar}), 7.04 (d, 2 H, J = 8.1 Hz, H^{Ar}), 6.82 (t, 2 H, J = 7.2 Hz, H^{Ar}), 4.01 (m, 1 H, C-2), 3.88 - 3.58 (m, 13 H, 2 x CH_3, C-3, C-4, C-5, C-6, C-7), 2.74 (d, 2 H, J = 8.4 Hz, C-1), 2.30 (s, 3,H, CH_3) ppm.
^{13}C NMR (75.5 MHz, $CDCl_3$) δ = 163.4 (ipso C-12), 154.3 (ipso C-11), 144.2 (ipso C-8), 139.3, 139.1 (2 x CH^{Ar}), 136.5 (ipso C-13), 132.6, 130.7, 125.0, 111.2 (4 x CH^{Ar}), 73.3, 72.9, 72.4 (C-3, C-4, C-5), 64.7 (C-7), 63.1 (C-6), 60.8 (C-1), 56.1 (2 x CH_3), 42.5 (CH_3) ppm.

Heptakis{6-O-[p-(Bis(o-methoxy)phenyl)bismuthyl]benzyl-2,3-di-O-methyl}cyclomaltoheptaose

Following General Procedure G, to a solution of **67** (CD) (100 mg, 0.075 mmol) in a mixture of THF/DMF 3:1 (v/v) (50 ml), NaH (60 % in mineral oil, 15.14 mg, 0.631 mmol) was added at 0 °C. After 30 min of stirring, a solution of bismuth compound **60** (44.56 mg, 0.075 mmol) in 10 ml THF was added dropwise. The reaction mixture was allowed to warm to ambient temperature and after completed conversion, the reaction was diluted with CH_2Cl_2 and successively washed with HCl (6 %) and saturated $NaHCO_3$. The combined organic layers were dried over Na_2SO_4, filtrated off and evaporated to dryness. The residue was purified on silica gel (C/EA 10:1 v/v) to afford compound **68** (325 mg, 0.066 mmol, 88 %) as white solid.

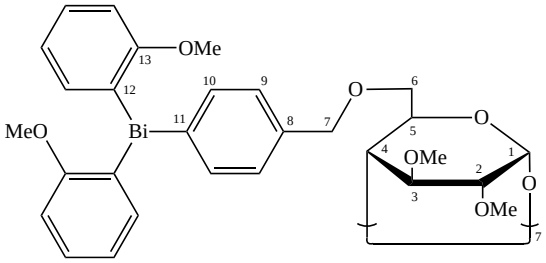

Compound: **68**
$C_{203}H_{231}Bi_7O_{49}$
MW: 4917.89 $\frac{g}{mol}$

^{1}H NMR (300 MHz, $CDCl_3$) δ = 7.58 - 7.28 (m, 4 H, H^{Ar}), 7.27 - 6.95 (m, 4 H, H^{Ar}), 6.94 - 6.65 (m, 4 H, H^{Ar}), 5.06 (s, 1 H, H-1), 4.25 (s, 2 H, H-7), 3.95 - 2.94 (m, 18 H, 4 x CH_3, H-4, H-2, H-3, H-5, H-6) ppm.
^{13}C NMR (75.5 MHz, $CDCl_3$) δ = 162.0 (ipso C-12), 153.0 (ipso C-11), 143.5 (ipso C-8), 138.8, 138.0 (2 x CH^{Ar}), 137.4 (ipso C-13), 129.5, 129.2, 124.2, 110.0 (4 x CH^{Ar}), 98.8 (C-1), 82.1 (C-2), 82.0 (C-3), 80.0 (C-4), 73.5 (C-7), 71.3 (C-5), 69.4 (C-6), 61.5, 58.6 (2 x CH_3), 55.6 (2 x CH_3) ppm.

5.3.7 Polymerization of bismuth compounds

{p-[Bis(o-methoxy)phenyl]bismuthyl}benzene modified polystyrene

Compound **22** (0.22 g, 0.42 mmol) and styrene **69** (0.35 g, 3.37 mmol) are solved in 10 ml dry toluene in a ratio of 1:8. The initiator AIBN (3.5 mg, 0.02 mmol) was added to the solution and the reaction mixture was heated to 80 °C under nitrogen atmosphere for 48 h. The solution was allowed to cool to room temperature and the solvent was removed under reduced pressure. The residue was taken up in 4 ml THF and added dropwise to vigorously stirred cold methanol. A colourless precipitate is formed, filtrated and dried. The bismuth-polystyrene **70** is obtained as a colourless powder.

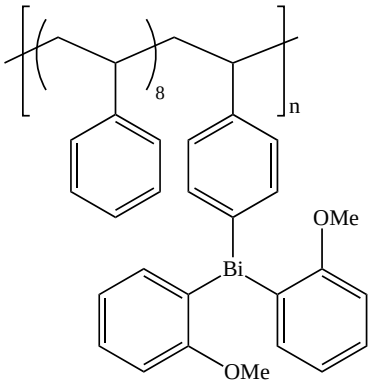

Compound: **70**
T_G: 139-141 °C

^{1}H NMR (300 MHz, $CDCl_3$): see appendix (Fig. 6.21)
^{13}C NMR (75.5 MHz, $CDCl_3$): see appendix (Fig. 6.22)

6 Appendix

6.1 Selected NMR spectra

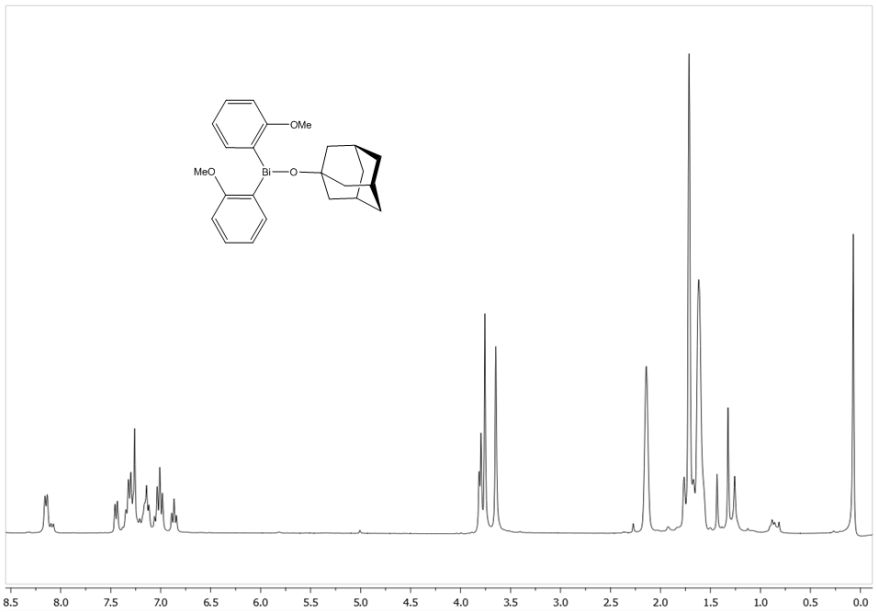

Fig. 6.1: ^{1}H-spectrum of compound **40**.

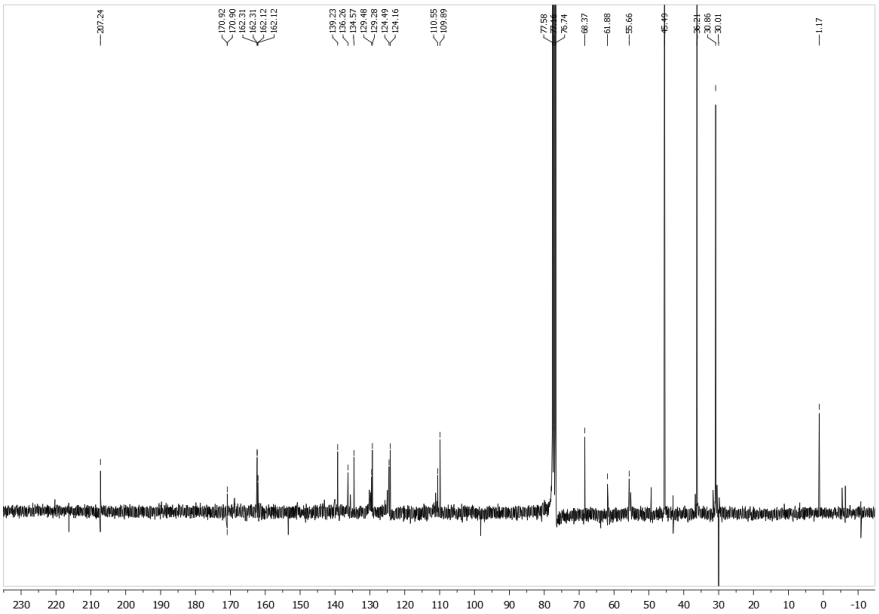

Fig. 6.2: ^{13}C-spectrum of compound **40**.

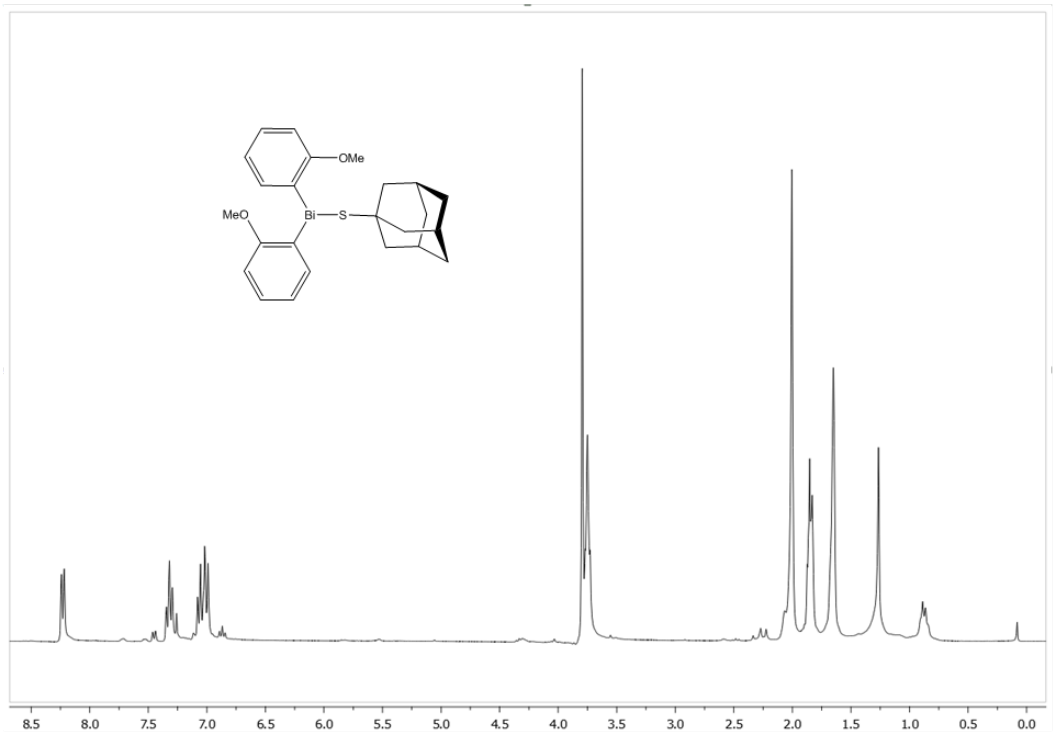

Fig. 6.3: ^{1}H-spectrum of compound **41**.

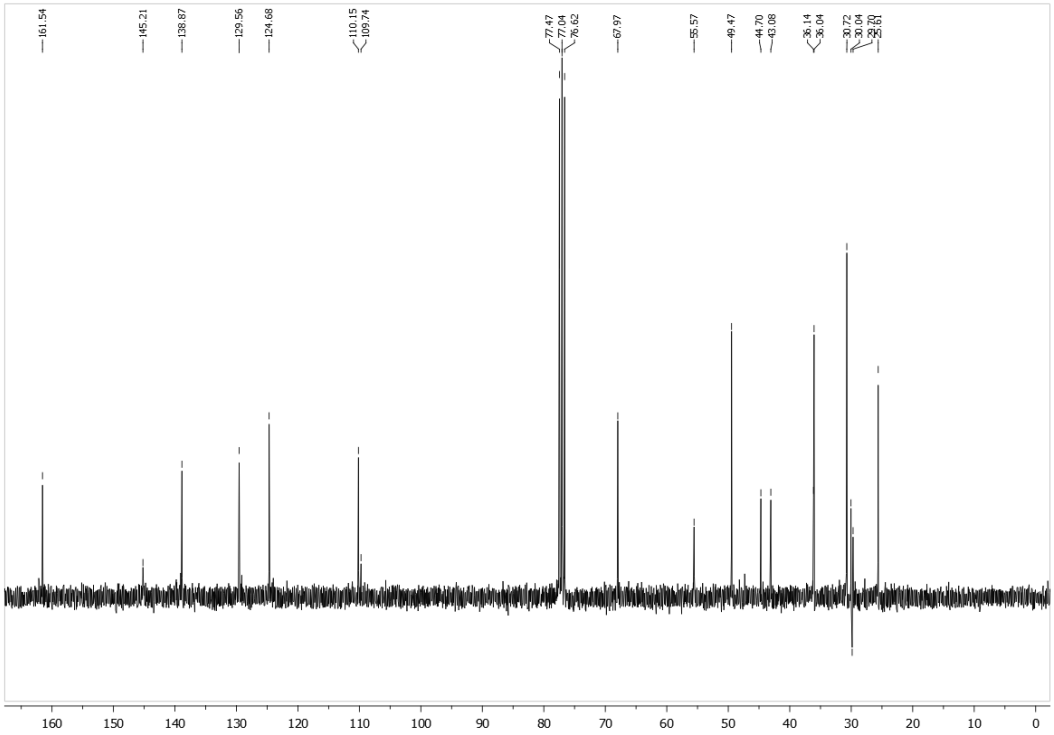

Fig. 6.4: ^{13}C-spectrum of compound **41**.

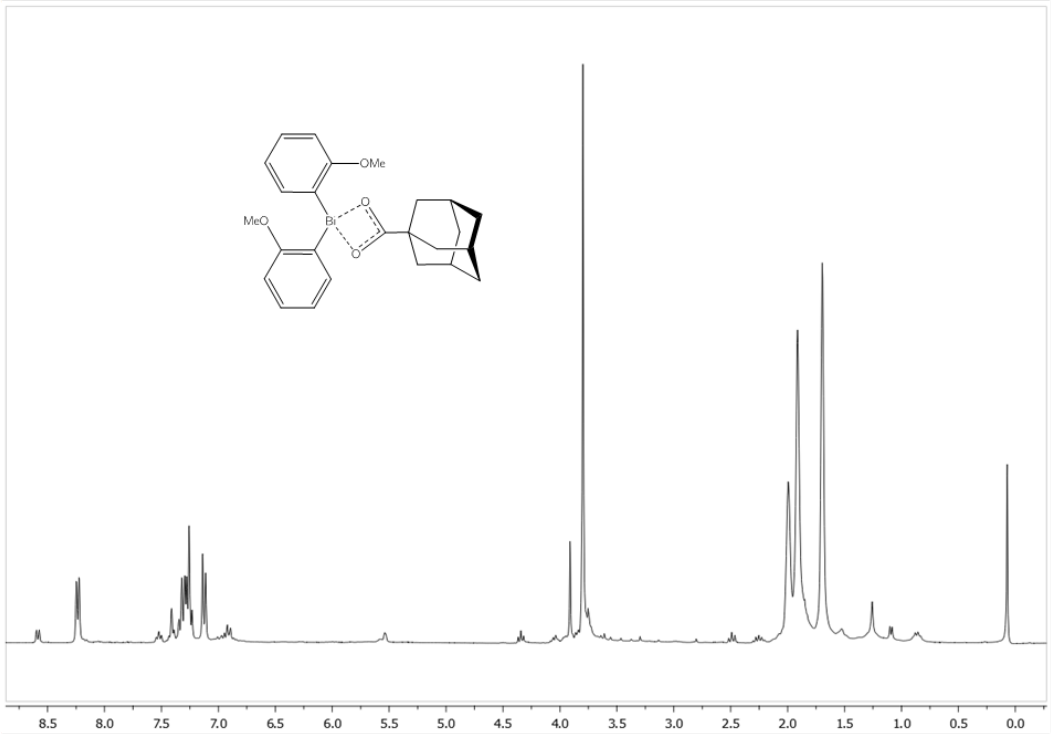

Fig. 6.5: ^{1}H-spectrum of compound **42**.

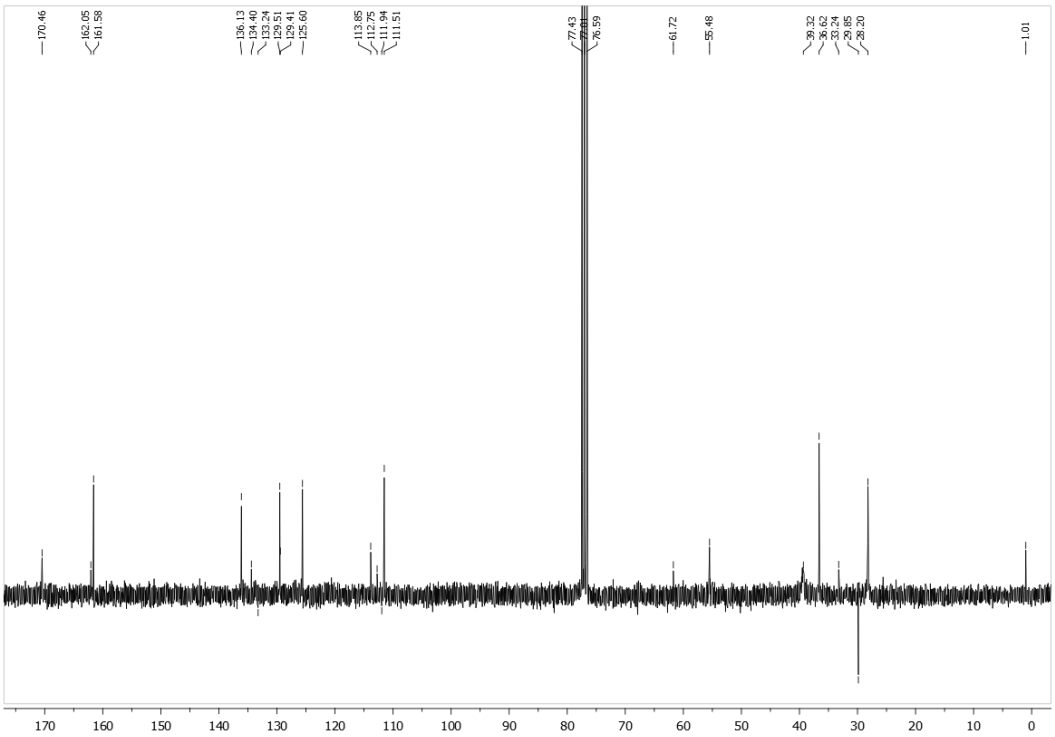

Fig. 6.6: ^{13}C-spectrum of compound **42**.

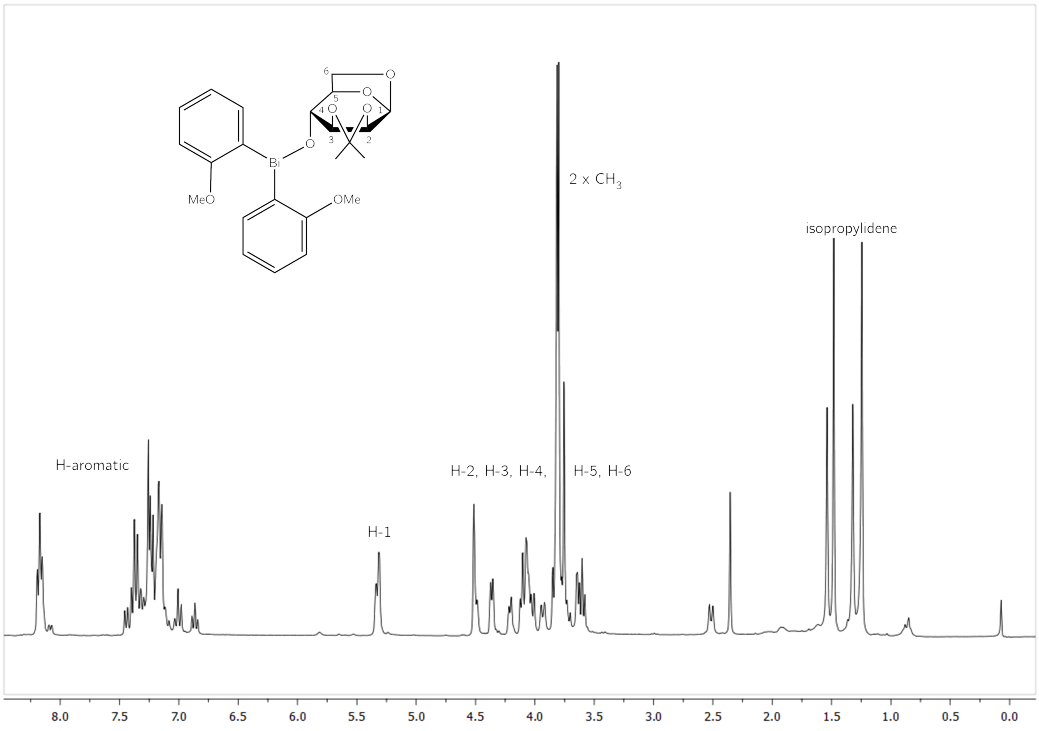

Fig. 6.7: ^{1}H-spectrum of compound **44** (t = 0 h).

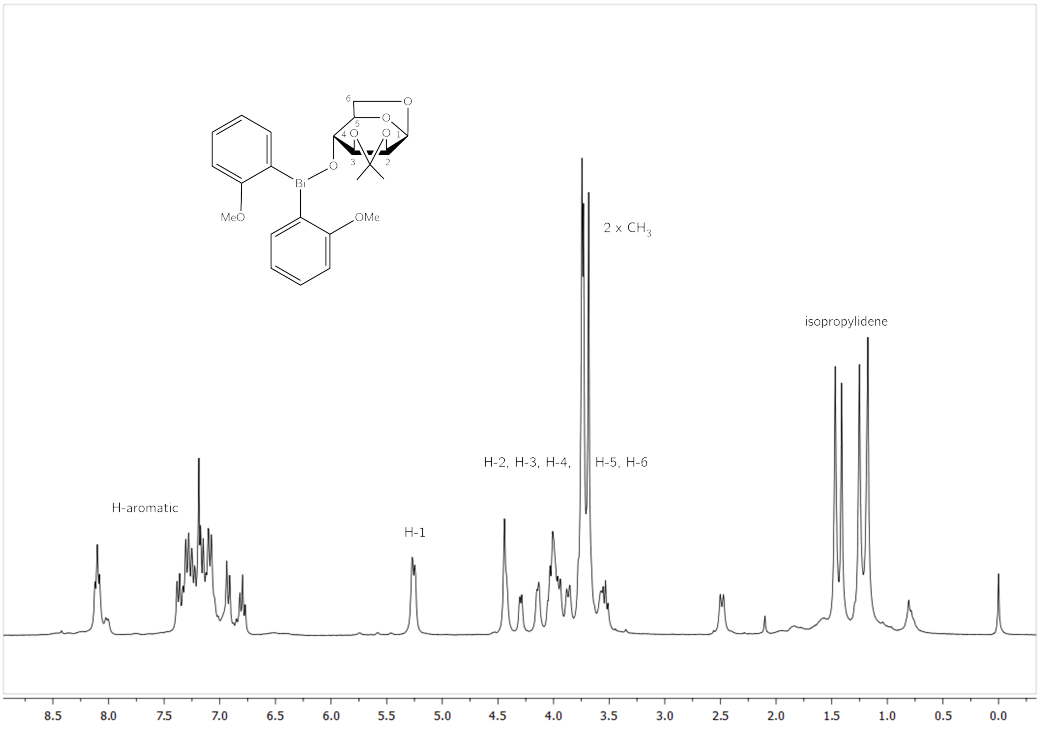

Fig. 6.8: ^{1}H-spectrum of compound **44** (t = 72 h).

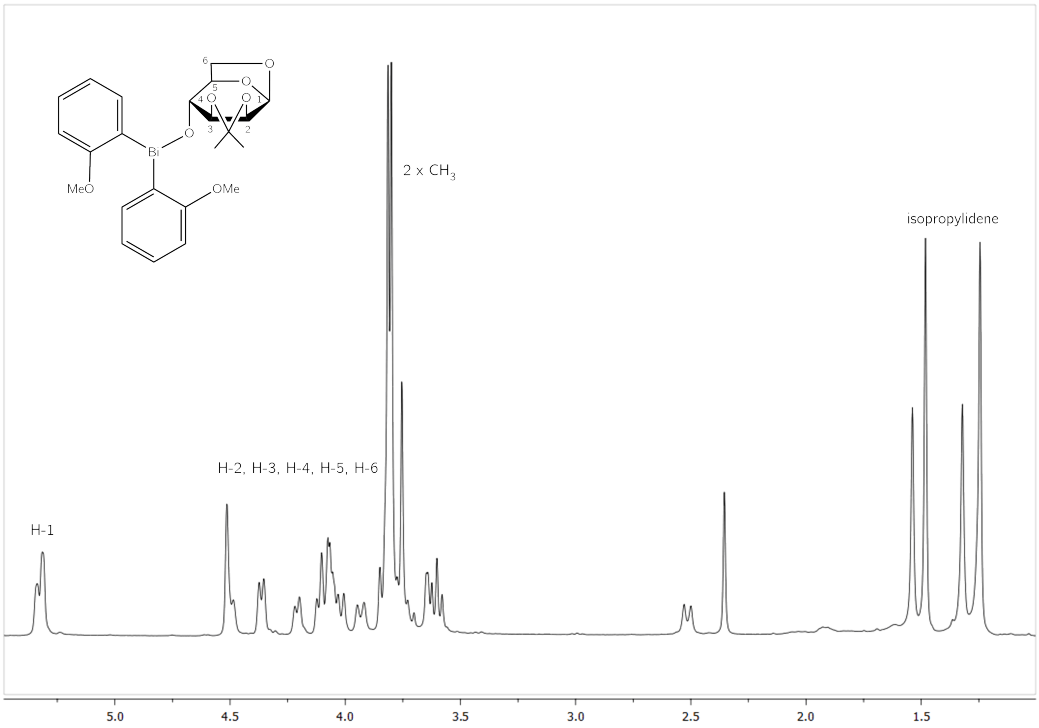

Fig. 6.9: Partial view of ^{1}H-spectrum of compound **44** (t = 0 h).

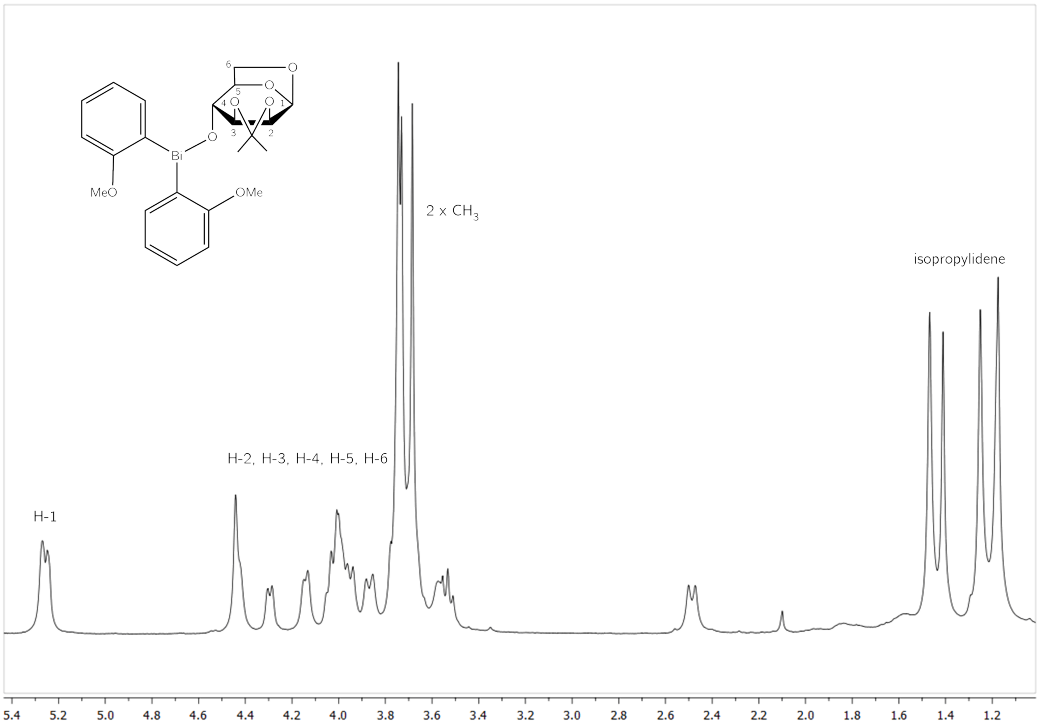

Fig. 6.10: Partial view of ^{1}H-spectrum of compound **44** (t = 72 h).

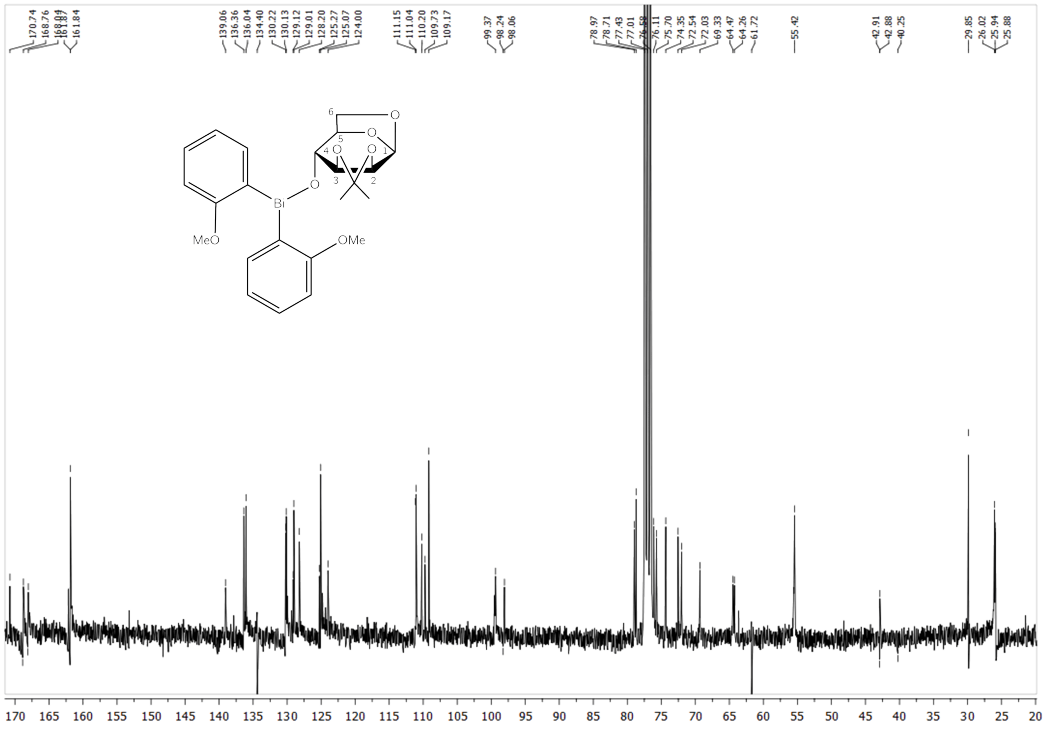

Fig. 6.11: ^{13}C-spectrum of compound **44** (t = 0 h).

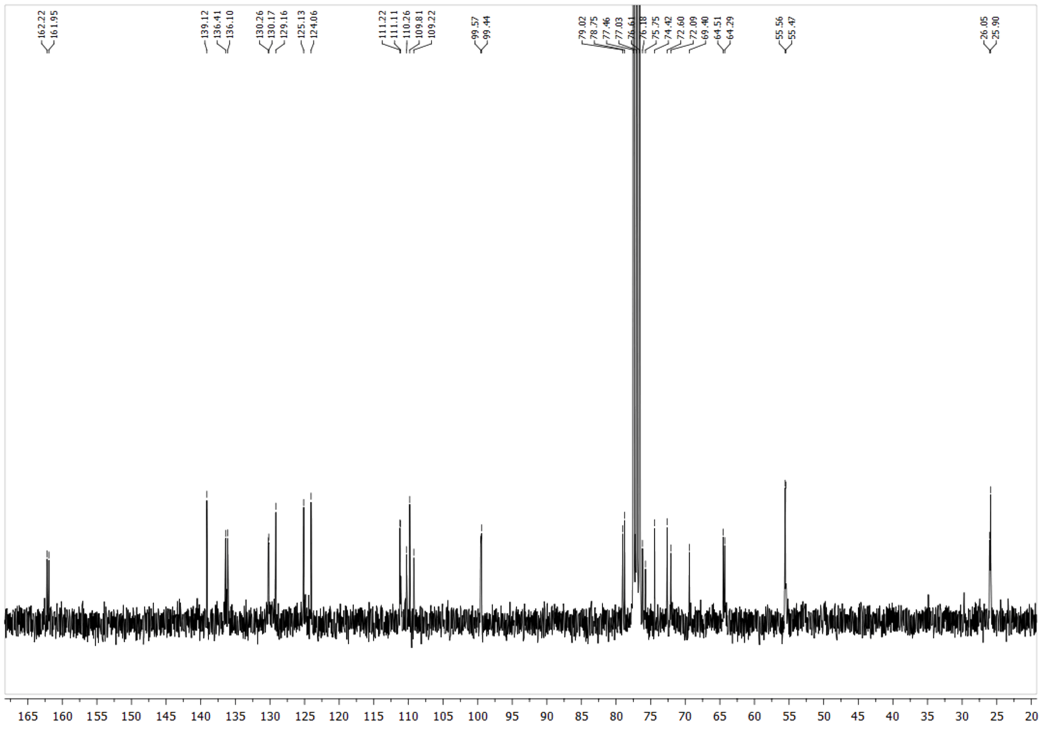

Fig. 6.12: ^{13}C-spectrum of compound **44** (t = 72 h).

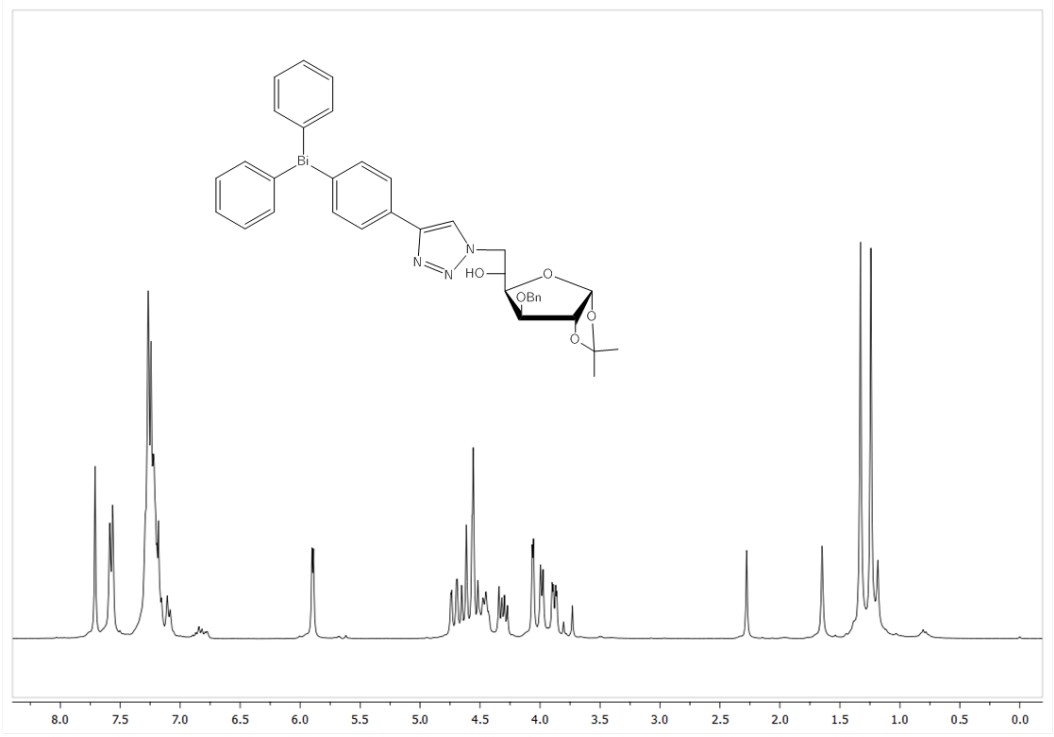

Fig. 6.13: ^{1}H-spectrum of compound **51**.

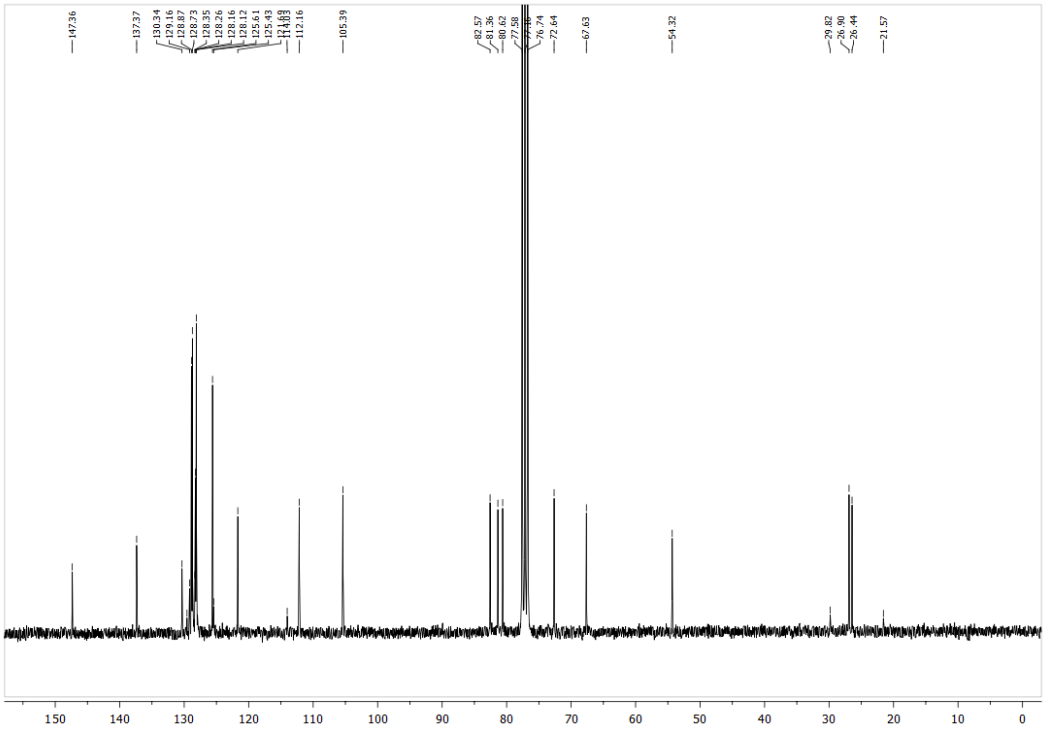

Fig. 6.14: ^{13}C-spectrum of compound **51**.

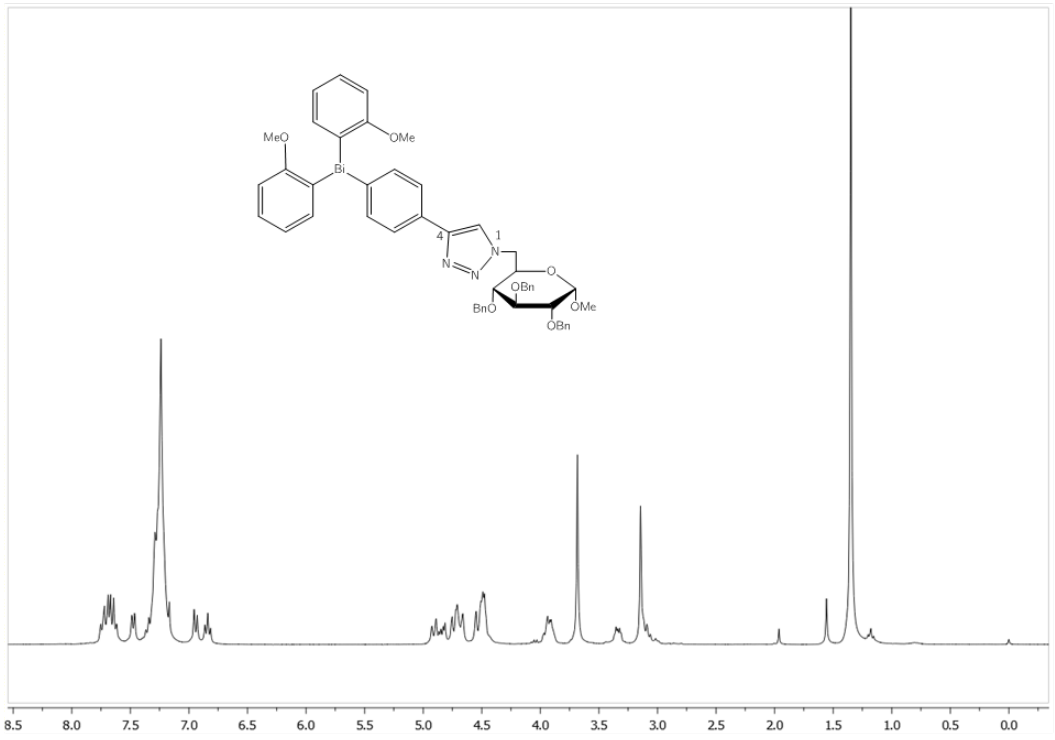

Fig. 6.15: ^{1}H-spectrum of compound **52**.

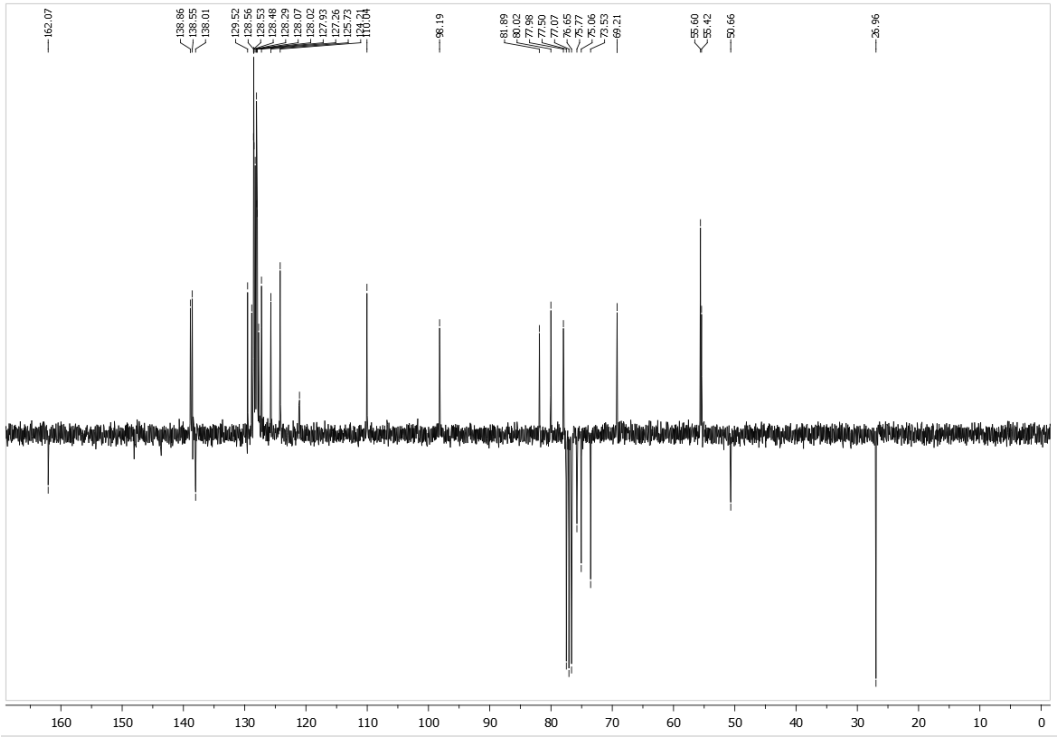

Fig. 6.16: ^{13}C-spectrum of compound **52**.

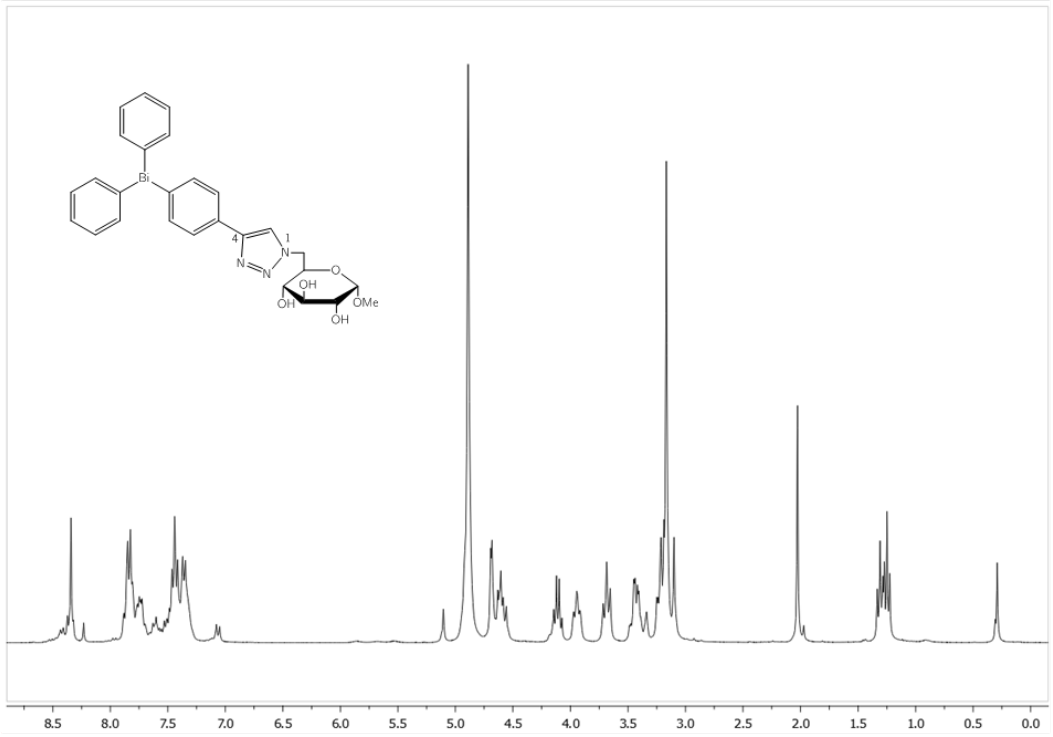

Fig. 6.17: ^{1}H-spectrum of compound **53**.

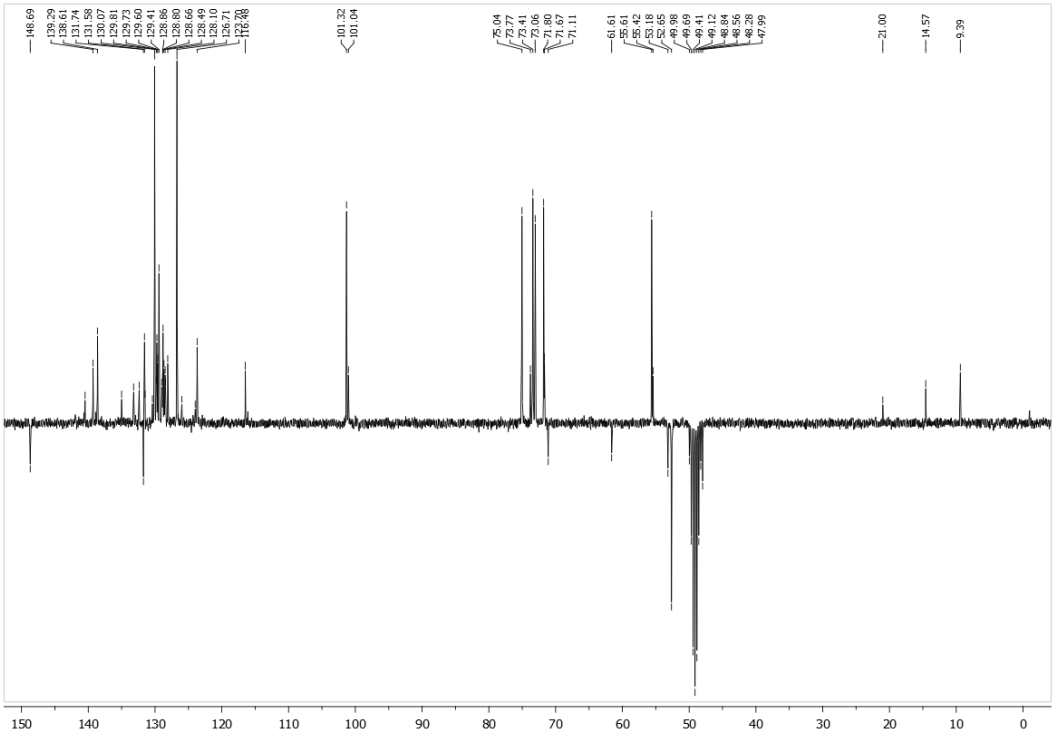

Fig. 6.18: ^{13}C-spectrum of compound **53**.

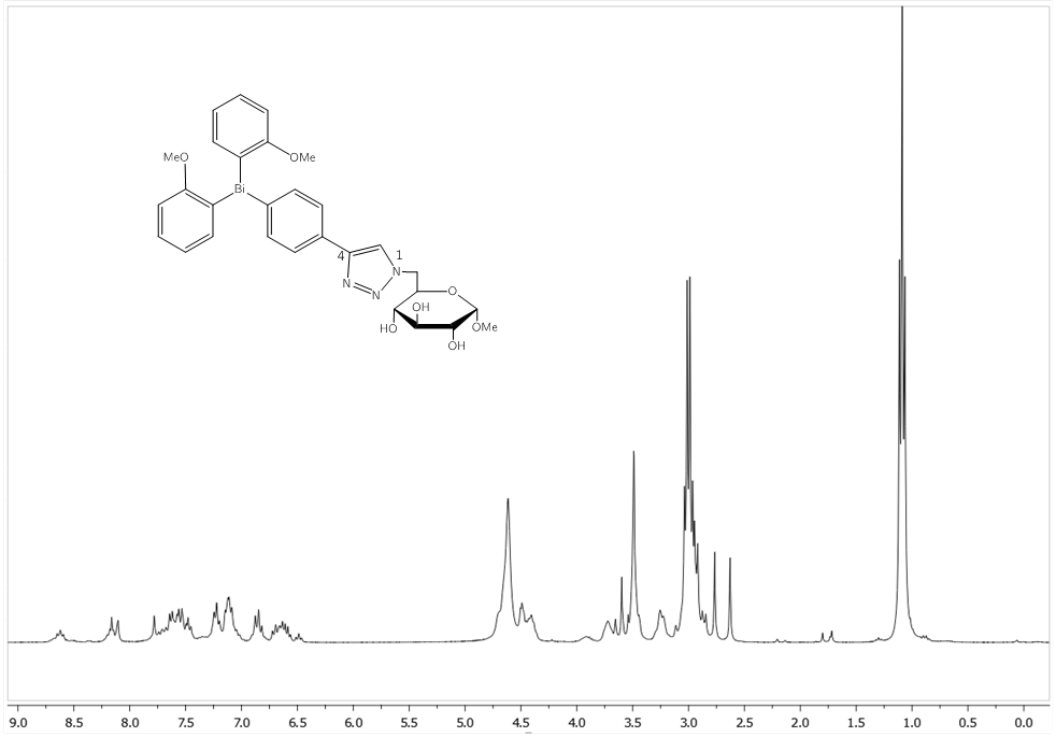

Fig. 6.19: ^{1}H-spectrum of compound **54**.

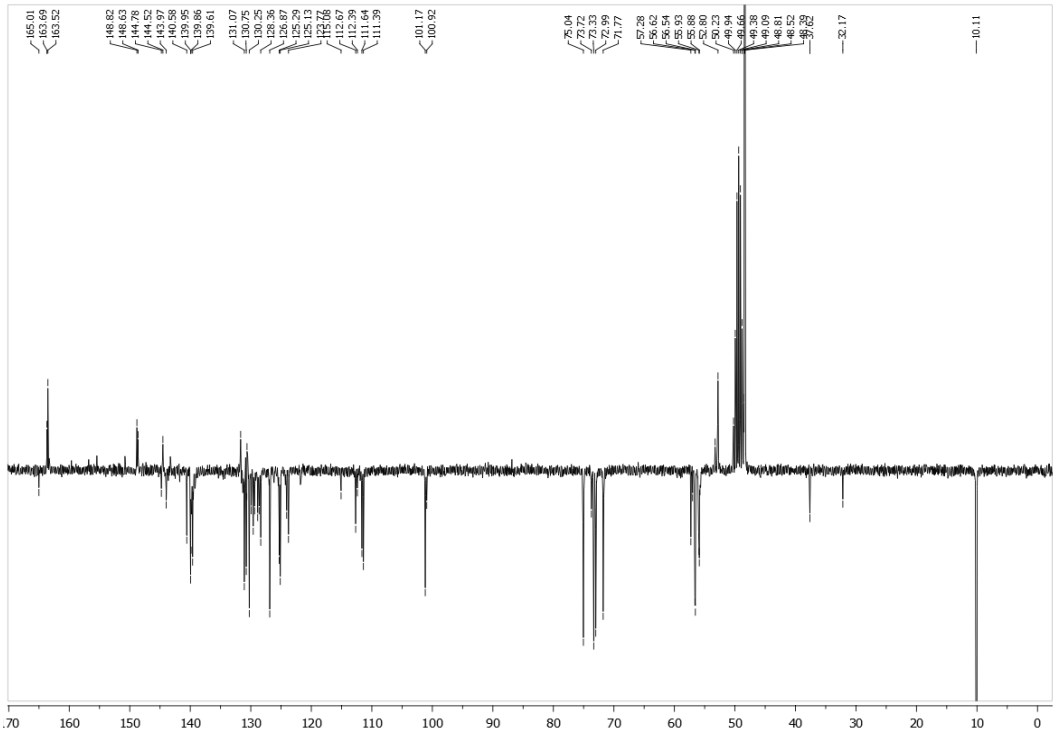

Fig. 6.20: ^{13}C-spectrum of compound **54**.

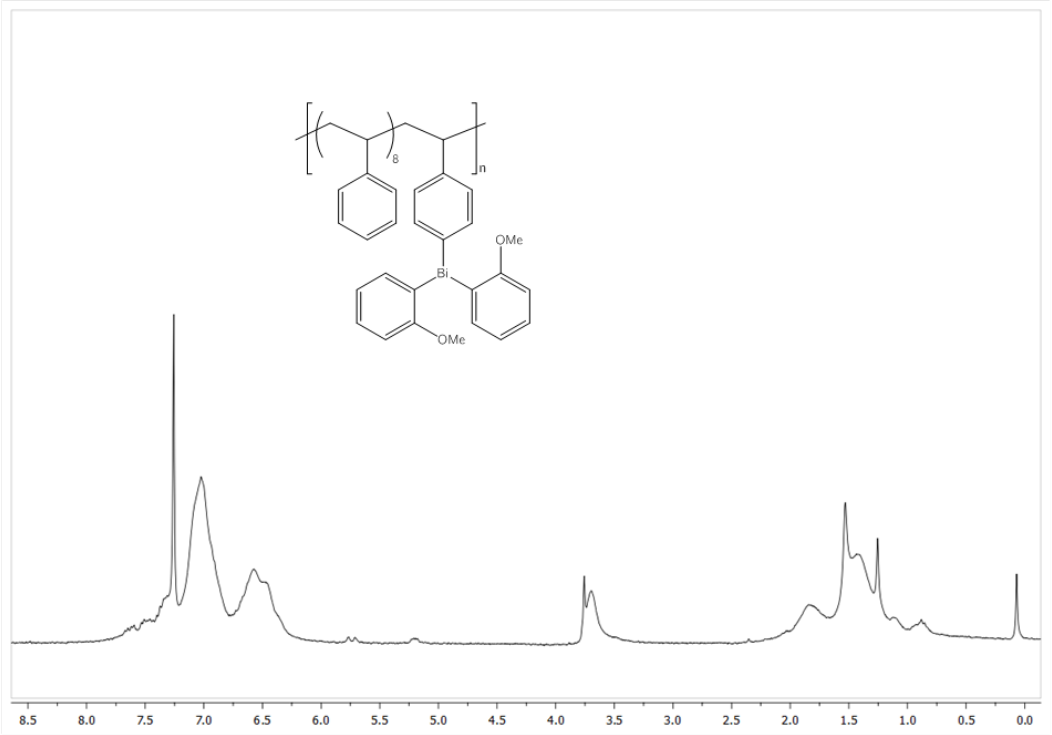

Fig. 6.21: ^{1}H-spectrum of compound **70**.

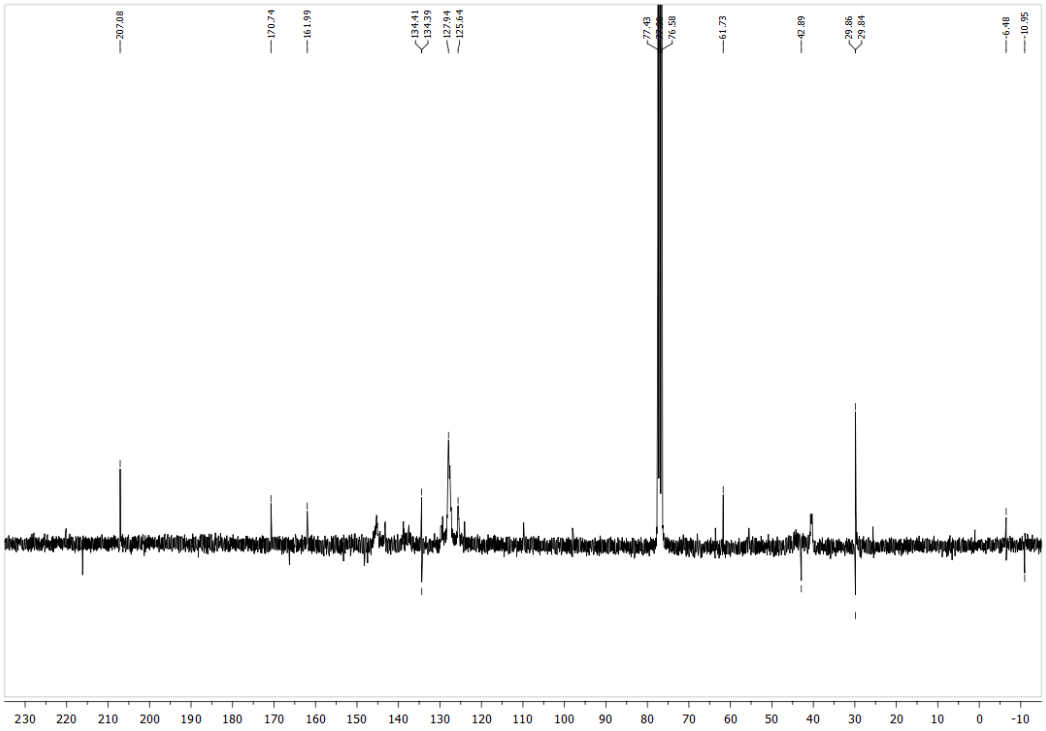

Fig. 6.22: ^{13}C-spectrum of compound **70**.

6.2 XRD Analysis Data

Table 6.1: Crystal data and structure refinement for compound **10**.

Compound	**10**, $BiPh_3$(d)
Empirical formula	$C_{18}H_{15}Bi$
Formula weight	440.28 $\frac{g}{mol}$
Temperature	100(2) K
Wavelength	0.71073 Å
Crystal system	Monoclinic
Space group	C2/c
Unit cell dimensions	a = 27.5842(15) Å, $\alpha = 90\,^\circ$
	b = 5.7415(3) Å, $\beta = 114.315(2)\,^\circ$
	c = 20.3318(11) Å, $\gamma = 90\,^\circ$
Volume	2934.4(3) $Å^3$
Z	8
Density (calculated)	1.993 mg/m^3
Absorption coefficient	12.000 mm^{-1}
F(000)	1648
Theta range for data collection	1.620 to 30.182 °
Index ranges	-38<=h<=38, -8<=k<=8, -28<=l<=28
Reflections collected	43860
Independent reflections	4303 [R(int) = 0.0805]
Completeness to theta = 25.242 °	100.0 %
Refinement method	Full-matrix least-squares on F^2
Data / restraints / parameters	4303 / 0 / 172
Goodness-of-fit on F2	1.062
Final R indices [I>2sigma(I)]	R1 = 0.0281, wR2 = 0.0627
R indices (all data)	R1 = 0.0373, wR2 = 0.0697
Largest diff. peak and hole	1.666 and -1.940 $e.Å^{-3}$

Table 6.3: Crystal data and structure refinement for compound **11**.

Compound	**11**, $BiTol_3$
Empirical formula	$C_{21}H_{21}Bi$
Formula weight	482.36 $\frac{g}{mol}$
Temperature	100(2) K
Wavelength	0.71073 Å
Crystal system	Triclinic
Space group	P-1
Unit cell dimensions	a = 6.3644(2) Å, α = 91.632(2) °
	b = 10.4568(4) Å, β = 91.587(2) °
	c = 13.9258(5) Å, γ = 107.494(2) °
Volume	882.92(5) $Å^3$
Z	2
Density (calculated)	1.814 mg/m^3
Absorption coefficient	9.979 mm^{-1}
F(000)	460
Crystal size	0.31 x 0.22 x 0.14 mm^3
Theta range for data collection	1.46 to 28.00 °
Index ranges	-8<=h<=8, -13<=k<=13, -18<=l<=18
Reflections collected	57430
Independent reflections	4277 [R(int) = 0.0628]
Completeness to theta = 28.00 °	100.0 %
Max. and min. transmission	0.3356 and 0.1479
Refinement method	Full-matrix least-squares on F^2
Data / restraints / parameters	4277 / 0 / 202
Goodness-of-fit on F2	1.071
Final R indices [I>2sigma(I)]	R1 = 0.0154, wR2 = 0.0405
R indices (all data)	R1 = 0.0165, wR2 = 0.0408
Largest diff. peak and hole	1.192 and -0.899 $e.Å^{-3}$

Table 6.5: Crystal data and structure refinement for compound **13**.

Compound	**13**, Bi(p–NMe_2Ph)$_3$
Empirical formula	$C_{24}H_{30}BiN_3$
Formula weight	569.49 $\frac{g}{mol}$
Temperature	100(2) K
Wavelength	0.71073 Å
Crystal system	Triclinic
Space group	P-1
Unit cell dimensions	a = 11.2464(7) Å, α = 110.690(4) °
	b = 11.3612(8) Å, β = 102.796(3) °
	c = 11.3921(7) Å, γ = 111.117(3) °
Volume	1164.42(14) Å^3
Z	2
Density (calculated)	1.624 mg/m^3
Absorption coefficient	7.584 mm^{-1}
F(000)	556
Crystal size	0.230 x 0.190 x 0.180 mm^3
Theta range for data collection	2.118 to 28.000 °
Index ranges	-14<=h<=14, -14<=k<=14, -15<=l<=15
Reflections collected	42541
Independent reflections	5601 [R(int) = 0.0914]
Completeness to theta = 28.000°	99.9 %
Refinement method	Full-matrix least-squares on F^2
Data / restraints / parameters	5601 / 0 / 259
Goodness-of-fit on F2	1.014
Final R indices [I>2sigma(I)]	R1 = 0.0340, wR2 = 0.0727
R indices (all data)	R1 = 0.0411, wR2 = 0.0754
Largest diff. peak and hole	1.375 and -1.503 e.Å^{-3}

Table 6.7: Crystal data and structure refinement for compound **14**.

Compound	**14**, Bi(p–OMePh)$_3$
Empirical formula	$C_{21}H_{21}BiO_3$
Formula weight	530.36 $\frac{g}{mol}$
Temperature	100(2) K
Wavelength	0.71073 Å
Crystal system	Trigonal
Space group	R-3
Unit cell dimensions	a = 13.0002(3) Å, α = 90 °
	b = 13.0002(3) Å, β = 90 °
	c = 18.8816(5) Å, γ = 120 °
Volume	2763.56(15) Å^3
Z	6
Density (calculated)	1.912 mg/m^3
Absorption coefficient	9.586 mm^{-1}
F(000)	1524
Theta range for data collection	3.134 to 27.999 °
Index ranges	-17<=h<=17, -17<=k<=17, -24<=l<=24
Reflections collected	32482
Independent reflections	1486 [R(int) = 0.2211]
Completeness to theta = 27.999 °	99.9 % [
Refinement method	Full-matrix least-squares on F^2
Data / restraints / parameters	1486 / 0 / 77
Goodness-of-fit on F2	0.574
Final R indices [I>2sigma(I)]	R1 = 0.0272, wR2 = 0.0708
R indices (all data)	R1 = 0.0304, wR2 = 0.0730
Largest diff. peak and hole	0.961 and -1.603 e.Å^{-3}

Table 6.9: Crystal data and structure refinement for compound **15**.

Compound	**15**, Bi(o–OMePh)$_3$
Empirical formula	$C_{21}H_{21}BiO_3$
Formula weight	529.60 $\frac{g}{mol}$
Temperature	100(2) K
Wavelength	0.71073 Å
Crystal system	Trigonal
Space group	R-3
Unit cell dimensions	a = 15.8380(3) Å, α = 94.5870(10) °
	b = 15.8380(3) Å, β = 94.5870(10) °
	c = 15.8380(3) Å, γ = 94.5870(10) °
Volume	3932.5(2) Å^3
Z	8
Density (calculated)	1.789 mg/m^3
Absorption coefficient	8.982 mm^{-1}
F(000)	2026
Crystal size	0.280 x 0.240 x 0.190 mm^3
Theta range for data collection	1.295 to 30.157 °
Index ranges	-22<=h<=21, -22<=k<=22, -22<=l<=22
Reflections collected	289361
Independent reflections	7741 [R(int) = 0.3529]
Completeness to theta = 25.242 °	100.0 %
Refinement method	Full-matrix least-squares on F^2
Data / restraints / parameters	7741 / 0 / 314
Goodness-of-fit on F2	1.157
Final R indices [I>2sigma(I)]	R1 = 0.0693, wR2 = 0.1960
R indices (all data)	R1 = 0.0816, wR2 = 0.2023
Largest diff. peak and hole	2.627 and -4.856 e.Å^{-3}

Table 6.11: Crystal data and structure refinement for compound **16**.

Compound	**16**, Bi(di−*o*−OMePh)$_3$
Empirical formula	$C_{24}H_{27}BiO_6$
Formula weight	620.43 $\frac{g}{mol}$
Temperature	100(2) K
Wavelength	0.71073 Å
Crystal system	Monoclinic
Space group	$P2_1/c$
Unit cell dimensions	a = 15.9319(7)Å, $\alpha = 90°$
	b = 20.5709(9)Å, $\beta = 110.616(2)°$
	c = 15.1264(6)Å, $\gamma = 90°$
Volume	4640.0(3) Å^3
Z	8
Density (calculated)	1.776 mg/m^3
Absorption coefficient	7.636 mm^{-1}
F(000)	2416
Theta range for data collection	1.366 to 27.999 °
Index ranges	-20<=h<=21, -27<=k<=27, -19<=l<=19
Reflections collected	182421
Independent reflections	11191 [R(int) = 0.1317]
Completeness to theta = 27.999°	100.0 %
Refinement method	Full-matrix least-squares on F^2
Data / restraints / parameters	11191 / 0 / 571
Goodness-of-fit on F2	0.997
Final R indices [I>2sigma(I)]	R1 = 0.0356, wR2 = 0.0739
R indices (all data)	R1 = 0.0507, wR2 = 0.0807
Largest diff. peak and hole	2.518 and -3.368 e.Å^{-3}

Table 6.13: Crystal data and structure refinement for compound **19**.

Identification code	**19**, $(o\text{–OMePh})_2$BiCl
Empirical formula	$C_{14}H_{14}BiClO_2$
Formula weight	458.68 $\frac{g}{mol}$
Temperature	100(2) K
Wavelength	0.71071Å
Crystal system	Triclinic
Space group	P-1
Unit cell dimensions	a = 8.949(3) Å, α = 104.514(11) °
	b = 8.958(2) Å, β = 100.225(11) °
	c = 9.196(3) Å, γ = 95.169(10)°
Volume	695.43 $Å^3$
Z	2
Density (calculated)	2.191 mg/m^3
Absorption coefficient	12.860 mm^{-1}
F(000)	428
Crystal size	0.230 x 0.130 x 0.120 mm^3
Theta range for data collection	2.336 to 26.988 °
Index ranges	-11<=h<=11 -11<=k<=11
	-0<=l<=11
Reflections collected	3033
Independent reflections	3033 [R(int) = 0.2185]
Completeness to theta = 26.988 °	99.9 %
Refinement method	Full-matrix least-squares on F^2
Data / restraints / parameters	3033 / 0 / 166
Goodness-of-fit on F2	1 084
Final R indices [I>2sigma(I)]	R1 = 0.0555, wR2 = 0.1195
R indices (all data)	R1 = 0.0693, wR2 = 0.1281
Largest diff. peak and hole	2.236 and -2.357 e.$Å^{-3}$

Table 6.15: Crystal data and structure refinement for compound **22**.

Identification code	**22**, (o–OMePh)$_2$BiC$_6$H$_4$Vinyl
Empirical formula	$C_{22}H_{21}BiO_2$
Formula weight	526.37 $\frac{g}{mol}$
Temperature	293(2) K
Wavelength	0.7107 Å
Crystal system	Monoclinic
Space group	P 2_1/c
Unit cell dimensions	a = 16.2608(7) Å, α = 90 °
	b = 8.7673(4) Å, β = 91.692(2) °
	c = 13.3805(5) Å, γ = 90 °
Volume	1906.74(14) Å^3
Z	4
Density (calculated)	1.834 mg/m^3
Absorption coefficient	9.258 mm^{-1}
F(000)	1008
Theta range for data collection	1.25 to 30.14 °
Index ranges	-22<=h<=22, -12<=k<=12, -18<=l<=18
Reflections collected	70312
Independent reflections	5602 [R(int) = 0.1271]
Completeness to theta = 30.14 °	99.5 %
Refinement method	Full-matrix least-squares on F^2
Data / restraints / parameters	5602 / 0 / 228
Goodness-of-fit on F2	1.035
Final R indices [I>2sigma(I)]	R1 = 0.0322, wR2 = 0.0688
R indices (all data)	R1 = 0.0480, wR2 = 0.0826
Largest diff. peak and hole	1.840 and -1.593 e.Å^{-3}

Table 6.17: Crystal data and structure refinement for compound **28**.

Identification code	**28**, Bi−trialkyne
Empirical formula	$C_{24}H_{15}Bi$
Formula weight	512.34 $\frac{g}{mol}$
Temperature	100(2) K
Wavelength	0.71073 Å
Crystal system	Monoclinic
Space group	P 2_1/c
Unit cell dimensions	a = 8.9684(6) Å, α = 90 °
	b = 13.5576(10) Å, β = 93.912(3) °
	c = 15.5016(12) Å, γ = 90 °
Volume	1880.4(2) Å^3
Z	4
Density (calculated)	1.810 mg/m^3
Absorption coefficient	9.378 mm^{-1}
F(000)	968
Theta range for data collection	1.998 to 29.998 °
Index ranges	-12<=h<=12, -19<=k<=18, -21<=l<=21
Reflections collected	94806
Independent reflections	5480 [R(int) = 0.0830]
Completeness to theta = 29.998 °	100.0 %
Refinement method	Full-matrix least-squares on F^2
Data / restraints / parameters	5480 / 0 / 226
Goodness-of-fit on F2	1.029
Final R indices [I>2sigma(I)]	R1 = 0.0206, wR2 = 0.0455
R indices (all data)	R1 = 0.0266, wR2 = 0.0479
Largest diff. peak and hole	1.817 and -1.026 e.Å^{-3}

Table 6.19: Crystal data and structure refinement for compound **34**.

Identification code	**34**, $(o\text{–OMePh})_2BiNEt_2$
Empirical formula	$C_{18}H_{24}BiNO_2$
Formula weight	495.36 $\frac{g}{mol}$
Temperature	100(2) K
Wavelength	0.71073 Å
Crystal system	Triclinic
Space group	P-1
Unit cell dimensions	a = 7.8387(7) Å, α = 96.770(5) °
	b = 8.0694(7) Å, β = 99.399(4) °
	c = 14.8306(13) Å, γ = 102.820(4) °
Volume	890.77(14) $Å^3$
Z	2
Density (calculated)	1.847 mg/m^3
Absorption coefficient	9.903 mm^{-1}
F(000)	476
Theta range for data collection	1.410 to 27.000 °
Index ranges	-10<=h<=10, -10<=k<=10, -18<=l<=18
Reflections collected	21853
Independent reflections	3844 [R(int) = 0.0971]
Completeness to theta = 27.000 °	98.9 %
Refinement method	Full-matrix least-squares on F^2
Data / restraints / parameters	3844 / 0 / 203
Goodness-of-fit on F2	1.029
Final R indices [I>2sigma(I)]	R1 = 0.0342, wR2 = 0.0671
R indices (all data)	R1 = 0.0432, wR2 = 0.0800
Largest diff. peak and hole	1.881 and -1.838 $e.Å^{-3}$

Table 6.21: Crystal data and structure refinement for compound **35**.

Identification code	**35**, $(o\text{–}OMePh)_2BiNiPr_2$
Empirical formula	$C_{20}H_{28}BiNO_2$
Formula weight	523.41 $\frac{g}{mol}$
Temperature	100(2) K
Wavelength	0.71073 Å
Crystal system	Triclinic
Space group	P-1
Unit cell dimensions	a = 7.7643(5) Å, α = 88.067(2) °
	b = 8.2845(5) Å, β = 77.025(2) °
	c = 16.1630(9) Å, γ = 74.920(3) °
Volume	977.89(10) $Å^3$
Z	2
Density (calculated)	1.778 mg/m^3
Absorption coefficient	9.026 mm^{-1}
F(000)	508
Theta range for data collection	1.293 to 28.996 °
Index ranges	-10<=h<=10, -11<=k<=11, -22<=l<=22
Reflections collected	58691
Independent reflections	5207 [R(int) = 0.0585]
Completeness to theta = 25.242 °	100.0 %
Refinement method	Full-matrix least-squares on F^2
Data / restraints / parameters	5207 / 0 / 223
Goodness-of-fit on F2	1.188
Final R indices [I>2sigma(I)]	R1 = 0.0158, wR2 = 0.0384
R indices (all data)	R1 = 0.0183, wR2 = 0.0472
Largest diff. peak and hole	1.175 and -0.826 e.$Å^{-3}$

Table 6.23: Crystal data and structure refinement for compound **36**.

Identification code	**36**, $(o\text{–OMePh})_2\text{BiNTMS}_2$
Empirical formula	$C_{20}H_{32}BiNO_2Si_2$
Formula weight	583.63 $\frac{g}{mol}$
Temperature	100(2) K
Wavelength	0.71073 Å
Crystal system	Triclinic
Space group	P-1
Unit cell dimensions	a = 8.4764(6) Å, α = 93.196(4) °
	b = 9.3837(6) Å, β = 100.505(4) °
	c = 14.9103(11) Å, γ = 96.893(4) °
Volume	1153.99(14) $Å^3$
Z	2
Density (calculated)	1.680 mg/m^3
Absorption coefficient	7.756 mm^{-1}
F(000)	572
Crystal size	0.41 x 0.16 x 0.15 mm^3
Theta range for data collection	2.19 to 28.00 °
Index ranges	-11<=h<=11, -12<=k<=12, -19<=l<=19
Reflections collected	43867
Independent reflections	5568 [R(int) = 0.1048]
Completeness to theta = 28.00 °	99.9 %
Max. and min. transmission	0.3891 and 0.1432
Refinement method	Full-matrix least-squares on F^2
Data / restraints / parameters	5568 / 0 / 243
Goodness-of-fit on F2	1.012
Final R indices [I>2sigma(I)]	R1 = 0.0315, wR2 = 0.0689
R indices (all data)	R1 = 0.0368, wR2 = 0.0707
Largest diff. peak and hole	2.787 and -2.810 e.$Å^{-3}$

Table 6.25: Crystal data and structure refinement for (o–OMePh)$_2$Bi–O–Bi(o–OMePh)$_2$

Identification code	(o–OMePh)$_2$Bi–O–Bi(o–OMePh)$_2$
Empirical formula	$C_{28}H_{28}Bi_2O_5$
Formula weight	431.23 $\frac{g}{mol}$
Temperature	100(2) K
Wavelength	0.71073 Å
Crystal system	Monoclinic
Space group	P 2_1/c
Unit cell dimensions	a = 20.8387(9) Å, α = 90 °
	b = 8.4051(4) Å, β = 94.374(2) °
	c = 15.4436(8) Å, γ = 90 °
Volume	2697.1(2) Å^3
Z	8
Density (calculated)	2.124 mg/m^3
Absorption coefficient	13.066 mm^{-1}
F(000)	1608
Theta range for data collection	2.61 to 30.00 °
Index ranges	-27<=h<=29, -11<=k<=11, -21<=l<=21
Reflections collected	106895
Independent reflections	7838 [R(int) = 0.0902]
Completeness to theta = 30.00 °	99.8 %
Refinement method	Full-matrix least-squares on F^2
Data / restraints / parameters	7838 / 0 / 320
Goodness-of-fit on F2	0.996
Final R indices [I>2sigma(I)]	R1 = 0.0265, wR2 = 0.0471
R indices (all data)	R1 = 0.0386, wR2 = 0.0504
Largest diff. peak and hole	1.733 and -1.838 e.Å^{-3}

Table 6.27: Crystal data and structure refinement for compound **40**.

Identification code	**40**, $(o\text{–}OMePh)_2BiOAda$
Empirical formula	$C_{24}H_{29}BiO_3$
Formula weight	574.45 $\frac{g}{mol}$
Temperature	296(2) K
Wavelength	0.71073 Å
Crystal system	Monoclinic
Space group	P-1
Unit cell dimensions	a = 7.9324(4) Å, α = 71.148(2) °
	b = 11.9411(6) Å, β = 81.518(2) °
	c = 12.3340(5) Å, γ = 77.298(3) °
Volume	1074.86(9) $Å^3$
Z	2
Density (calculated)	1.775 mg/m^3
Absorption coefficient	8.223 mm^{-1}
F(000)	560
Theta range for data collection	1.83 to 29.00 °
Index ranges	-10<=h<=10, -16<=k<=16, -16<=l<=16
Reflections collected	55441
Independent reflections	5720 [R(int) = 0.0803]
Completeness to theta = 29.00 °	99.9 %
Refinement method	Full-matrix least-squares on F^2
Data / restraints / parameters	5720 / 0 / 255
Goodness-of-fit on F2	0.893
Final R indices [I>2sigma(I)]	R1 = 0.0235, wR2 = 0.0397
R indices (all data)	R1 = 0.0310, wR2 = 0.0435
Largest diff. peak and hole	1.429 and -1.144 $e.Å^{-3}$

Table 6.29: Crystal data and structure refinement for compound **41**.

Identification code	**41**, $(o\text{–}OMePh)_2BiSAda$
Empirical formula	$C_{24}H_{29}BiO_2S$
Formula weight	590.51 $\frac{g}{mol}$
Temperature	100(2) K
Wavelength	0.71073 Å
Crystal system	Monoclinic
Space group	$P2_1/c$
Unit cell dimensions	a = 11.2486(9 Å, $\alpha = 90\,^\circ$
	b = 15.4514(15) Å, $\beta = 98.571(4)\,^\circ$
	c = 12.9688(12) Å, $\gamma = 90\,^\circ$
Volume	2228.9(3) $Å^3$
Z	4
Density (calculated)	1.760 mg/m^3
Absorption coefficient	8.020 mm^{-1}
F(000)	1152
Theta range for data collection	2.064 to 26.496 °
Index ranges	-14<=h<=13, 0<=k<=19, 0<=l<=16
Reflections collected	4903
Completeness to theta = 26.496 °	99.6 %
Refinement method	Full-matrix least-squares on F^2
Data / restraints / parameters	4903 / 6 / 250
Goodness-of-fit on F2	1.041
Final R indices [I>2sigma(I)]	R1 = 0.0553, wR2 = 0.0905
R indices (all data)	R1 = 0.0826, wR2 = 0.0988
Largest diff. peak and hole	3.140 and -1.221 $e.Å^{-3}$

Table 6.31: Crystal data and structure refinement for compound **42**.

Identification code	**42**, $(o\text{–OMePh})_2BiO_2CAda$
Empirical formula	$C_{25}H_{29}BiO_4$
Formula weight	602.46 $\frac{g}{mol}$
Temperature	100(2) K
Wavelength	0.71073 Å
Crystal system	Monoclinic
Space group	C2/c
Unit cell dimensions	a = 29.9406(16) Å, α = 90 °
	b = 11.3481(6) Å, β = 112.106(3) °
	c = 14.7663(8) Å, γ = 90 °
Volume	4648.3(4) $Å^3$
Z	8
Density (calculated)	1.722 mg/m^3
Absorption coefficient	7.613 mm^{-1}
F(000)	2352
Theta range for data collection	1.939 to 29.997 °
Index ranges	-42<=h<=42, -15<=k<=15, -20<=l<=20
Reflections collected	105777
Independent reflections	6782 [R(int) = 0.0853]
Completeness to theta = 29.997 °	99.9 %
Refinement method	Full-matrix least-squares on F^2
Data / restraints / parameters	6782 / 72 / 355
Goodness-of-fit on F2	1.000
Final R indices [I>2sigma(I)]	R1 = 0.0298, wR2 = 0.0643
R indices (all data)	R1 = 0.0590, wR2 = 0.0760
Largest diff. peak and hole	1.688 and -1.751 $e.Å^{-3}$

Table 6.33: Crystal data and structure refinement for compound **59**.

Identification code	**59**, $(o\text{–OMePh})_2$BiBzOH
Empirical formula	$C_{21}H_{20}BiO_3$
Formula weight	529.35 $\frac{g}{mol}$
Temperature	100(2) K
Wavelength	0.71073 Å
Crystal system	Tetragonal
Space group	I-4
Unit cell dimensions	a = 23.5775(9) Å, $\alpha = 90°$
	b = 23.5775(9) Å, $\beta = 90°$
	c = 6.9357(4) Å, $\gamma = 90°$
Volume	3855.5(4) $Å^3$
Z	8
Density (calculated)	1.824 mg/m^3
Absorption coefficient	9.161 mm^{-1}
F(000)	2024
Theta range for data collection	1.221 to 27.997°
Index ranges	-31<=h<=31, -31<=k<=31, -9<=l<=9
Reflections collected	60913
Independent reflections	4655 [R(int) = 0.0859]
Completeness to theta = 27.997°	100.0 %
Refinement method	Full-matrix least-squares on F^2
Data / restraints / parameters	4655 / 151 / 255
Goodness-of-fit on F2	1.087
Final R indices [I>2sigma(I)]	R1 = 0.0298, wR2 = 0.0721
R indices (all data)	R1 = 0.0338, wR2 = 0.0795
Absolute structure parameter	0.404(6)
Largest diff. peak and hole	1.099 and -0.579 $e.Å^{-3}$

Table 6.35: Crystal data and structure refinement for compound **60**.

Identification code	**60**, $(o\text{–OMePh})_2$BiBzBr
Empirical formula	$C_{21}H_{20}BiBrO_2$
Formula weight	593.26 $\frac{g}{mol}$
Temperature	100(2) K
Wavelength	0.71073 Å
Crystal system	Monoclinic
Space group	$P2_1/c$
Unit cell dimensions	a = 14.9230(4) Å, α = 90 °
	b = 8.1273(2) Å, β = 102.8440(10) °
	c = 16.6251(5) Å, γ = 90 °
Volume	1965.90(9) $Å^3$
Z	4
Density (calculated)	2.004 mg/m^3
Absorption coefficient	11.012 mm^{-1}
F(000)	1120
Theta range for data collection	1.400 to 27.996 °
Index ranges	-18<=h<=19, -10<=k<=10, -21<=l<=21
Reflections collected	92153
Independent reflections	4741 [R(int) = 0.1303]
Completeness to theta = 27.996 °	100.0 %
Refinement method	Full-matrix least-squares on F^2
Data / restraints / parameters	4741 / 0 / 228
Goodness-of-fit on F2	1.089
Final R indices [I>2sigma(I)]	R1 = 0.0264, wR2 = 0.0566
R indices (all data)	R1 = 0.0347, wR2 = 0.0725
Largest diff. peak and hole	0.722 and -1.524 e.$Å^{-3}$

Bibliography

[1] N. Akeroyd and B. Klumperman. "The combination of living radical polymerization and click chemistry for the synthesis of advanced macromolecular architectures". In: European Polymer Journal 47.6 (2011), pp. 1207–1231.

[2] H. Althaus et al. "Synthesis and Characterization of R 2 BiCl and RBiCl 2 [R = CH(SiMe 3) 2]". In: Organometallics 18.3 (1999), pp. 328–331.

[3] P. C. Andrews et al. "Anti-leishmanial activity of novel homo- and heteroleptic bismuth(iii) thiocarboxylates". In: Australian Journal of Chemistry 66.10 (2013), pp. 1297–1305.

[4] D. H. R. Barton et al. "Pentavalent organobismuth reagents. Part vi. Comparative migratory aptitudes of aryl groups in the arylation of phenols and enols by pentavalent bismuth reagents". In: Tetrahedron 42.12 (1986), pp. 3111–3122.

[5] G. Bauer. Handbuch der Anorganischen Chemie. Vol. 140. 1975, pp. 1081–1081.

[6] R. H. Blessing. "An empirical correction for absorption anisotropy". In: Acta Crystallographica Section A 51.1 (1995), pp. 33–38.

[7] H. J Breunig et al. "Hypervalent organobismuth(iii) carbonate, chalcogenides and halides with the pendant arm ligands 2-(Me2NCH2)C6H4 and 2,6-(Me2NCH2)2C6H3." In: Dalton transactions (Cambridge, England : 2003) 9226.14 (2008), pp. 1831–1842.

[8] A. Brown. "Bismuth Nanoparticles as Medical X-ray Contrast Agents: Synthesis, Characterization and Applications". In: Dissertations Thesis (2013).

[9] F. Challenger. "Organo-derivatives of bismuth". In: Journal of the American Chemical Society 105 (1914), p. 2210.

[10] J. Chen, T. Murafuji, and R. Tsunashima. "Insertion of benzyne into a Bi-S bond: A new synthetic route to ortho -functionalized bismuthanes and its application to the synthesis of dibenzothiophene". In: Organometallics 30.17 (2011), pp. 4532–4538.

[11] M. K. W. Choi and P. H. Toy. "Soluble polystyrene-based sulfoxide reagents for Swern oxidation reactions". In: Tetrahedron 59.36 (2003), pp. 7171–7176.

[12] S. Condon, C. Pichon, and M. Davi. “Preparation and synthetic applications of trivalent arylbismuth compounds as arylating reagents. A review”. In: Organic Preparations and Procedures International 46.2 (2014), pp. 89–131.

[13] R. H. Crabtree and D. M. Mingos. Comprehensive Organometallic CHemistry III. 2007, pp. 425–452.

[14] G.-L. Davies, I. Kramberger, and J. J. Davis. “Environmentally responsive MRI contrast agents”. In: Chemical Communications 49.84 (2013), p. 9704.

[15] L. Dawara, S. C. Joshi, and R. V. Singh. “Synthesis, Characterization, and Antimicrobial and Antispermatogenic Activity of Bismuth(III) and Arsenic(III) Derivatives of Biologically Potent Nitrogen and Sulfur Donor Ligands”. In: International Journal of Inorganic Chemistry 2012.Iii (2012), pp. 1–9.

[16] R. Diemer et al. “Synthesis, Characterization and Molecular Structures of some Bismuth(III) Complexes with Thiosemicarbazones and Dithiocarbazonic Acid Methylester Derivatives with Activity against Helicobacter Pylori.” In: Metal-based drugs 2.5 (1995), pp. 271–292.

[17] W. J. Evans, J. H. Hain, and J. W. Ziller. “Synthesis and first X-ray crystal structure of a Bi(OR)3 complex: tris(2,6-dimethylphenoxo)bismuth”. In: J. Chem. Soc., Chem. Commn. 0 (1989), pp. 1628–1629.

[18] L. D. Freedman and G. O. Doak. “Preparation, Reactions, and Physical Properties of Organobismuth Compounds”. In: Chemical Reviews 82.1 (1982), pp. 15–57.

[19] A. Gagnon, J. Dansereau, and A. Le Roch. “Organobismuth Reagents: Synthesis, Properties and Applications in Organic Synthesis”. In: Synthesis 49.08 (2017), pp. 1707–1745.

[20] H. Gilman and H. L. Yablunky. “Unsymmetrical Organobismuth Compounds”. In: Journal of the American Chemical Society 63.1 (1941), pp. 207–211.

[21] C. Gösweiner et al. “Novel smart MRI contrast agents based on nuclear quadrupole cross relaxation – pre-selection of promising compounds”. In: Magnetic Resonance Materials in Physics, Biology and Medicine 29.S1 (2016), pp. 371–372.

[22] C. Gösweiner et al. “Tuning nuclear quadtupole spin resonance”. In: (2018).

[23] M. Gynane et al. “Bulky Alkyls, Amides and Aryloxides of Main Group 5 Elements”. In: J.C.S. Dalton 15.86 (1986), pp. 3–7.

[24] A. Hassan et al. “Organobismuth(III) and Organobismuth(V) Complexes Containing Pyridyl and Amino Functional Groups.” In: Organometallics 15.26 (1996), pp. 5613–5621.

[25] M. Hébert et al. “Synthesis of highly functionalized triarylbismuthines by functional group manipulation and use in palladium- and copper-catalyzed arylation reactions”. In: Journal of Organic Chemistry 81.13 (2016), pp. 5401–5416.

[26] D. V. Hingorani, A. S. Bernstein, and M. D. Pagel. “A review of responsive MRI contrast agents: 2005–2014”. In: Contrast Media Mol Imaging 10 (2015), pp. 245–265.

[27] R. Huisgen et al. “1.3-Dipolare Cycloadditionen, XXIII. Einige Beobachtungen zur Addition organischer Azide an CC-Dreifachbindungen”. In: Chemische Berichte 98.12 (1965), pp. 4014–4021.

[28] F. Ignatious et al. “Anionic polymerization of arylbismuth, lead and tin derivatives of styrene and α-methylstyrene”. In: Makromolekulare Chemie. Macromolecular Symposia 60.1 (1992), pp. 247–257.

[29] F. Ignatious et al. “Organobismuth polymers as X-ray contrast materials: synthesis, characterization and properties”. In: Polymer 33.8 (1992), pp. 1724–1730.

[30] P. G. Jones et al. “Redetermination of the crystal structure of triphenylbismuth, (C6H5)3Bi”. In: Zeitschrift für Kristallographie 210.5 (1995), pp. 377–378.

[31] D. M. Keogan and D. M. Griffith. “Current and potential applications of bismuth-based drugs”. In: Molecules 19.9 (2014), pp. 15258–15297.

[32] R. Kimmich and E. Anoardo. Field-cycling NMR relaxometry. Vol. 44. 3-4. 2004, pp. 257–320.

[33] X. Kou et al. “Bismuth aryloxides”. In: Inorganic Chemistry 48.23 (2009), pp. 11002–11016.

[34] R. B. Lauffer. “Paramagnetic Metal Complexes as Water Proton Relaxation Agents for NMR Imaging: Theory and Design”. In: Chemical Reviews 87.5 (1987), pp. 901–927.

[35] W. Levason, B. Sheikh, and F. McCullough. “The synthesis and properties of substituted tertiary bismuthine ligands”. In: Journal of Coordination Chemistry 12.1 (1982), pp. 53–57.

[36] L. Liu et al. “Synthesis and Characterization of Bismuth (III) and Antimony (III) Calixarene Complexes”. In: Inorganic Chemistry 47.23 (2008), pp. 11143–11153.

[37] J. M. Lobez and T. M. Swager. “Radiation Detection : Resistivity Responses in Functional Poly (Olefin Sulfone)/ Carbon Nanotube Composites”. In: Angewandte Chemie (2010), pp. 95–98.

[38] J. M. Lobez and T. M. Swager. “Radiation detection: Resistivity responses in functional poly(olefin sulfone)/carbon nanotube composites”. In: Angewandte Chemie - International Edition 49.1 (2010), pp. 95–98.

[39] J. Luan, L. Zhang, and Z. Hu. “Synthesis, properties characterization and applications of various organobismuth compounds”. In: Molecules 16.5 (2011), pp. 4191–4230.

[40] D. J. Lurie. “Quadrupole-Dips Measured by Whole-Body Field-Cycling Relaxometry and Imaging”. In: Proc. Intl. Soc. Magn. Reson. Med. 292.1982 (1998), p. 1998.

[41] M. R. Mason et al. “Synthesis and characterization of chelating triamide complexes of bismuth and antimony”. In: Inorganic Chemistry 39.17 (2000), pp. 3931–3933.

[42] Y. Matano, S. A. Begum, and H. Suzuki. “A New Synthesis of Triarylbismuthanes via Directed Ligand Coupling of Oxazoline-Substituted Tetraarylbismuthonium Salts: Synthesis of Polystyrenes Bearing the Diarylbismuthino Group”. In: Synthesis 2001.07 (2001), pp. 1081–1085.

[43] D. Mendoza-Espinosa and T. A. Hanna. “Facile synthesis of bismuth(III) and antimony(III) complexes supported by silylated calix[5]arenes.” In: Inorganic chemistry 48.21 (2009), pp. 10312–10325.

[44] D. Mendoza-Espinosa and T. A. Hanna. “Synthesis, X-ray structures and reactivity of calix[5]arene bismuth(III) and antimony(III) complexes”. In: Dalton Transactions 26 (2009), p. 5211.

[45] D. Mendoza-Espinosa and T.A. Hanna. “Heterobimetallic bismuth(III)/Molybdenum(VI) and Antimony(III)/ Molybdenum(VI) Calix[5]arene complexes, progress toward modeling the SOHIO catalyst”. In: Inorganic Chemistry 48.15 (2009), pp. 7452–7456.

[46] D. Mendoza-Espinosa, A. L. Rheingold, and T. A. Hanna. “Synthesis of bismuth and antimony complexes of the ”larger” calix[n]arenes (n = 6–8); from mononuclear to tetranuclear complexes”. In: Dalton Transactions 26 (2009), p. 5226.

[47] T. Murafuji et al. “Activity of antifungal organobismuth(III) compounds derived from alkyl aryl Ketones against S. cerevisiae: Comparison with a heterocyclic bismuth scaffold consisting of a diphenyl sulfone”. In: Molecules 19.8 (2014), pp. 11077–11095.

[48] B. Nekoueishahraki et al. “Addition of Dimethylaminobismuth to Aldehydes, Ketones, Alkenes and Alkynes”. In: Angew. Chem. Int. Ed 48 (2009), pp. 4517–4520.

[49] B. Nekoueishahraki et al. “Organobismuth(III) and dibismuthine complexes bearing N,N’- disubstituted 1,8-diaminonaphthalene ligand: Synthesis, structure, and reactivity”. In: Organometallics 31.18 (2012), pp. 6697–6703.

[50] I. Norvick. “Interchange of Heavy Atoms in Organo-Metallic Compounds”. In: Nature 135 (1935), pp. 1038–1039.

[51] T. Ogawa et al. “Selective activation of primary carboxylic acids by electron-rich triarylbismuthanes. Application to amide and ester synthesis under neutral conditions”. In: J. Chem. Soc. Perkin Trans. 1 0.23 (1994), pp. 3473–3478.

[52] O. Rabin et al. “An X-ray computed tomography imaging agent based on long-circulating bismuth sulphide nanoparticles”. In: Nature Materials 5.2 (2006), pp. 118–122.

[53] A. F. M. Rahman et al. “Effect of π-accepting substituent on the reactivity and spectroscopic characteristics of triarylbismuthanes and triarylbismuth dihalides”. In: Journal of Organometallic Chemistry 689.21 (2004), pp. 3395–3401.

[54] D. W. H. Rankin, N. W. Mitzel, and C. A. Morrison. Structural Methods in Molecular Inorganic Chemistry. 1. 2013.

[55] M. L.N. Rao, D. Banerjee, and S. Giri. “Palladium-catalyzed cross-couplings of allylic carbonates with triarylbismuths as multi-coupling atom-efficient organometallic nucleophiles”. In: Journal of Organometallic Chemistry 695.10-11 (2010), pp. 1518–1525.

[56] V. V. Rostovtsev et al. “A Stepwise Huisgen Cycloaddition Process Catalyzed by Copper (I): Regioselective Ligation of Azides and Terminal Alkynes”. In: Angew. Chem. Int. Ed. 41.14 (2002), pp. 2596–2599.

[57] M. Rusek et al. “Bismuth amides as promising ALD precursors for Bi2Te3films”. In: Journal of Crystal Growth 470 (2017), pp. 128–134.

[58] H. Scharfetter. “An electronically tuned wideband probehead for NQR spectroscopy in the VHF range”. In: Journal of Magnetic Resonance 271 (2016), pp. 90–98.

[59] H. Scharfetter. CONQUER. 2017. URL: http://conquer.at/.

[60] H. Scharfetter. "Contrast by quadrupole enhanced relaxation (CONQUER): A concept for novel smart MRI contrast agents". In: Abstracts of the 1st workshop of the COST action CA15209 EURELAX. 2017.

[61] H. Scharfetter and Graz University of Technology. CONQUER - Innovative Contrast Agents for a Clear View in Medicine. URL: https://www.tugraz.at/en/research/fields-of-expertise/human-biotechnology/conquer-innovative-contrast-agents-for-a-clear-view-in-medicine/.

[62] H. Scharfetter and Graz University of Technology. Nuclear Quadrupol Resonance. 2018. URL: https://www.tugraz.at/institute/imt/research/nuclear-quadrupole-resonance/.

[63] H. Scharfetter et al. "A no-tune no-match wideband probe for nuclear quadrupole resonance spectroscopy in the VHF range". In: Measurement Science and Technology 25.12 (2014).

[64] G. M. Sheldrick. GM SHELXS97 and SHELXL97. Universitaet Goettingen, Goettingen, Germany, 2002.

[65] G. M. Sheldrick. SADABS Version 2.10 Siemens Area Detector Correction. Universitaet Goettingen, Goettingen, Germany, 2003.

[66] G. M. Sheldrick. SHELXTL Version 6.1. Bruker AXS, Inc. Madison, WI, 2002.

[67] S. Shimada et al. "Synthesis and structure of 5,6,7,12-tetrahydrodibenz[c,f][1,5]azabismocines". In: Journal of Organometallic Chemistry 689.19 (2004), pp. 3012–3023.

[68] C. Silvestru, H. J. Breunig, and H. Althaus. "Structural Chemistry of Bismuth Compounds. I. Organobismuth Derivatives". In: Chemical Reviews 99.11 (1999), pp. 3277–3328.

[69] C. P. Slichter. Principles of Magnetic Resonance. Springer-Verlag, 1989.

[70] J. A. S. Smith. "Nuclear Quadrupole Resonance Spectroscopy". In: Journal of Chemical Education 48.1 (1971), pp. 39–48.

[71] A. L. Spek. "Single-crystal structure validation with the program PLATON". In: Journal of Applied Crystallography 36.1 (2003), pp. 7–13.

[72] A. L. Spek. "Structure validation in chemical crystallography". In: Acta Crystallographica Section D: Biological Crystallography 65.2 (2009), pp. 148–155.

[73] B. H Suits. “Nuclear Quadrupole Resonance Spectroscopy”. In: (1958).

[74] H. Suzuki and Y. Matano. Organobismuth Chemistry. 2001.

[75] D. V. Talapin and W. Heiss. “Highly Monodisperse Bismuth Nanoparticles and Their Three-Dimensional”. In: Journal of the American Chemical Society (2010), pp. 15158–15159.

[76] H. Tamber, J. Smid, and I. Cabasso. “Radiopaque Copolymers of Styryldiphenylbismuth Vinylbenzylphosphonate and Methyl Methacrylate”. In: Chemistry of Materials 9.6 (1997), pp. 1335–1341.

[77] C. W. Tornoe, C. Christensen, and M. Meldal. “Peptidotriazoles on solid phase: [1,2,3]-Triazoles by regiospecific copper(I)-catalyzed 1,3-dipolar cycloadditions of terminal alkynes to azides”. In: Journal of Organic Chemistry 67.9 (2002), pp. 3057–3064.

[78] M. Vehkamaeki. “Bismuth precursors for atomic layer deposition of bismuth-containing oxide films”. In: Journal of Materials Chemistry 14.21 (2004), p. 3191.

[79] B. T. Worrell, S. P. Ellery, and V. V. Fokin. “Copper(I)-catalyzed cycloaddition of bismuth(III) acetylides with organic azides: Synthesis of stable triazole anion equivalents”. In: Angewandte Chemie - International Edition 52.49 (2013), pp. 13037–13041.